UNIVERSIDAD DE MURCIA

FACULTAD DE BIOLOGÍA

The Zebrafish (*Danio rerio*) as a Model to Study *In Vivo* the Role of Telomerase in Hematopoiesis

El Pez Zebra (*Danio rerio*) como Modelo de Estudio *In Vivo* del Papel de la Telomerasa en la Hematopoyesis

Dña. Francisca Alcaraz Pérez

2014

UNIVERSIDAD DE MURCIA

FACULTAD DE BIOLOGÍA

DEPARTAMENTO DE BIOLOGÍA CELULAR E HISTOLOGÍA

THE ZEBRAFISH (*Danio rerio*) AS A MODEL TO STUDY *IN VIVO* THE ROLE OF TELOMERASE IN HEMATOPOIESIS

EL PEZ CEBRA (*Danio rerio*) COMO MODELO DE ESTUDIO *IN VIVO* DEL PAPEL DE LA TELOMERASA EN LA HEMATOPOYESIS

Memoria que presenta

Dña. Francisca Alcaraz Pérez

para optar al grado de Doctor Internacional

por la Universidad de Murcia

Febrero 2014

Index

Abbreviations

AGM	Aorta-Gonad-Mesonephros
ALM	Anterior Lateral plate Mesoderm
ALT	Alternative Lengthening of Telomeres
ATM	Ataxia Telangiectasia Mutated
ATR	ATM and Rad3-related
BSA	Bovine Serum Albumin
cDNA	complementary DNA
CFU	Colony Forming Units
CHT	Caudal Hematopoiestic Tissue
ChIRP	Chromatin Isolation by RNA Purification
CMV	Cytomegalovirus
CSF	Colony Stimulating Factor
CTC1	Conserved telomere maintenance component 1
DC	Dyskeratosis congenita
DDR	DNA Damage Response
DKC1	Dyskerin 1
D-loop	Displacement loop
DMSO	Dimethyl sulphoxide
DNA	Deoxyribonucleic Acid
DNase	Deoxyribonuclease
dNTP	Deoxynucleotide Triphosphate
dpf	days post-fertilization
dsDNA	double-stranded DNA
dsRNA	double-stranded RNA

DTT	Dithiothreitol …
*Ec*LPS	*Escherichia coli* LPS
EDTA	Ethylenediaminetetraacetic acid
EF1α	Elongation factor 1α
EGFP	Enhanced GFP
EGTA	Ethylene glycol bis (2-aminoethyl ether)-N, N, N', N'-tetraacetic acid
EMPs	Erythromyeloid Progenitors
F	Direct primer
FACS	Fluorescence-Activated Cell Sorting
FCS	Fetal Calf Serum
FITC	Fluorescein isothiocyanate
FISH	Fluorescence *In Situ* Hybridization
fMLP	N-formyl-methyonyl-leucyl-phenylalanine
GAPDH	Glyceraldehyde-3-phosphate dehydrogenase
GAR1	H/ACA ribonucleoprotein complex subunit 1
GATA1a	GATA binding protein 1 (globin transcription factor 1)
gDNA	Genomic DNA
GFP	Green fluorescent protein
GMCSF	Granulocyte/macrophage CSF
hpf	hours post-fertilization
hpi	hours post-infection
hpm	hours post-microinjection
hpw	hours post-wound
HSCs	Hematopoietic Stem Cells
HTA	Head Trunk Angle

ICM	Intermediate Cell Mass
IFN	Interferon
IL-1β	Interleukin-1β
iPS	induced Pluripotent Stem cells
LPS	Lipopolysaccharide
LTL	Leukocyte Telomere Length
lyz	lysozyme
Luc	Luciferase
MCSF	Macrophage-CSF
MO	Morpholino
MOI	Multiplicity Of Infection
MPX	myeloperoxidase
mRNA	messenger RNA
$mTR^{-/-}$	mouse TR deficient
MYC	v-myc avian myelocytomatosis viral oncogene homolog
NAF1	Nuclear Assembly Factor 1 ribonucleoprotein
ND	Not Detected
NF-κB	Nuclear Factor-κB
NHEJ	Non-Homologous-End-Joining
NHP2	H/ACA ribonucleoprotein complex subunit 2
NOLA3	NOP10 encoding gene
NOP10	Nucleolar Protein 10
n.s.	not significant
nt	nucleotides

PAMP	Pathogen-Associated Molecular Pattern
PBI	Posterior Blood Island
PBS	Phosphate Buffered Saline
PBT	Phosphate Buffered solution with 0.1 % Tween-20
PCR	Polymerase Chain Reaction
PFA	Paraformaldehyde
PLB	Passive Lysis Buffer
PMA	Phorbol 12-myristate acetate
POT1	Protection of Telomeres 1
Q-FISH	Quantitative-FISH
Q-TRAP	Quantitative-TRAP
R	Reverse primer
RdRP	RNA-dependent RNA Polymerase
RMRP	RNA component of Mitochondrial RNA Processing endoribonuclease
RNA	Ribonucleic Acid
RNase	Ribonuclease
RNP	Ribonucleoprotein
ROS	Reactive Oxygen Species
RPS11	ribosomal protein subunit 11
rRNA	ribosomal RNA
RT	Room Temperature
RTA	Relative Telomerase Activity
RT-qPCR	Reverse transcription – quantitative polymerase chain reaction
SEM	Standard Error of the Mean

siRNA	small interfering RNA
ssDNA	single-stranded DNA
SPI1	spleen focus forming virus (SFFV) proviral integration oncogene
STE	Stem-Terminus Element
Std	Standard
STN1	Suppressor of cdc thirteen homolog
SWI/SNF	SWItch/Sucrose NonFermentable
TBE	Template Boundary Element
TCAB1	Telomerase Cajal Body protein 1
TEN1	CST complex subunit TEN1
TERC	Telomerase RNA Component
TERRA	Telomeric-Repeat-containing RNA
TERT	Telomerase catalytic subunit
TIF1γ	transcription intermediate factor-1γ
TIN2	TRF1-Interacting Nuclear factor 2
TK	Thymidine Kinase
t-loop	telomeric DNA loop
TLR	Toll-Like Receptors
TMG	Tri-Methyl Guanosine
TMM	Telomere Maintenance Mechanism
TPP1	TIN2 and POT1-interacting Protein 1
TR	Telomerase RNA component
TRF1	Telomeric Repeat binding Factor 1

TRF2	Telomeric Repeat binding Factor 2
TSA	Tyramide Signal Amplification
UTP	Uridine triphosphate
*Va*DNA	*Vibrio anguillarum* genomic DNA
WISH	Whole-mount RNA *In Situ* Hybridization
wt	wild type
ZIRC	Zebrafish International Resource Center
ZFNs	Zinc Finger Nucleases
zf	zebrafish

Summary

During the development of this Doctoral Thesis, we have exploited the unquestionable advantages of the zebrafish to generate a new tool to study *in vivo* the promoter and gene function and to develop a new zebrafish model to study dyskeratosis congenita (DC).

Firstly, we have adapted the classical dual luciferase reporter assay from cell lines to whole zebrafish embryos/larvae. The result is a rapid and sensitive technique that can be used as a new tool to characterize the minimum promoter region of a gene as well as the *in vivo* response of inducible promoters to different stimuli. We have illustrated the usefulness of this system for studying both constitutive and inducible promoters. This assay has several advantages compared with the classical *in vitro* (cell lines) and *in vivo* (transgenic mice) approaches. Among others, the assay allows a rapid and quantitative measurement of the effects of particular genes or drugs in a given promoter in the context of a whole organism and it can also be used in high throughput screening experiments.

We have showed several evidences supporting the zebrafish as a new model to study the role of the telomerase RNA component (*TR*) in DC, which is an inherited premature disease whose patients usually die of bone marrow failure. In this model, genetic depletion of *TR* results in impaired myelopoiesis, despite normal development of hematopoietic stem cells (HSCs). Interestingly, the neutropenia caused by *TR* depletion is independent of telomere length and telomerase activity. Genetic analysis shows that *TR* modulates the myeloid-erythroid fate decision by controlling the levels of the master myeloid and erythroid transcription factors *spi1* and *gata1,* respectively, through stimulation of *gcsf* and *mcsf*. This model of *TR* deficiency in the zebrafish illuminates the non-canonical roles of *TR*, and could establish therapeutic targets for DC.

Introduction

1. Telomeres

Genomic stability is the prerequisite of species survival as ensures that all required information will be passed on to the next generations. In contrast to single-cell-species, higher order organisms, in order to preserve their genomic information, require more efficient DNA repair mechanisms due to later onset of reproduction. Therefore, a remarkable ability of cells to recognize and repair DNA damage and progress through the cell cycle, in a regulated and orderly manner, has been developed.

A vulnerable portion of the genome, especially in eukaryotic organisms whose genome is organised in linear chromosomes, is their edges called telomeres (after the greek words '*τέλος*' (*télos*) and '*μέρος*' (*méros*) meaning 'the ending part'). For this, telomeres form specialized structures at the ends of linear chromosomes that ensure their integrity by 'hiding' the free-ends of the chromosome from the mechanisms within the cell that monitor DNA damage. They are also needed to overcome the 'end-replication problem' [Greider, 1996].

Telomeres are long tracts of DNA at the linear chromosome's ends composed of tandem repeats of a guanine rich sequence motif that vary in length from 2 to 20 kb, according to species. This motif is conserved in lower eukaryotes and in mammalian cells [Greider, 1998]. Usually, but not always, the telomeric DNA is heterochromatic and contains direct tandemly repeated sequences of the form $(T/A)_xG_y$ where x is between 1 and 4 and y is greater than 1 (**Table I**).

Table I: The following table shows the diversity of telomeric DNA. *Adapted from Sfeir (2012).*

Organism	Sequence	Length
H. sapiens	TTAGGG	5-15 kb
M. musculus	TTAGGG	20-100 kb
D. rerio	TTAGGG	12-20 kb
S. pombe	$GGTTACA_{0-1}C_{0-1}G_{0-1}$	5 kb
S. cerevisiae	TG_{1-3}	300 bp
T. brucei	GGGTTA	2-26 kb
T. thermophila	TTGGGG	120-420 bp
C. elegans	TTAGGC	4-9 kb
A. thaliana	TTTAGGG	2-5 kb
Oxytricha	TTTTGGGG	20 bp

Exceptionally, the chromosome ends of a few insect species (*Drosophila* and some dipterans), instead of telomeric motifs, possess tandem arrays of retrotransposons [Abad *et al.*, 2004].

1.1. Structure and function

Telomeric DNA is double stranded with a single-stranded terminus that is on average 130-210 nucleotides (nt) long in human cells [Makarov *et al.*, 1997]. Under normal conditions, in most somatic cells of an adult organism, telomeres shorten in each cell division (i.e. in humans by about 50-150 nt). The basic telomere DNA repeat unit in vertebrates is the hexamer TTAGGG, in which the strand running 5'→ 3' outwards the centromere is usually guanine-rich and referred to as G-tail (**Fig. 1**).

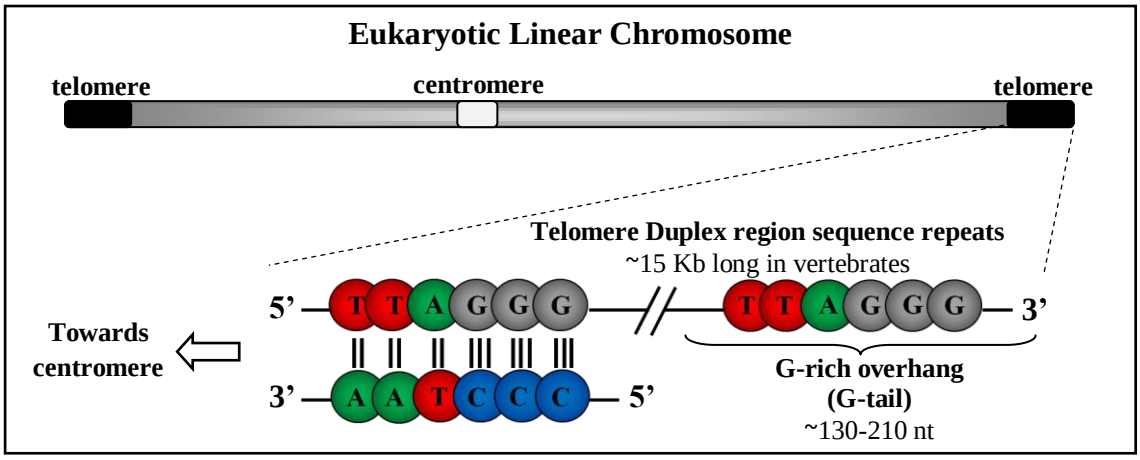

Figure 1: Telomere primary structure scheme.

In order not to leave exposed a single stranded overhang, this G-rich strand protrudes its complementary DNA-strand and by bending on itself it folds back to form a telomeric DNA loop (t-loop), while the G-tail 3' end invades into the double strand forming a triple-stranded structure called displacement loop (D-loop) inside the t-loop [Griffith *et al.*, 1999]. As a result, the t-loop protects the G-tail from being recognized as a double-stranded DNA (dsDNA) break by sequestering the 3'-overhang into a higher order DNA structure (**Fig. 2**).

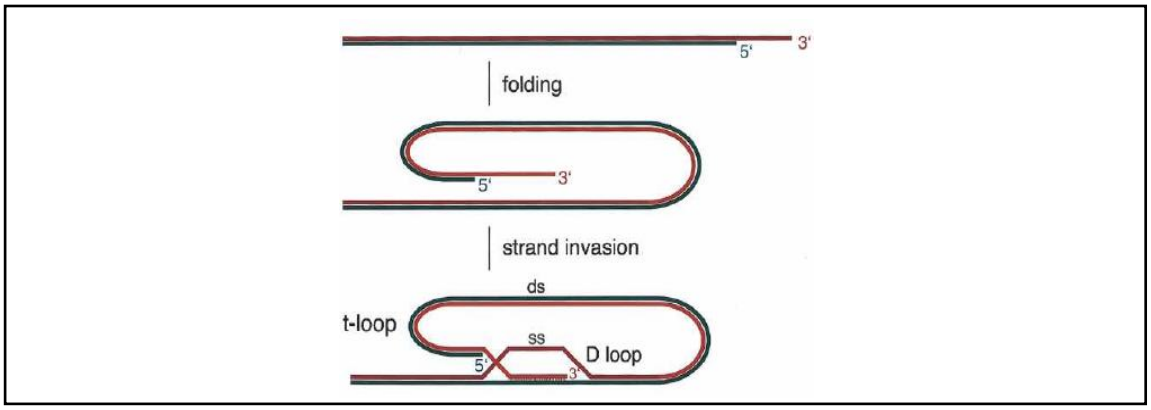

Figure 2: Telomere secondary structure scheme. The single stranded overhang folds back and forms a telomeric DNA loop, t-loop. Then, the 3' overhang is strand-invaded into the adjacent duplex telomeric repeat array, forming a D-loop. The size of the loop is variable. *Adapted from de Lange (2005).*

In vertebrates, the role of chromosome end protection in order to be distinguished from chromosome breaks is attributed to a specific complex of proteins collectively referred to as shelterin. Shelterin complex is basically composed by six proteins: TRF1 (telomeric repeat binding factor 1), TRF2 (telomeric repeat binding factor 2), POT1 (protection of telomeres 1), RAP1 (repressor activator protein 1), TIN2 (TRF1-interacting nuclear factor 2) and TPP1 (TIN2 and POT1-interacting protein 1). Two members of the shelterin complex, TRF1 and TRF2 (from Telomere Repeat-binding Factor 1 and 2) bind directly to double stranded telomeric sequence, while POT1 binds single-stranded DNA (ssDNA). TRF2 interacts with and recruits RAP1, while TIN2 mediates TPP1-POT1 binding to the TRF1/TRF2 core complex. POT1 binds to and protects the 3´ ssDNA overhang of telomeres (G-tail), while TIN2 likely links the ssDNA and dsDNA binding complexes, especially in the area of the telomeric D-loop formation [de Lange, 2005; Stewart *et al.*, 2012] (**Fig. 3**).

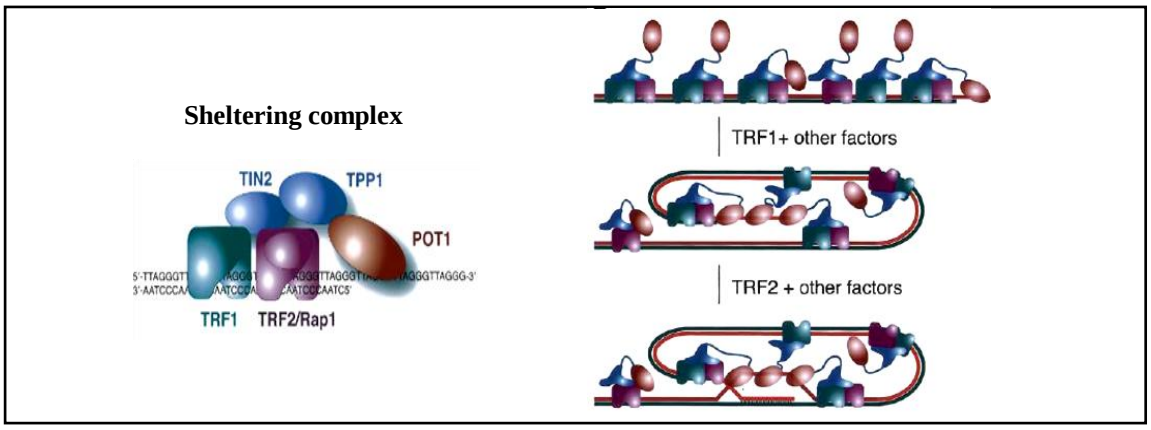

Figure 3: Speculative model for t-loop formation by shelterin. TRF1 has the ability to bend, loop, and pair telomeric DNA *in vitro* and could potentially fold the telomere. *Adapted from de Lange (2005).*

It seems that this core shelterin complex is mainly located at the telomere end (also referred to as telosome) and serves both in stabilizing t-loop structure, protecting it at the same time from being recognized by the DNA damage detection machinery as dsDNA breaks and repaired by Non-Homologous-End-Joining (NHEJ) repair activities. Additionally, shelterin regulates access to restoration processes of telomeric DNA after each genome replication. In general, shelterin complex seems to function as a platform regulating recruitment of a growing list of factors involved in chromatin remodelling, DNA replication, DNA damage repair, recombination and telomerase function, thus regulating telomere access/modification by diverse cellular processes, recently reviewed by Diotti *et al.* (2011).

Apart from shelterin and interacting partners, another significant complex has recently emerged to be also involved in telomere biology, the CST complex. The CST complex is composed of three subunits: CTC1 (conserved telomere maintenance component 1), STN1 (suppressor of cdc thirteen homolog) and TEN1 (CST complex subunit TEN1), and has been attributed the rescue of stalled replication forks during replication stress. The CST complex interconnects telomeres to genome replication and protection independently of the POT1 pathway [Stewart *et al.*, 2012; Miyake *et al.*, 2009].

An RNA component called telomeric-repeat-containing RNA (TERRA), has been identified as the third entity of the telomere nucleoprotein complex [Azzalin *et al.*, 2007]. TERRA transcription is mediated by RNA polymerase II and is initiated from

the sub-telomeric regions that are found near chromosome ends [Porro *et al*., 2010]. TERRA levels are regulated during the cell cycle, and its localization at telomeres is modulated by the nonsense-mediated decay machinery [Azzalin *et al*., 2007]. It has been postulated that this non-coding RNA is important for telomere maintenance and function [Redon *et al*., 2010; Flynn *et al*., 2011], yet the molecular mechanisms underlying this proposed function remain to be uncovered.

The structure of telomeres is intrinsically dynamic, as chromosome ends should relax during genome replication and then re-establish their 'capped' state after replication. Consequently, telomeres may switch between closed (protected) and open (replication-competent) states during the cell cycle. Each state is governed by a number of interactions with specific factors and can lead the cell to either cell division or senescence/apoptosis under normal conditions, or to disorders/cancer in abnormal cases [Harley *et al.*, 1990; d'Adda di Fagagna *et al.*, 2003]. Moreover, during development and in certain cell types in adults, telomere length should be preserved. Thus, multiple physiological processes guarantee functional and structural heterogeneity of telomeres concerning their length and nucleoprotein composition. A functional chromosome end structure is essential for genome stability, as it must prevent chromosome shortening and chromosome end fusion as well as degradation by the DNA repair machinery. Hence, structure and function of telomeres are highly conserved throughout evolution [Silvestre & Londoño-Vallejo, 2010].

1.2. The 'end-replication problem'

The primary difficulty with telomeres is the replication of the lagging strand. Because DNA synthesis requires a RNA template (that provides the free 3'-OH group) to prime DNA replication, and this template is eventually degraded, a short single-stranded region would be left at the end of the chromosome (referred to as the 'end-replication problem'). This region would be susceptible to enzymes that degrade ssDNA. In the absence of any compensatory mechanism, the result would be that the length of the chromosome would be shortened after every cell division, resulting in cumulative telomere attrition during aging [Watson, 1972; Olovnikov, 1973]. In addition, loss of telomere DNA also occurs due to post-replicative degradation of the 5' strand that generates long 3' G-rich overhangs [Wellinger *et al.*, 1996] (**Fig.4**).

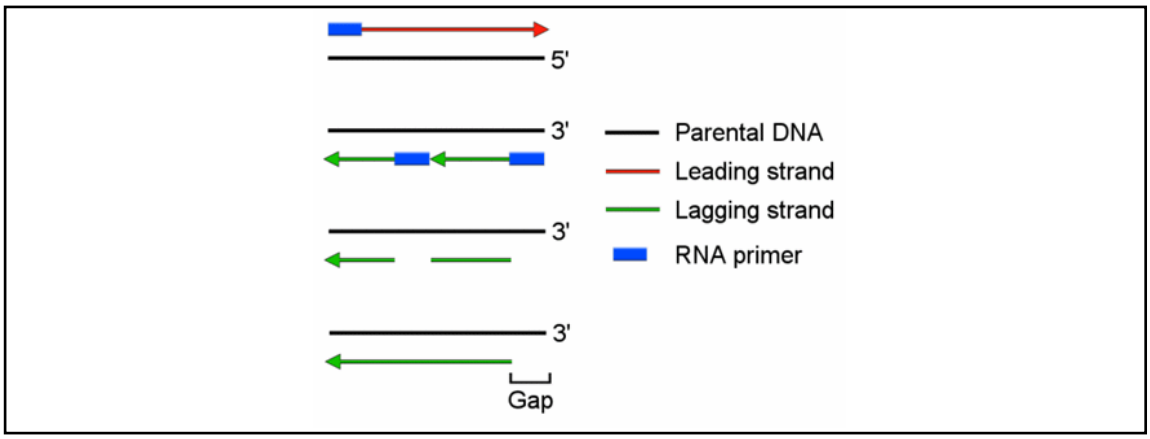

Figure 4: The 'end-replication problem'. DNA polymerase requires an RNA primer to initiate synthesis in the 5'-3' direction. At the end of a linear chromosome, DNA polymerase can synthesize the leading strand until the end of the chromosome. In the lagging strand, however, DNA polymerase's synthesis is based on a series of fragments, called Okazaki, each requiring an RNA primer. Without DNA to serve as template for a new primer, the replication machinery is unable to synthesize the sequence complementary to the final primer event. The result is an end-replication problem in which sequence is lost at each round of DNA replication.

Upon each genome duplication, cells would otherwise keep losing genetic material, eventually resulting in premature cell death, a critical problem for both the species and an individual's survival. This issue is even more prominent especially in multi-cellular organisms with late onset of reproduction.

2. Telomerase complex

During ontogenesis, eukaryotic organisms solved the 'end replication problem' by preventing telomere attrition in dividing cells, through recruitment of telomerase, a specialized and unique RNA-dependent DNA polymerase that synthesizes telomeric repeats at the end of eukaryotic chromosomes [Blackburn, 2005], thereby maintaining them at a 'constant' length, as a limited telomere length is a prerequisite for cell replication [Blackburn *et al*., 2006] (**Fig. 5**).

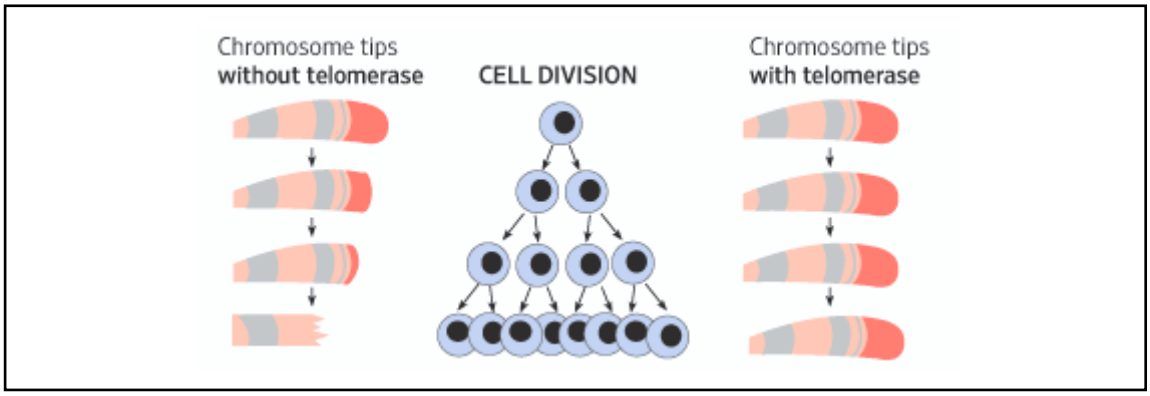

Figure 5: Telomerase synthesizes telomeres. Without telomerase, chromosomes get shorter over time and cells eventually stop dividing. *Adapted from The Nobel Committee for Physiology or Medicine.*

Telomerase is routinely active only during embryogenesis and development, while in adults is expressed only to rapidly dividing cells (i.e. proliferative skin and gastrointestinal cells, activated lymphocytes, specific bone marrow stem cells and dividing male germ cell lineages) [Ulaner *et al.*, 1997]. In most adult cells telomerase is not expressed. Consequently, after a number of cell divisions, telomeres reach a critical length and chromosomes become uncapped (**Fig. 6**).

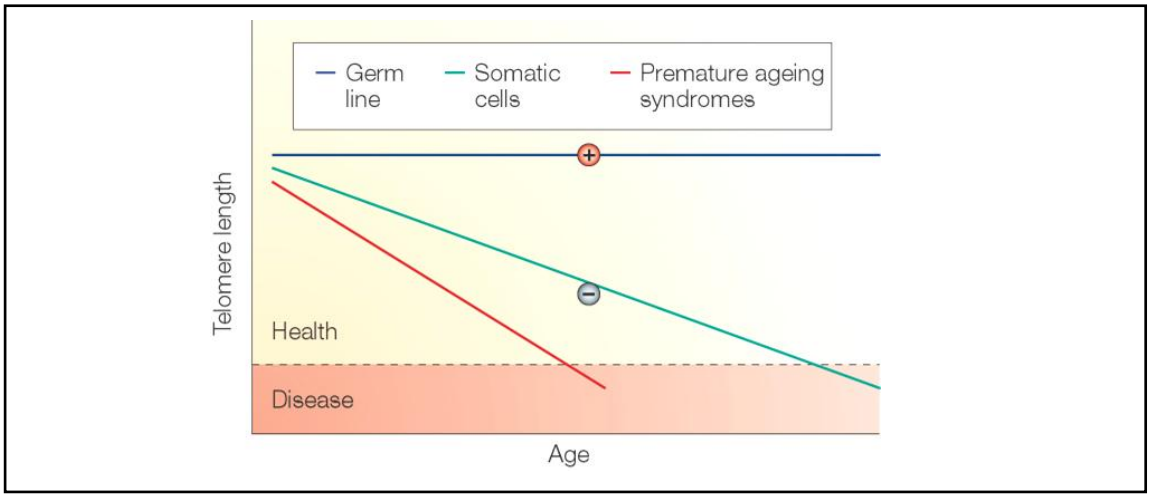

Figure 6: Telomeres undergo characteristic length changes over time in normal somatic and germ line cells, and in premature ageing syndromes. In contrast to germ cells, which have high telomerase activity (indicated by the plus symbol) and maintain telomere length with age, most somatic cells show progressive telomere shortening owing to low or absent telomerase activity (indicated by the minus symbol). In addition, several human premature ageing syndromes show an accelerated rate of telomere shortening, therefore resulting in an early onset of ageing-related pathologies. *Adapted from Blasco (2005).*

This progressive telomere loss eventually leads to critically short telomeres which leads, depending on the cellular context in which the uncapping occurs, a DNA damage response (DDR) that results in chromosomal end-to-end fusions or a permanent cell cycle arrest (termed cellular senescence) or apoptosis (programmed cell death) [Blasco, 2005; Galati *et al.*, 2013]. This loss of cell viability associated with telomere shortening is thought to contribute not only to the onset of degenerative diseases that occur during human ageing, but also to several age associated diseases such as cancer, coronary artery disease, and heart failure [Sherr & McCormick, 2002; Ogami *et al.*, 2004; Starr, 2007; Donate & Blasco, 2011]. Cells programmed to enter senescence may escape this procedure due to checkpoint dysfunction and instead continue infinite proliferation, leading to oncogenesis. In such cases genomic stability has to be re-established and telomere length has to be restored by a telomere maintenance mechanism (TMM). In most of tumor cells telomere maintenance is achieved by re-expression of telomerase. Interestingly, tumors have been described where telomerase could not be detected.

Further studies revealed that in addition to the role of telomerase in maintaining telomere length, homologous recombination constitute an alternative method (ALT ‘alternative lengthening of telomeres’) to maintain telomere DNA in telomerase-

deficient cells. ALT TMM, in contrast to telomerase dependent TMM, results in telomeres with high heterogeneity in length and at least in the well-studied model of *S. cerevisiae*, consists of two pathways. While the bulk of cancer and immortalized cells utilize telomerase re-expression to maintain telomere length, about 10-15% of tumors described operate using the ALT mechanism [Lundblad & Blackburn, 1993; Teng & Zakian, 1999; Teng *et al*., 2000], (**Fig.7**).

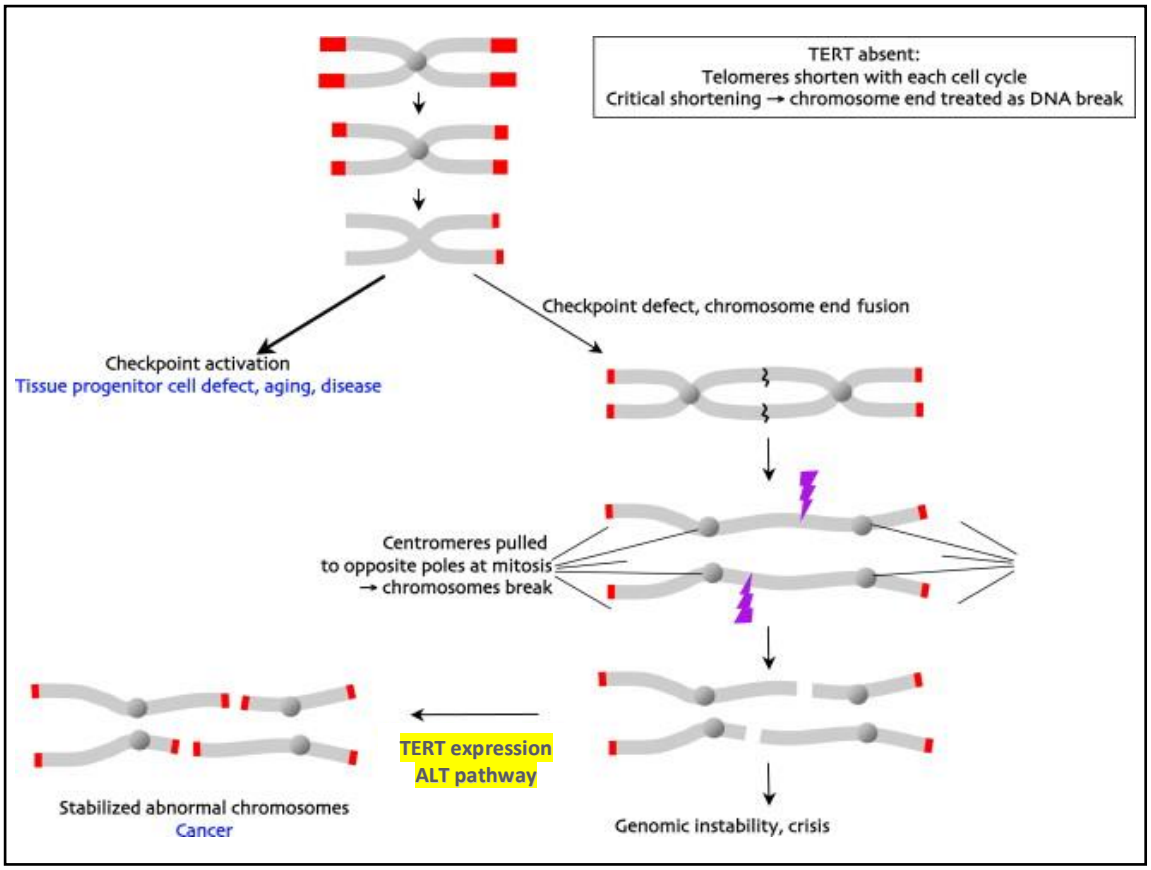

Figure 7: Telomere shortening causes senescence and chromosome instability. In cells with insufficient telomerase, DNA replication-dependent telomere attrition results in critically short telomeres, which activate the DDR, leading to senescence or apoptosis. However, in cells lacking a robust DNA-damage checkpoint response, inappropriate 'repair' reactions act on telomeres. One result of this is the end fusion depicted, which produces a dicentric chromosome that breaks randomly if the centromeres are pulled to opposite poles by the mitotic spindle. This scenario can lead to cell death or to widespread chromosomal rearrangement through cycles of chromosomal fusion and breakage, which can drive tumor development. Telomerase upregulation (or, rarely, an alternative telomere maintenance pathway) stabilizes the telomeres, allowing the propagation of aberrant genomes associated with many cancers. *Adapted from Artandi & Cooper (2009).*

2.1. Structure and function

The telomerase complex is a ribonucleoprotein (RNP) composed by a catalytic subunit (TERT), a RNA component (*TR*) which acts as a template for the addition of the telomere sequence in the 3' end of the telomere and species-specific accessory proteins. The accessory proteins regulate telomerase biogenesis, subcellular localization and its function *in vivo* [Wyatt *et al.*, 2010]. In human telomerase, seven associated proteins have been identified: Dyskerin, NHP2 (H/ACA ribonucleoprotein complex subunit 2), NOP10 (nucleolar protein 10), Pontin, Reptin, GAR1 (H/ACA ribonucleoprotein complex subunit 1) and TCAB1 (telomerase Cajal body protein 1) [Fu & Collins, 2007] (**Fig. 8**).

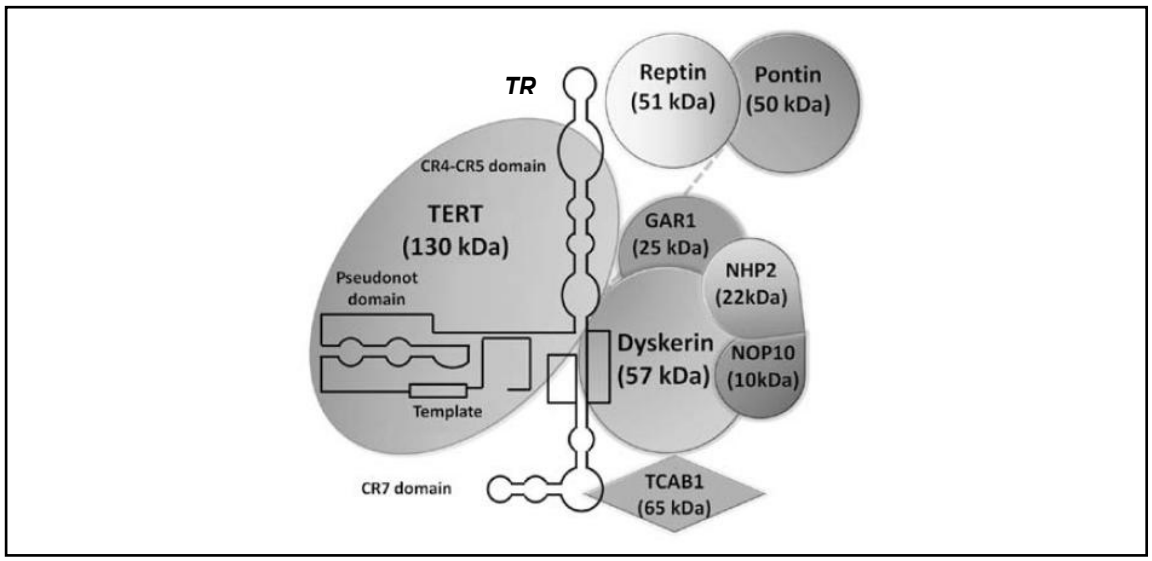

Figure 8: Schematic representation of human telomerase and its associated proteins. *Adapted from Gómez et al. (2012).*

Dyskerin, NHP2 and NOP10 are required for the stability and accumulation of human *TR in vivo* [Fu & Collins, 2007]. Pontin and reptin are two closed ATPases necessary for the stability of dyskerin and *TR in vivo* [Veinteicher *et al.*, 2008]. The current model is that dyskerin, pontin and reptin form a scaffold that recruits and stabilizes *TR*, and assembles the telomerase ribonucleoprotein particle. Once this complex is formed, pontin and reptin are believed to dissociate from the complex and release the catalytically active enzyme [Veinteicher *et al.*, 2008]. The subcellular location of telomerase complex assembly is the cajal body, and it appears to be

regulated by the TCAB1 protein [Zhong *et al.*, 2011]. Also, while one study claims that the human telomerase holoenzyme contains only dyskerin, TERT, and *TR* [Cohen *et al.*, 2007], other studies establish that the human telomerase holoenzyme assembles all of the core proteins [Fu & Collins, 2007].

The action of the telomerase complex ensures that the ends of the lagging strands are replicated correctly. Elongation of the telomere by telomerase is a process that happens in different stages. First, the nucleotides of the 3' extreme of the telomeric DNA are hybridized to the end of the RNA template, inside the RNA domain of the telomerase complex. The template sequence of 11 nucleotides is complementary to almost two telomeric repeats. Next, the gap in the extreme of the template is completed by synthesis, using triphosphate nucleotides in the catalytic site of the enzyme (TERT). In this way, a complete hexanucleotidic repeat is assembled in the template. Then, telomerase relocates and the cycle is repeated, extending the telomere in the 3'-direction. Finally, the DNA polymerase can synthesize the lagging strand and thus, the end of the chromosome is faithfully replicated (**Fig. 9**).

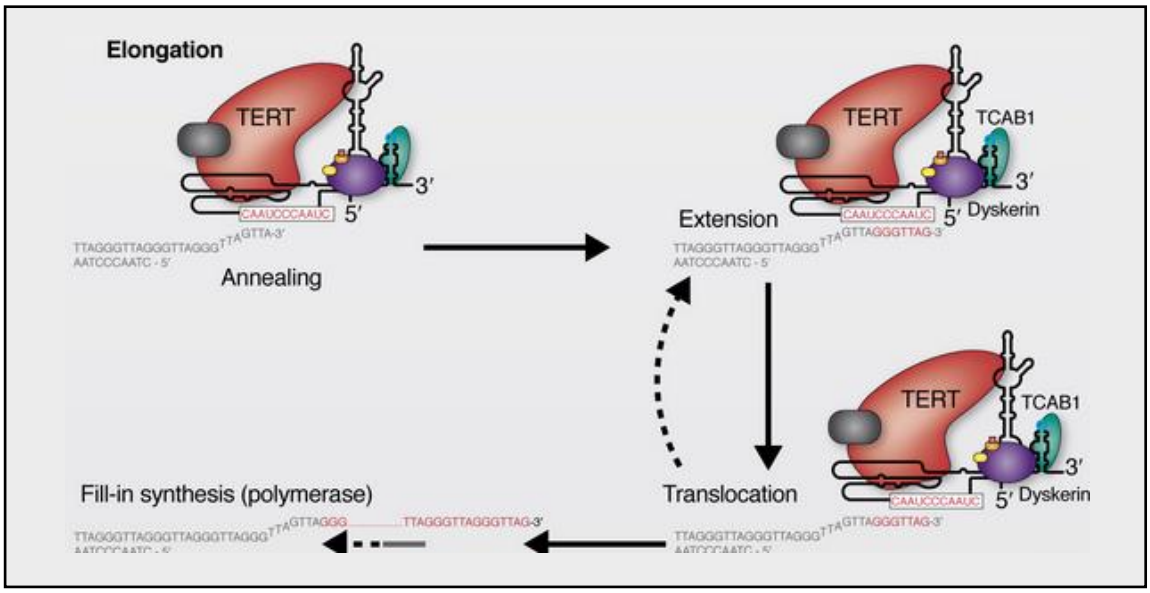

Figure 9: Telomere maintenance. Telomerase, consisting mainly of the protein (TERT) and RNA subunit (*TR*), binds to 3' flanking end of telomere that is complementary to *TR*, and bases are added using *TR* as template. Then, telomerase relocates and telomere is extended in the 3'-direction. Finally, the DNA polymerase can synthesize the lagging strand. This process can maintain telomere length or lead to telomere lengthening. *Adapted from Sfeir (2012).*

2.2. The RNA component

The RNA component of telomerase, *TR*, has been isolated from ciliates, yeasts, and mammals and is essential for telomerase activity [Blasco *et al.*, 1996], but is not a limiting factor for telomerase [Cairney & Keith, 2008]. In vertebrates, *TR* has an extension between 382 and 559 nucleotides [Tsao *et al.*, 1998], and in humans in particular *TR* has an extension of 451 nucleotides of length and contains a sequence of 11 bp (5-CUAACCCUAAC-3') that encodes for telomeric repeats [Morin, 1989].

Phylogenetic comparative analysis of vertebrate *TR* predicts three conserved domains: (1) the pseudoknot/template core domain, (2) the CR4/CR5 domain and (3) a box H/ACA domain [Chen *et al.*, 2000]. The pseudoknot/template core domain contains a template region for telomeric DNA synthesis, and a conserved pseudoknot structure essential for telomerase activity *in vitro* and *in vivo*. The CR4/CR5 domain together with the pseudoknot/template domain are both required for reconstituting active telomerase *in vitro*, and the box H/ACA domain is essential for *TR* stability, processing, nuclear localization and telomerase activity *in vivo* [Theimer & Feigon, 2006]. Within the H/ACA domain, two additional motifs have been defined: (1) the CAB box, which binds TCAB1 to promote RNP concentration in Cajal bodies [Richard *et al.*, 2003; Jády *et al.*, 2004; Tycowski *et al.*, 2009; Venteicher *et al.*, 2009] and (2) the BIO box, which cooperates with other elements to promote mature RNP accumulation *in vivo* [Fu & Collins, 2003; Egan & Collins, 2012] (**Fig. 10**).

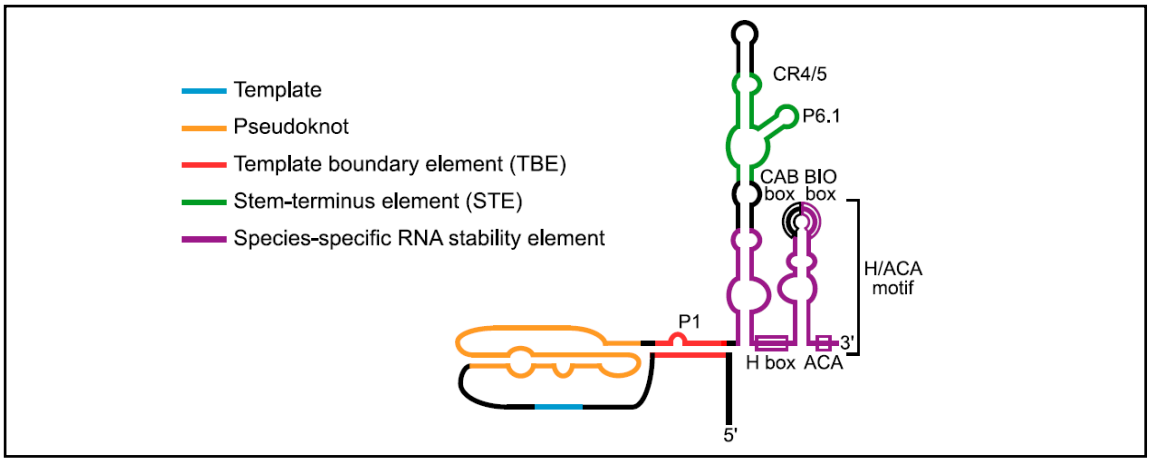

Figure 10: The minimum consensus structure of vertebrate telomerase RNA. *Adapted from Egan & Collins (2012).*

Vertebrate *TR*s are synthesized as 3'-extended precursors by RNA Polymerase II, the same enzyme that synthesizes mRNA. Many steps of processing are required to convert an incompletely defined *TR* precursor into the mature form. These events must distinguish a nascent *TR* transcript from other transcripts such that the precursor acquires features of *TR* rather than a processed mRNA.

Specifically, human *TR* is transcribed by RNA polymerase II as a precursor that cotranscriptionally assembles with the H/ACA core protein heterotrimer of dyskerin, NHP2, and NOP10 bound to the H/ACA RNP assembly chaperone NAF1 (nuclear assembly factor 1 ribonucleoprotein) [Trahan & Dragon, 2010]. Then, the *TR* precursor transcript is processed at its 3' end by an unknown mechanism so that the mature form lacks the poly-adenosine tail, characteristic of mRNA. At the 5' end, the G-quadruplex structure is resolved by the helicase DHX36. [Feng *et al*., 1995; Fu & Collins, 2006]. Cellular accumulation of mature *TR* requires a region within the RNA that folds to form a so-called H/ACA motif. After transcription, assembly with H/ACA core proteins, and RNA processing, *TR* is routed through Cajal bodies by some transport factors. Cajal bodies are also sites of RNP remodelling, likely including the exchange of the RNP assembly factor NAF1 for the mature RNP component GAR1 [Darzacq *et al*., 2006] and the modification of the 5' cap to tri-methyl guanosine (TMG) rather than mono-methyl guanosine cap. Finally, TCAB1 and TERT bind to *TR* in the active telomerase holoenzyme (**Fig. 11**).

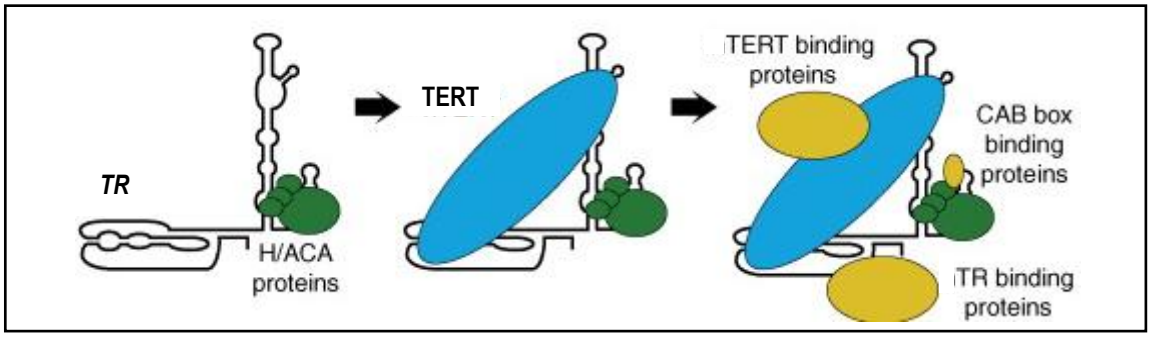

Figure 11: Model for human telomerase RNP assembly. Assembly of *TR* with the H/ACA-motif binding proteins (in green) dyskerin, NHP2 and NOP10 is essential for its accumulation *in vivo*. Once transported to Cajal bodies, these proteins recruit the fourth shared H/ACA-motif binding protein, GAR1. RNP assembly on the *TR* H/ACA motif would be predicted to influence the relative orientation of the *TR* binding surfaces for human TERT (in blue), potentially promoting *TR*-TERT interaction. The numerous proteins that are proposed to regulate human telomerase function *in vivo* (in yellow) may interact with the catalytically active TERT RNP and/or with telomerase RNP or TERT assembly intermediates. *Adapted from Collins (2008)*.

2.3. 'Extracurricular' roles

Telomerase is essential for the long-term proliferation potential of stem cells and cancer cells, and for normal tissue renewal. However, other functions have been described beyond its action at the telomeric level, so-called 'extracurricular' or non-canonical roles. Indeed, human TERT can function as a transcriptional modulator of the Wnt-β-catenin signaling pathway, as a cofactor in a β-catenin transcriptional complex through interactions with BRG1, which is an SWI/SNF (SWItch/Sucrose NonFermentable) related chromatin remodeling protein [Park *et al.*, 2009]. In addition, human TERT forms a complex with RMRP (RNA component of mitochondrial RNA processing endoribonuclease) and acts as an RNA-dependent RNA polymerase. The TERT-RMRP complex acts as an RNA-dependent RNA Polymerase (RdRP) and processes RMRP into double-stranded RNA (dsRNA), which is then processed by the endoribonuclease Dicer into small interfering RNA (siRNA), which controls RMRP endogenous levels [Maida et al., 2009]. Some evidence has been found for a role for telomerase in the regulation of apoptosis in a telomere maintenance-independent manner [Cong & Shay, 2008]. Human TERT contains a mitochondrial localization signal peptide at its N-terminal that targets TERT to mitochondria where it is active. Furthermore, it was shown that telomerase sensitizes mitochondrial DNA to hydrogen peroxide-induced oxidative damage, probably through the modulation of metal homeostasis [Santos *et al.*, 2004]. The mitochondrial localization of telomerase also has an important role in apoptosis [Santos *et al.*, 2006]. Moreover, human TERT contribution to epithelial proliferation, tumorigenesis and aging is also mediated by a telomere length-independent mechanism [Choi *et al.*, 2008; Sarin *et al.*, 2005; Stewart *et al.*, 2002; Geserick & Blasco, 2006].

In contrast to TERT, repressed at the transcriptional level in most somatic cells, *TR* is constitutively expressed in human cells, and it ubiquitously assembles as a stable RNP complex [Cong *et al.*, 2002; Cairney & Keith, 2007], suggesting a non-canonical role also for *TR*. For example, the cancer promoting activity of *TR* may also occur independently of telomerase activity [Blasco *et al.*, 1996; Cayuela *et al.*, 2005; Fragnet *et al.*, 2003; Li *et al.*, 2005]. Although the mechanism involved in this activity of *TR* is largely unknown, a recent study identified 2198 *TR* binding sites in the genome using chromatin isolation by RNA purification (ChIRP), which represents a large resource to study potential non-canonical functions of human *TR* and TERT [Chu *et al.*, 2011]. *TR*

occupied multiple *Wnt* genes directly and several binding sites near the *MYC* (v-myc avian myelocytomatosis viral oncogene homolog) gene, concordant with previously documented binding sites of TERT [Chu *et al.*, 2011].

3. Telomere diseases

Telomere function is directly implicated in cellular senescence and therefore is expected to play a fundamental role in aging processes. Large epidemiological studies have reported an association between shorter telomere length in peripheral leukocytes and several inflammatory diseases of the elderly including diabetes, atherosclerosis and, recently, periodontitis [Steffens *et al.*, 2012]. To date, leukocyte telomere length (LTL) serves in many cases as a predictor of age-related diseases and mortality. The potential role of telomere attrition in the onset or evolution of chronic inflammatory diseases, although requiring further investigation, could serve as a monitor of disease progression and effectiveness of treatment schemes. Furthermore, a recent work provides preliminary evidence in humans, supporting a correlation of maternal psychological stress during pregnancy with the setting of newborn leukocyte telomere length [Entriger *et al.*, 2013].

Telomerase mutations have been detected in the context of several premature aging syndromes: dyskeratosis congenita (DC), a multisystem disorder characterized by defects in skin, blood, and lung, among other tissues [Walne & Dokal, 2008]; aplastic anemia, a hematological disorder characterized by reduced red blood cell counts, bone marrow failure and liver and lung disease [Vulliamy *et al.*, 2002]; Hoyeraal-Hreidarsson syndrome, a multisystem disorder characterized by bone marrow failure, immunodeficiency and severe growth retardation [Nishio & Kojima, 2010]; and idiopathic pulmonary fibrosis, a chronic, progressive, and fatal disease that is defined by irreversible lung fibrosis [Armanios, 2012]. The unifying molecular characteristic of these diseases is that patients harbor telomeres that are significantly shorter than age-matched control subjects [Armanios, 2009]. Telomerase mutations have also been identified in familial cases of pulmonary fibrosis and in sporadic cases of aplastic anemia. The full spectrum of telomerase mutations in human disease remains to be identified, and additional work in this area will continue to provide new insights into the pathophysiology of degenerative diseases and human aging [García *et al.*, 2007] (**Fig.12**).

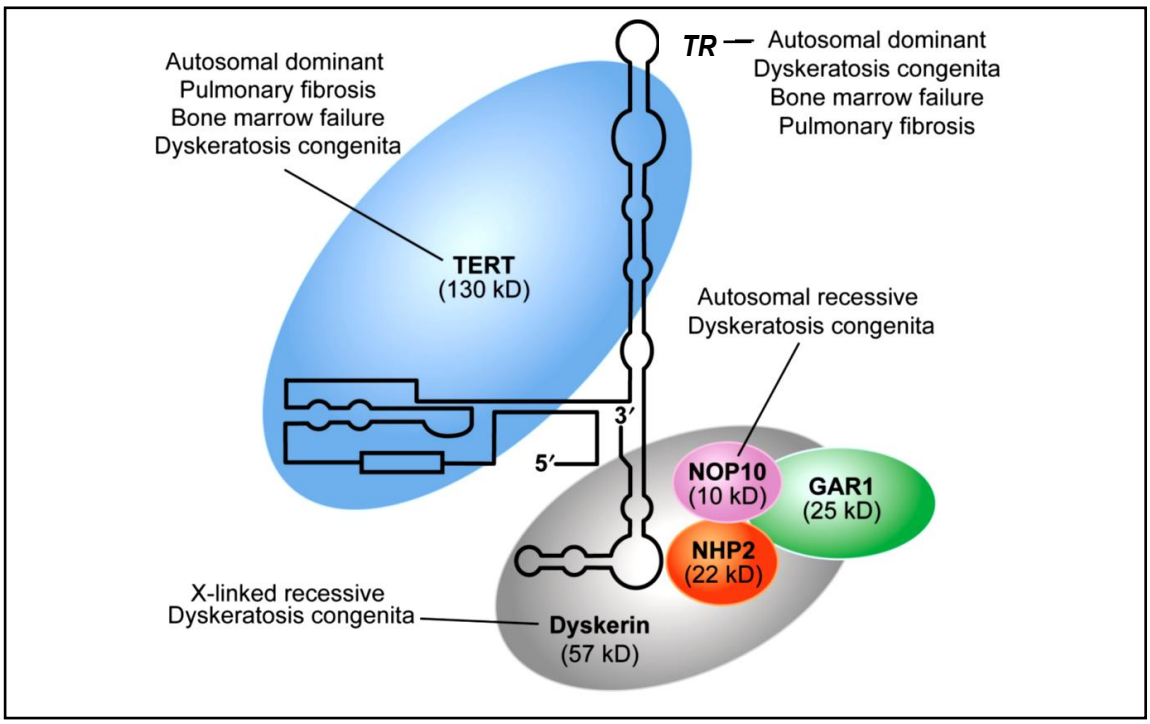

Figure 12: Schematic structure of the telomerase complex and diseases associated with mutations in the genes encoding each protein within the complex. *Adapted from García et al. (2007).*

Apart from aging and specific syndromes directly related to telomere dysfunction, abnormal telomere biology critically interferes with cancer [Prescott *et al.*, 2012]. One of the hallmarks of cancer is unlimited cell proliferation, therefore tumour cells require a telomere maintenance mechanism in order to retain the ability of infinite propagation. Telomere maintenance in cancer is achieved by two major mechanisms. In most of the cases telomere attrition in cancer cells is counteracted by telomerase upregulation [Shay, 1997] but in about 10-15% of tumour telomeres are preserved by telomerase independent mechanisms referred to as the ALT pathways which are based on homologous recombination [Royle *et al.*, 2009; Cesare & Reddel, 2010], (**Fig. 13**).

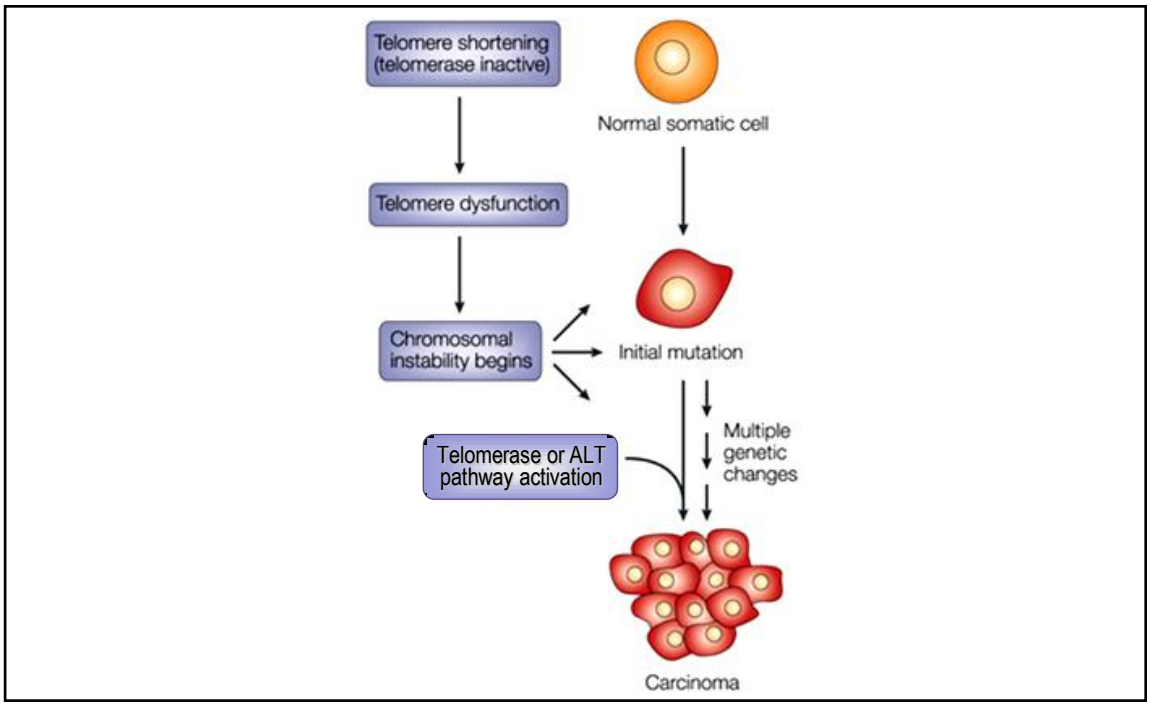

Figure 13: Telomere shortening in a simplified cancer-progression model. Normal somatic cells lose telomeric repeats as they divide in the absence of telomerase. Eventually, telomeres become dysfunctional and can cause chromosomal instability. Chromosomal instability occurs very early in tumorigenesis. It begins either before or soon after the initial mutation in a tumour suppressor or oncogene. Chromosomal instability then drives the multiple genetic changes that are required for the formation of a carcinoma. Telomerase or ALT pathway activation occurs late in tumorigenesis, increasing the replicative potential of a tumour by facilitating tumour growth. *Adapted from Feldser et al. (2003).*

The relevance of telomere shortening induced by dysfunctional telomerase to physiological aging is suggested by the phenotypes of a telomerase deficient mouse model [Blasco *et al.*, 1997; Lee *et al.*, 1998]. Early generations of mouse *TR* deficient ($mTR^{-/-}$) mice do not show abnormalities presumably because laboratory mice have a much longer telomere length (20–150 kb) than humans (5–15 kb). However, late generations of $mTR^{-/-}$ mice have defects in cell viability of highly proliferative tissues. They have a shorter life span compared with wild-type (wt) mice and show hair loss or early graying of hair, decreased capacity for wound healing and a slight increased incidence of cancer. However, the telomerase deficient mouse models may not completely mirror human diseases of telomerase dysfunction as they have longer telomeres [Blasco *et al.*, 1997; Zijlmans *et al.*, 1997], express telomerase activity in most tissues [Prowse & Greider, 1995; Martin-Rivera *et al.*, 1998] and do not use

telomere shortening as a counting mechanism [Wright & Shay, 2000]. For these reasons, an alternative animal model able to reproduce the human symptoms of telomere diseases is needed.

3.1. Dyskeratosis congenita

The first disease associated with mutations in human telomerase were identified in patients afflicted with a rare, inherited multisystem disorder called dyskeratosis congenita, DC [Walne & Dokal, 2008]. The prevalence is approximately 1 in 1,000,000 individuals, with death occurring at a median age of 16 [Drachtman & Alter, 1995]. The clinical manifestations of DC generally appear during childhood and include a monocutaneous triad of abnormal skin pigmentation, nail dystrophy and oral leukoplasia. The symptoms are accompanied by a spectrum of other somatic abnormalities such as developmental delay, premature hair loss and organ failure. Bone marrow failure is the principal cause of premature mortality, followed by pulmonary disease and cancer [Marciniak & Guarente, 2001] (**Fig.14**).

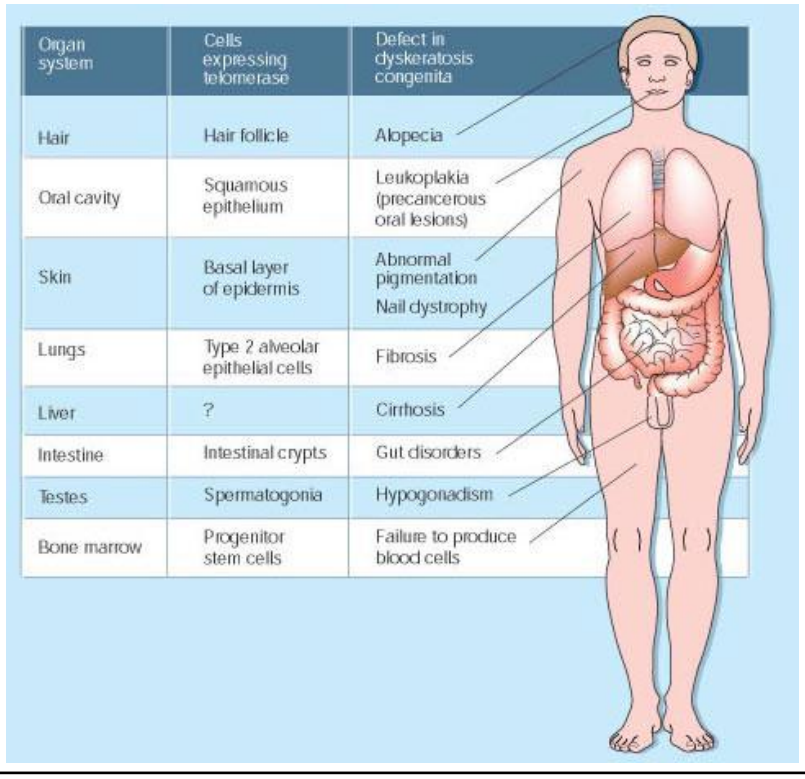

Figure 14: Characteristic of the human disease dyskeratosis congenita. Patients typically appear healthy at birth and develop the mucocutaneous features later in life as well as a wide

range of somatic abnormalities including bone marrow, pulmonary, gastrointestinal, endocrine, skeletal, urologic, immunologic and neurologic abnormalities. Bone marrow failure is the leading cause of death, followed by pulmonary disease and cancer. Defects are seen most often in tissues in which cells divide rapidly and often. *Adapted from Marciniak & Guarente (2001).*

There is evidence that all DC patients have some defects in telomere biology, and that those defects affect the renewing capabilities of hematopoietic stem cells. Furthermore, all DC causal mutations identified to date are found in telomerase components or in telomere stabilizing components [Hockemeyer *et al*., 2008; Savage *et al*., 2008; Vulliamy & Dokal, 2008; Vulliamy *et al*., 2008].

Three modes of inheritance of DC have been identified: X-linked recessive, autosomal dominant-DC and autosomal recessive-DC. In its X-linked form, DC is caused by mutations in the RNA-binding protein dyskerin, a telomerase holoenzyme component critical for stabilizing *TR* [Heiss *et al*., 1998]. Autosomal dominant forms of DC are caused by mutations in TERT and *TR*, clearly showing that the disease is caused by a failure of telomerase [Vulliamy *et al.*, 2001; Vulliamy *et al.*, 2004]. In addition, mutations in the telomere binding protein TIN2 can also cause DC and severe telomere shortening is a universal feature of the disease, further establishing telomere dysfunction as the underlying problem. Homozygosity mapping of one large consanguineous Saudi Arabian family with autosomal recessive-DC led to the identification of a homozygous missense mutation in the *NOLA3* gen (encoding the protein NOP10) that segregated with the phenotype [Walne *et al*., 2007].

Regardless of the pattern of genetic inheritance, all patients with DC have very short telomeres, implying a common pathway underlying the mechanism of this disease [Mitchell *et al.*, 1999; Vulliamy *et al*., 2004; Armanios *et al*., 2005; Vulliamy *et al*., 2001]. When patients with mutations in the *DKC1* gene (encoding dyskerin) are categorized by disease severity, those with the most severe phenotypes have shorter telomeres than those with the mildest phenotypes (age over 15 years with no coexistent aplastic anemia) [Vulliamy *et al.*, 2006]. Using the telomere flow-FISH assay and a cut off of total LTL below the first percentile, DC patients could be distinguished from their unaffected relatives with 100% sensitivity and 90% specificity [Alter *et al*., 2007]. Interestingly, DC families with mutations in either *TR* or *TERT* genes demonstrate genetic anticipation with a worsening of disease severity and an earlier onset of

symptoms with successive generations [Vulliamy *et al*., 2004; Armanios *et al*., 2005]. The onset and severity of disease correlates with progressive telomere shortening in later generations. Siblings that do not inherit the mutated *TR* gene do not have symptoms. Even though these siblings inherit short telomeres from the affected parent, the non-mutated telomerase preferentially acts on the shortest telomeres to normalize their lengths [Goldman *et al*., 2005]. Thus, DC patients have to inherit both short telomeres and have a mutation in one of the components of telomerase in order to show anticipation. Most clinical presentations of DC are associated with an impaired proliferative capacity of tissues [Dokal *et al*., 1992]. In addition, the number of hematopoietic progenitor cells is decreased in DC patients [Marsh *et al*., 1992].

4. The zebrafish as a vertebrate model

Zebrafish (*Danio rerio*) is a tropical freshwater teleost fish belonging to the Cyprinidae family, order Cypriniformes. Since it was first used in a scientific laboratory 30 years ago, its popularity in biomedical research has significantly increased due to their unquestionable advantages respect other vertebrate models: (1) As a vertebrate, zebrafish shares considerable genetic sequence similarity with humans. (2) High resistance to pathogens. (3) High fecundity and large production of embryos (around 200 eggs/female/week) makes phenotype-based forward genetics doable [Patton & Zon, 2001]. (4) Low maintenance cost, small space needed y easy to transfer among different labs by transporting their eggs. (5) Embryos are transparent and their develop following fertilization is external and fast, from embryo to larva in just three days, and to adult in three months (**Fig. 15**). (6) A variety of methods have been developed to manipulate gene function: chemical mutagenesis [Rohner *et al.*, 2011] and targeted mutagenesis [Leong *et al.*, 2011], transient gene knock down by using morpholinos [Ekker, 2004; Ekker & Larson, 2001; Nasevicius & Ekker, 2000; Sumanas & Larson, 2002], transient protein overexpression by injecting mRNA or plasmids, conditional transgene expression and generation of stable transgenic lines using zinc finger nucleases (ZFNs) [Meng *et al.*, 2008] and a transposon strategy [Kawakami, 2004], small molecules screening [Murphey & Zon, 2006], conditional targeted cell ablation [Curado *et al.*, 2007], *in vivo* cell physiology and imaging [Detrich, 2008].

The ease of accessibility and transparency of the embryo allows the effects of these manipulations to be analyzed at a cellular level of resolution unprecedented in a vertebrate model system.

All these advantages have lead to the increased interest of scientists using zebrafish as an animal model for the study of both, basic and applied science in the last years and, nowadays, zebrafish has been proposed as an excellent vertebrate model for the study of the immune system [Renshaw & Trede, 2012], hematopoiesis [Martin *et al.*, 2011], vascular development [Isogai *et al.*, 2009; Quaife *et al.*, 2012; Gore *et al.*, 2012], neurogenesis [Schmidt *et al.*, 2013] and cancer research [Mione & Trede, 2010], among others.

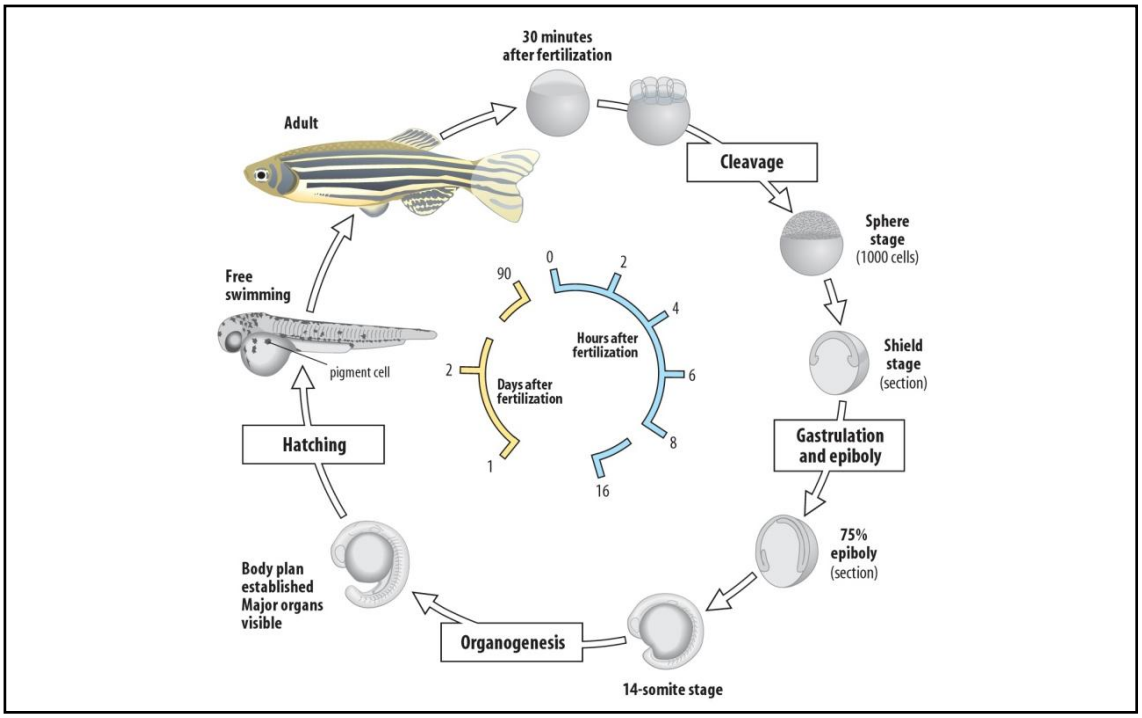

Figure 15: Schematic representation of zebrafish development from embryo to adulthood, highlighting both the speed of the development and the embryo transparency. *Adapted from www.daniorerio.com*

4.1. Hematopoiesis in the zebrafish embryo

Hematopoiesis is a vital process for invertebrate and vertebrate organisms. The ontogeny of blood cells from multiple hematopoietic organs appears to be a feature common to all organisms with multiple hematopoietic lineages [Evans *et al.*, 2003; Hartenstein & Mandal, 2006].

In the adulthood, all blood lineages come originally from the hematopoietic stem cells (HSCs), defined by their self-renewal and differentiation into all blood cell types in transplanted recipients previously irradiated. The process involves specific regulation of gene transcriptions and epigenetic modifications of genomes and includes controlling HSC homeostasis, balancing of diverse differentiated cell populations, making different cell fate decisions, and maintaining differentiated cell states. It has been supported by lineage tracing experiments in zebrafish, that HSCs are specified during embryonic development, not arising *de novo* in the adulthood [Bertrand *et al.*, 2010].

The better understandings of the regulation of hematopoietic stem cell biology and lineage differentiation is essential to improve the diagnosis and treatment of human hematopoietic disorders and bone marrow transplantation therapies.

As in all vertebrates, zebrafish also experience different waves of hematopoiesis during embryogenesis: the primitive and definitive waves of hematopoiesis [de Jong & Zon, 2005; Galloway & Zon, 2003; Chen & Zon, 2009]. These waves have been named differently regarding to the ability of the hematopoietic cells not to have or have self-renewal properties, respectively.

The primitive hematopoiesis begins at early somitogenesis stages in two intraembryonic locations called the intermediate cell mass (ICM) and the anterior lateral mesoderm (ALM). Primitive erythropoiesis is in the ICM, whereas myelopoiesis initiates in the ALM (**Fig. 16**).

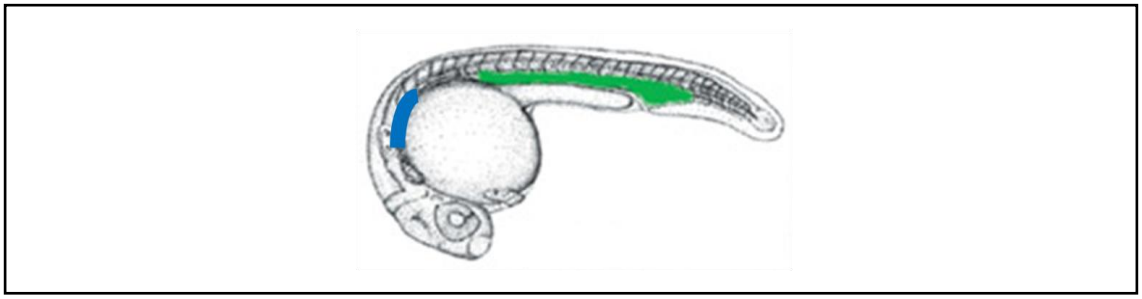

Figure 16: Sites of primitive hematopoiesis in the zebrafish embryo at 24 hpf. The ALM (in blue) gives rise to primitive macrophages, whereas primitive erythrocytes are produced at the ALM (in green).

The first wave of definitive hematopoiesis gives rise to erythromyeloid progenitors (EMPs) in the posterior blood island (PBI) of the zebrafish embryo between 24 and 48 hpf [Bertrand *et al.*, 2007]. These transient cells have erythroid and myeloid differentiation potential, but lack lymphoid potential. **The second wave of definitive hematopoiesis** starts in the floor of the dorsal aorta, at the aorta-gonad-mesonephros (AGM) at 2 days post-fertilization, giving rise to HSCs (**Fig. 17**).

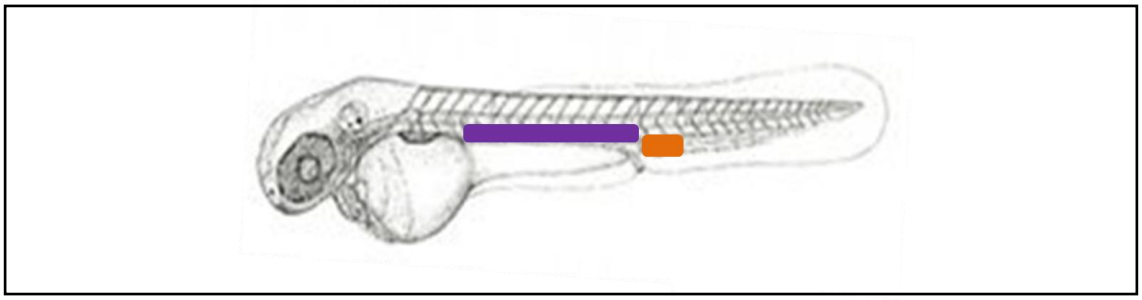

Figure 17: Sites of definitive hematopoiesis in the zebrafish embryo at 2 dpf. Between 24-48 hpf, a first wave of definitive hematopoiesis gives rise to EMPs in the PBI (in orange). From 2 dpf, the second wave of definitive hematopoiesis gives rise to HSCs in the AGM (in purple).

There are three different HSC migration and colonization events: AGM progenitor cells migrate to (1) the caudal hematopoietic tissue (CHT), which is an intermediate site of blood development; (2) the thymus, which is a site of T lymphocyte maturation; and (3) the developing kidney marrow, which is the larval and adult location for production of all hematopoietic cell types, and is comparable to the bone marrow of mammals (**Fig. 18**).

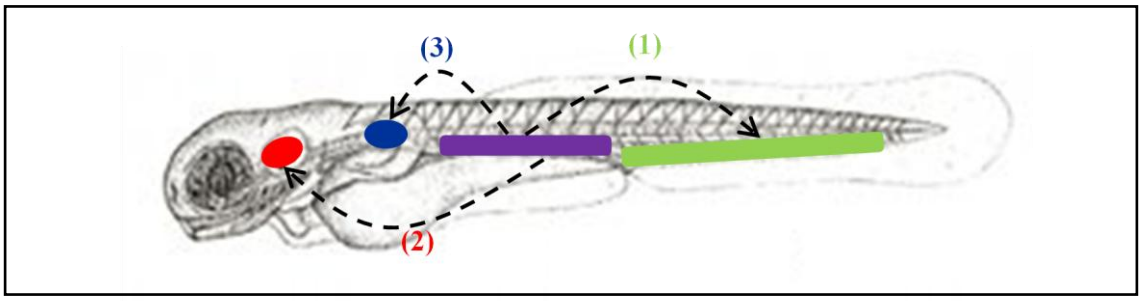

Figure 18: HSC migration and colonization events. From 3 dpf, AGM progenitor cells (in purple) migrate to: (1) the CHT (in green), (2) the thymus (in red), and (3) the kidney marrow (in blue).

4.2. Telomeres and telomerase in zebrafish

The coding sequence of zebrafish *tert* was revealed and cloned, and the expression of telomerase at mRNA, protein, and functional levels was assayed several years ago [Lau *et al.*, 2008]. Since then, the zebrafish has been considered as a potential model for aging, cancer, and regeneration studies.

In 2011, Anchelin and colleagues established the behaviour of telomere and telomerase during aging and regeneration in zebrafish, concluding that the expression of telomerase and telomere length are closely related during the entire life cycle of the fish and that these two parameters can be used as biomarkers of aging in zebrafish [Anchelin *et al*., 2011]. Thus, telomerase and telomere length are limiting for zebrafish lifespan, enabling the study of telomere shortening in naturally ageing individuals (**Fig. 19**).

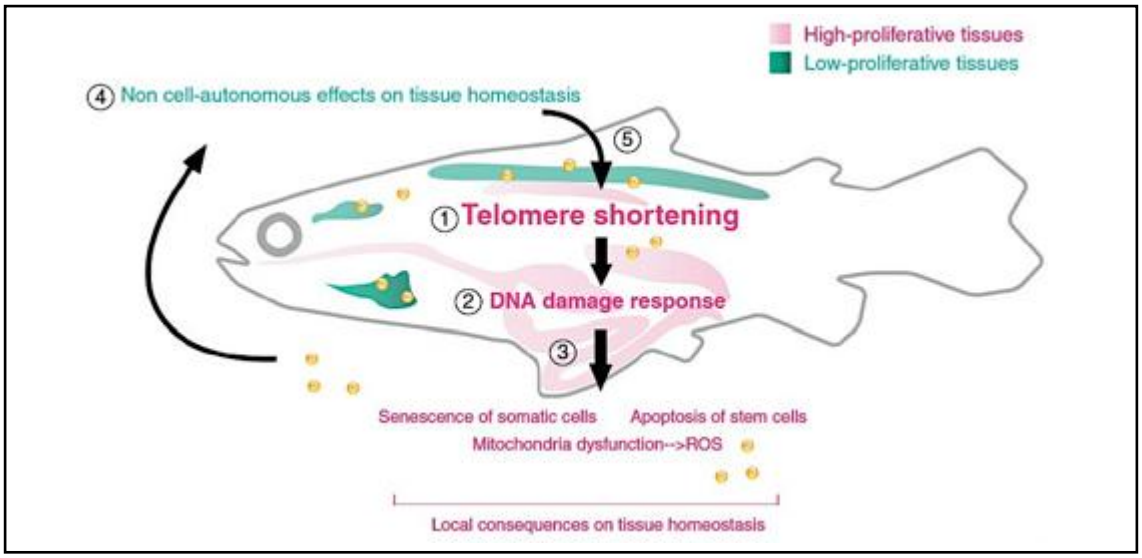

Figure 19: Tissue communication in response to telomere dysfunction. (1) Restriction of telomerase expression leads to telomere erosion throughout lifetime. (2) Organs with high-proliferative capacity, such as gonads and gut, become rate-limiting over time and initiate DDRs. (3) DDRs culminate in apoptosis of stem cells and senescence of somatic cells. Tissue homeostasis is locally perturbed both in a cell-autonomous and non-cell-autonomous manner. (4) Non-cell-autonomous signals spread to produce a systemic effect that extends to low-proliferating organs, such as the brain and muscle. (5) Systemic tissue damage leads to metabolic disorders that give rise to further reactive oxygen species (ROS) and cellular damage, thus creating a positive feedback loop capable of impairing whole body homeostasis. *Adapted from Henriques & Ferreira (2012).*

Zebrafish have restricted telomerase expression and human-like telomere length that, like these, acts as a cell division clock. Thus, the zebrafish have been established as a better model than the mouse model to study telomerase dysfunction diseases. In fact, two recent studies have determined that telomerase is required for zebrafish lifespan, as a telomerase-deficient zebrafish shows several premature aging symptoms from the first generation, like premature infertility, gastrointestinal atrophy, loss of body mass,

increased inflammation, sarcopaenia, spinal curvature, liver and retina degeneration. Furthermore, p53 was induced by telomere attrition, leading to growth arrest and apoptosis. Importantly, genetic inhibition of p53 rescued the adverse effects of telomere loss, indicating that the molecular mechanisms induced by telomere shortening are conserved from fish to mammals [Anchelin *et al*., 2013; Henriques *et al*., 2013].

Along the last two years, there have been three different zebrafish lines to study DC. The *nop10* mutant [Pereboom *et al.*, 2011], the *nola1* mutant (nola1 is the zebrafish homologous to the human GAR1 protein) and the *dkc1* morphant [Zhang *et al.*, 2012]. The three lines show hematopoietic defects mediated by p53 due to a defective 18S ribosomal RNA (rRNA) processing, but no changes in telomere length or telomerase activity are detected at the early stages of DC pathogenesis, suggesting that their role in telomere maintenance do not contribute to DC until later in life. Importantly, the *tert* mutant zebrafish line also reproduces the disease anticipation observed in humans with DC [Anchelin *et al*., 2013].

The presence of telomerase in different tissues may be associated with the indeterminate growth of teleost. However, *tert* is also expressed in teleost retinal neurons [Lau *et al*., 2008], which are post-mitotic cells that do not further divide under normal situation, suggesting that, like in humans, telomerase has functions other than the elongation of telomere. For example, zfTERT promotes the development of hematopoietic cells through a non-canonical mechanism that is independent of the authentic telomerase activity of TERT and the role of this enzyme in telomere lengthening [Imamura *et al*., 2008].

Objectives

The specific objectives of the present work are:

1. Development of a new luciferase-based reporter system for studying both constitutive and inducible promoters in the context of a whole organism.

2. Study the non-canonical role of the telomerase RNA component (*TR*) in hematopoiesis using the zebrafish.

Chapter I:

Application of the dual-luciferase reporter assay to the analysis of promoter activity in zebrafish embryos

Abstract

The dual luciferase assay has been widely used in cell lines to determine rapidly but accurately the activity of a given promoter. Although this strategy has proved very useful, it does not allow the promoter and gene function to be analyzed in the context of the whole organism. Here, we present a rapid and sensitive assay based on the classical dual-luciferase reporter technique which can be used as a new tool to characterize the minimum promoter region of a gene as well as the *in vivo* response of inducible promoters to different stimuli. We illustrate the usefulness of this system for studying both constitutive (telomerase) and inducible (NF-κB-dependent) promoters. The flexibility of this assay is demonstrated by induction of the NF-κB-dependent promoters using simultaneous microinjection of different pathogen-associated molecular patterns as well as with the use of morpholino-gene mediated knockdown. This assay has several advantages compared with the classical *in vitro* (cell lines) and *in vivo* (transgenic mice) approaches. Among others, the assay allows a rapid and quantitative measurement of the effects of particular genes or drugs in a given promoter in the context of a whole organism and it can also be used in high throughput screening experiments.

1. Introduction

The zebrafish has been established as an excellent model for studying any biological process. This organism possesses many advantages including ease of experimentation, optical clarity, drug administration, amenability to *in vivo* manipulation and feasibility of reverse and forward genetic approaches. The fish reach sexual maturity in only 3 to 4 months, and adult females are capable of producing 100 to 200 eggs weekly. Many thousands of animals can be kept in a fish facility requiring much less space than mice or other mammals, and hence the zebrafish is regarded as a cost-effective experimental vertebrate model for large-scale genetic screening [Patton & Zon, 2001]. Furthermore, the high degree of homology between the zebrafish genome and that of humans makes such discoveries especially pertinent to human disease and development [Nicoli & Presta, 2007; Pyati *et al.*, 2007].

Morpholino antisense oligonucleotides (MO) have been widely used to inhibit gene function in zebrafish embryos [Ekker, 2004; Ekker & Larson, 2001; Nasevicius & Ekker, 2000; Sumanas & Larson, 2002] and are usually used as sequence-specific translation-blocking or splicing-blocking agents. A few years ago, a quantitative assessment of the knockdown efficiency of morpholinos was performed in zebrafish embryos and its effectiveness proved [Kamachi *et al.*, 2007]. Furthermore, microinjection of DNA constructs into single-cell fertilized zebrafish embryos has also proven successful in the generation of transgenic zebrafish. The widespread use of fluorescent proteins in mammalian systems has been successfully adapted for use in zebrafish, which are well-suited to the use of fluorescence because of their optical clarity and external development. By linking a fluorescent protein such as GFP or DsRed to a gene or promoter of interest, expression can be easily visualized in living animals [Detrich, 2008].

The dual luciferase assay has been widely used in cell lines to determine rapidly and accurately the activity of a given promoter. Although this strategy has been very useful, it does not allow analysis of the promoter and gene function in the context of the whole organism. To overcome these limitations, we have developed a protocol based on the dual luciferase system in zebrafish embryos. We illustrate the usefulness of this system for studying the promoter of telomerase, a key enzyme in the fields of cancer, stem cells and aging [Blasco, 2007], and a NF-κB-dependent promoter, a master

regulator of the immune response [Kawai & Akira, 2007]. The luciferase reporter DNA plasmids were injected into zebrafish embryos at the one-cell developmental stage, together with MO or the expression constructs of interest, and the luciferase activity was determined in the time frame of MO activity (24-48 h later). In addition, the flexibility of this assay is also illustrated by activation of the NF-κB-dependent promoters by simultaneous microinjection of different pathogen-associated molecular patterns (PAMPs).

The protocol presented here is based on the methods used in our previous publication [Sepulcre *et al.*, 2009] and provides details of how to apply the dual luciferase assay to determining the activity of constitutive and inducible promoters in zebrafish embryos. This approach involves three steps: (1) cloning the promoter of interest in the firefly luciferase reporter construct, (2) microinjecting the embryos with this construct together with the appropriate *Renilla* luciferase reporter and (3) measuring the promoter activity with the dual luciferase system in whole embryo extracts. See all details in Annex I.

2. Materials and methods

2.1. Animals

Wild-type zebrafish (*Danio rerio* H. Cypriniformes, Cyprinidae) were obtained from the Zebrafish International Resource Center (ZIRC) and maintained in recirculating tanks as described in the zebrafish handbook [Westerfield, 2000]. Adult fish were maintained at 26 ºC, with a light:dark cycle of 14:10 hours and were fed twice daily, once with dry flake food (PRODAC) and once with live arthemia (MC 450, IVE AQUACULTURE). Zebrafish embryos were maintained in egg water at 28.5 ºC and were fed at 5days with NOVO TOM and with live arthemia at 11 days of life.

The experiments performed comply with the Guidelines of the European Union Council (86/609/EU) and they were approved by the Bioethical Committee of the University Hospital Virgen de la Arrixaca (Spain) under approval number (PI06/FIS0369/040706).

2.2. Microinjection

Zebrafish embryos within the one- to eight-cell developmental stage were microinjected with 0.5-1 nL of microinjecting mix containing 20 ng/μL of firefly luciferase and *Renilla* reporter plasmids (**Table I**). Add Buffer Tango 10x to a final concentration of 0.5x, and phenol red solution to a final concentration of 0.05%. When injecting morpholinos, they should be prepared to a final concentration of 1-10 μM. The injected embryos were incubated for 24-48 h at 28.5 ºC in egg water.

Table I- Reporter plasmids used in this study.

Plasmid name	Purpose	Relevant features
pEGFPLuc	Positive control for assaying the effectiveness of transfection	Kanamycin/neomycin marker. This reporter plasmid encodes a fusion of enhanced green fluorescent protein (EGFP) and luciferase from the firefly *Photinus pyralis* driven by the human CMV immediate early promoter (Clontech, Cat.# 6169-1).
plessEGFPLuc	Negative control	Kanamycin/neomycin marker. This vector was created by removing the CMV promoter of pEGFPLuc with the restriction enzymes AseI and NheI, followed by blunting of 5'-cohesive ends and autoligation.

Plasmid name	Purpose	Relevant features
zfpTERT(1/3Kb)-EGFPLuc	Determination of the zfTERT promoter activity	Kanamycin marker. This vector was created by replacing the CMV promoter of pEGFPLuc with a 1 or 3 Kb-fragment of the zebrafish telomerase promoter region.
pNF-κB::Luc	Assessment of NF-κB activation	Ampicillin marker. This vector carries a the cDNA encoding the firefly (*P. pyralis*) luciferase gene placed under the control of three synthetic copies of the κB consensus of the immunoglobulin κ-chain promoter cloned in the *Bam*HI site located upstream of the conalbumin transcription start site [Arenzana-Seisdedos *et al*., 1993].
pRL-CMV, pRL-TK and pRL-SV40	Normalization	Ampicillin marker. The pRL vectors contain the cDNA encoding *Renilla* luciferase cloned from the anthozoan coelenterate *Renilla reniformis* (sea pansy). Three different promoter configurations are available: CMV, TK and SV40.
pRL-EF1α	Normalization	Ampicillin marker. This vector was obtained by inserting the EF1α promoter in the pRL-null vector (Promega, Cat. # E2271).

2.3. Dual-luciferase reporter assay

Twenty-four to forty-eight hours after injection, collect live injected embryos and put three of them in a 1.5 mL microcentrifuge tube. Remove the egg water, wash the embryos with PBS and remove it completely. Incubate the embryos with 50 μL of PLB 1x [from the kit Dual-Luciferase Reporter Assay System (Promega, Cat.# E1910)], for 30 min at room temperature, shaking at 150 rpm. After incubation, homogenize the embryos with a pellet pestle. Spin the embryo extracts for 3 min at 13,000 rpm to remove cellular debris and measure firefly and *Renilla* luciferase activities according to the manufacturer.

2.4. Statistical analysis

Data were analyzed by analysis of variance (ANOVA) and a Tukey multiple range test to determine differences between groups. The differences between two samples were analyzed by the Student *t* test.

3. Results

3.1. Analysis of the promoter activity of zebrafish telomerase-reverse transcriptase

The protocol presented here should result in very sensitive and accurate measurement of promoter activity and analysis of gene function in the context of the whole organism, which represents an important advantage over traditional measurement in cell lines. We first illustrated the usefulness of our protocol to analyze the promoter activity of zebrafish telomerase-reverse transcriptase (zf*TERT*) (**Fig. 1**). At 24 hours post-injection (hpi), the 3 Kb fragment upstream of the zf*TERT* coding sequence was able to drive the expression of the firefly luciferase reporter, while the 1 Kb fragment failed to significantly increased the basal expression. Therefore, the relative promoter activity of each fragment could be quantitatively determined.

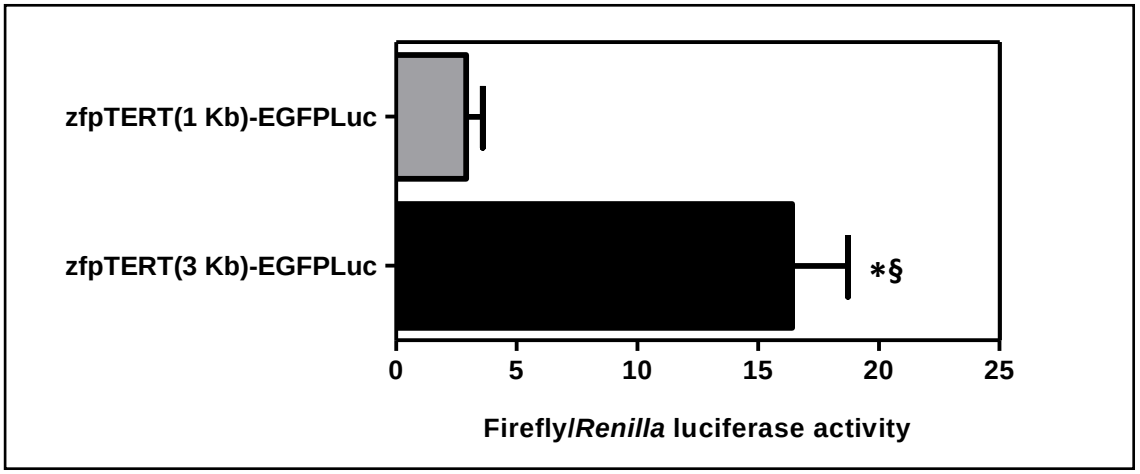

Figure 1. Analysis of zf*TERT* promoter activity in whole zebrafish embryos. Zebrafish one to eight-cell embryos were injected with plessEGFPLuc, zfpTERT(1Kb)-EGFPLuc or zfpTERT(3Kb)-EGFPLuc and the pRL-CMV (10:1) reporter vectors. Twenty-four hours after injection, the firefly and *Renilla* luciferase activity was measured using the Dual-Luciferase Reporter Assay System. The results are expressed as the mean ± SEM of normalized luciferase activity relative to plessEGFPLuc injected embryos. *$p < 0.05$ vs. plessEGFPLuc. §$p < 0.05$ vs. zfpTERT(1Kb)-EGFPLuc.

3.2. Optimization of the different *Renilla* luciferase reporter constructs

The critical step in the protocol presented here is the correct choice of the promoter used for normalization. The cytomegalovirus (CMV) immediate-early promoter is a strong promoter used for both the *in vitro* and *in vivo* expression of

proteins in signal transduction and gene therapy studies. However, CMV activity is induced by external stimuli such as endotoxin from Gram-negative bacteria (lipopolysaccharide, LPS), cytokines and phorbol esters [Ramanathan *et al.*, 2005]. Therefore, for the study of NF-κB activation, we first studied the effects of bacterial LPS and DNA in the expression of several *Renilla* luciferase reporter constructs. Among the four candidates tested, the CMV promoter was strongly induced by both PAMPs, i.e. *Escherichia coli* LPS (*Ec*LPS, strains 0111:B4 (Cat.# L4391) or 055:B5 (Cat.# L6529), from Sigma-Aldrich) and *Vibrio anguillarum* DNA (*Va*DNA, phenol-extracted genomic DNA from any bacteria), whereas the translation elongation factor EF1α promoter was inhibited by *Ec*LPS and, to some extent, by *Va*DNA. In contrast, the herpes simplex virus thymidine kinase (TK) promoter and the early SV40 enhancer/promoter region showed a more constant expression (**Fig. 2a and 2b**) and were therefore selected for further studies. Figure 2C illustrates the profound effects of the plasmid used for normalization in the measurement of the induction of NF-κB. When using *Ec*LPS, a 29 vs. 14 fold induction of NF-κB activity was obtained with the TK and the CMV promoters, respectively (**Fig. 2c**), indicating that induction of CMV by *Ec*LPS resulted in the underestimation of the NF-κB activation by this PAMP. Similarly, 21 vs. 738 fold induction of NF-κB was observed with *Va*DNA when using the SV40 and the TK promoters, respectively (**Fig. 2c**), indicating that the inhibition of the TK promoter by *Va*DNA resulted in the overestimation of the NF-κB induced by this PAMP.

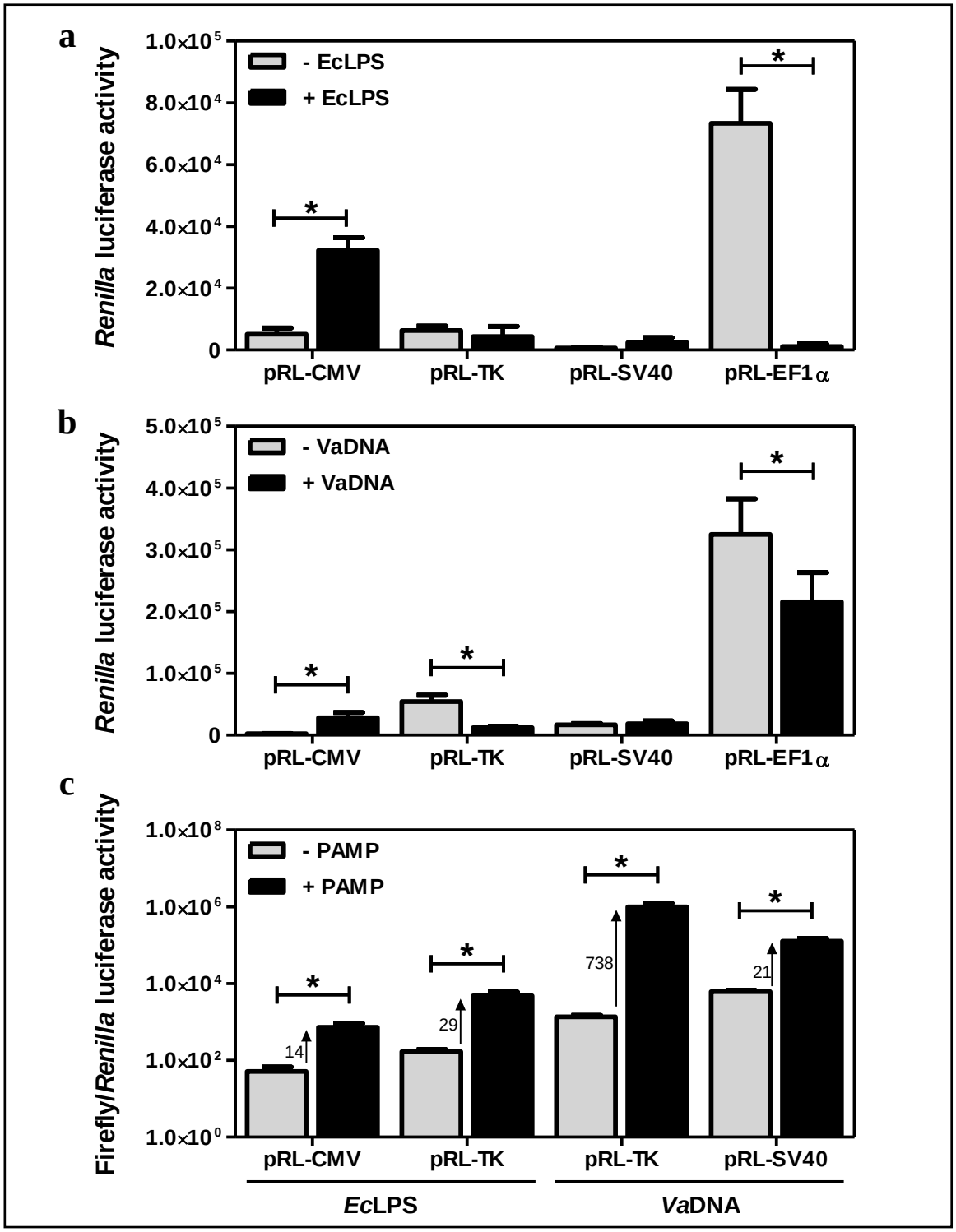

Figure 2. Optimization of the different *Renilla* luciferase reporter constructs. Zebrafish one- to eight-cell embryos were injected with 3.8 ng EcLPS **(a, c)** or 0.8 ng *Va*DNA **(b, c)** and NF-κB::Luc together with the pRL-CMV, pRL-TK, pRL-SV40 or pRL-EF1α (10:1) reporter vectors. Twenty-four hours after injection, the firefly and *Renilla* luciferase activity was measured using the Dual-Luciferase Reporter Assay System. The results are presented as the *Renilla* luciferase activity (**a, b**) or as the normalized luciferase activity (firefly/*Renilla*) (**c**). Each bar represents the mean ± SEM of ten replicate samples and the data are representative of three independent experiments. The asterisk denotes statistically significant differences between the indicated samples.

3.3. Analysis of the NF-κB signaling pathway by using MO-gene mediated knockdown

We finally validated the usefulness of this technique for studying a gene of interest by using MO-gene mediated knockdown. Figure 3 illustrates an example of the inhibition of the NF-κB activation triggered by *Va*DNA using a translation-blocking MO against MyD88 [van der Sar *et al.*, 2006], an adaptor protein involved in the downstream signalling following the engagement of bacterial DNA by its cognate receptor (TLR9) [O'neill & Bowie, 2007]. The results showed that injection of the MO against MyD88 resulted in a significant inhibition (>30%) of the NF-κB activation induced by bacterial DNA, while injection of a MO directed against TLR3, which is involved in the recognition of dsRNA [Vercammen *et al.*, 2008], failed to affect the NF-κB activation induced by bacterial DNA (**Fig. 3**).

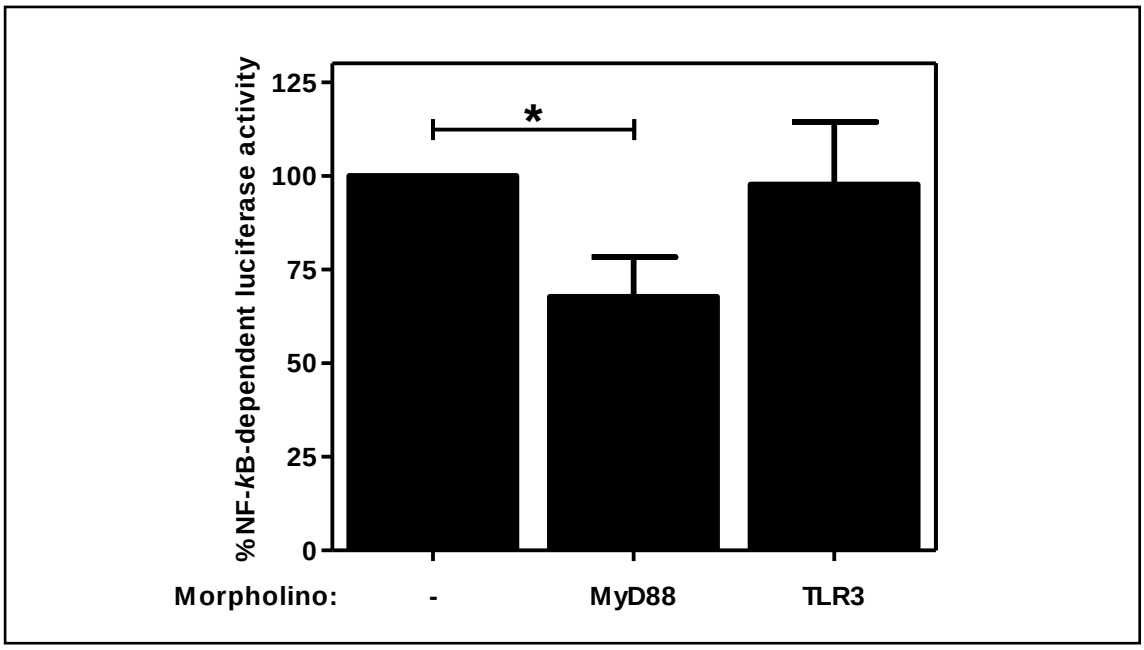

Figure 3. An example of the usefulness of MO-gene mediated knockdown in combination with the Dual-Luciferase Assay for the analysis of the NF-κB signaling pathway. Zebrafish one- to eight-cell embryos were injected with 0.8 ng *Va*DNA together with the firefly and *Renilla* reporter vectors as indicated in legend of **Figure 2** alone or in combination with 0.5 ng of the indicated morpholinos. Twenty-four hours after injection, activation of the NF-κB was measured using the Dual-Luciferase Reporter Assay System. The results are expressed as normalized luciferase activity relative to control embryos not injected with MOs. Each bar represents the mean ± SEM of ten replicate samples and the data are representative of three independent experiments. The asterisk denotes statistically significant differences between the indicated samples.

4. Discussion

The protocol presented here provides details of how to apply the dual-luciferase assay to determining the activity of both constitutive and inducible promoters in zebrafish embryos. Beyond genetics and experimental tools, the strength of the zebrafish resides in the analysis of phenotype [Patton & Zon, 2001]. Perhaps no other organism (and certainly no vertebrate) is better suited to high-throughput phenotyping. The scale that can be achieved in zebrafish experiments is impressive by vertebrate standards. Early zebrafish embryos are less than 1 mm in diameter, allowing several embryos to fit easily in a single well of a 384-well plate. Whole organisms offer several advantages over cell lines for forward chemical genetic screens, providing information on tissue specificity, toxicity and accounting for bioavailability. Furthermore, cells are not transformed and are in their normal physiological milieu of cell-cell and cell-extracellular matrix interactions [Zon & Peterson, 2005; Langheririch, 2003; Murphey & Zon, 2006]. Use of the whole organism can also allow the screening of processes that are not easily replicated *in vitro* such as organ development. The advantages of zebrafish screening over invertebrate model organisms are their closer evolutionary relationship to humans [Zon & Peterson, 2005; Langheririch, 2003; Murphey & Zon, 2006]. Therefore, the assay described here represents a promising route to the identification and validation of novel drug targets. Analysis of the promoter of newly identified genes that underlie zebrafish disease phenotypes might lead directly to the identification of novel drug targets or genes that can correct the phenotype.

Because zebrafish development occurs *ex uterus* and they have a large number of offspring, hundreds or thousands of embryos can be injected per day and the results of this assay can be obtained within 24-48 hours, although shorter time points can also be analyzed if either the mRNA coding for the gene under study or the recombinant protein are used. Although some variation was found between replicates, these can be easily avoided by the high number of technical replicates achievable. The high-fold induction of luciferase activity, together with barely detectable levels of basal expression, makes it an ideal system for the *in vivo* analysis of inducible promoters. In addition, the assay can be combined with powerful MO-gene mediated knockdown or gene over-expression to rapidly determine the functions of a particular gene (1-2 days compared with months-years needed for the generation of knockout mice). Therefore, this technique appears to be suitable for studying the activity and responses of different promoters and gene

functions as well as for the validation of genetic constructs. However, this technique does not provide spatial information on gene expression and, therefore, it might be useful as a complementary technique to *in situ* hybridization and fluorescent microscopy. To avoid this limitation, all our promoters drive the expression of a fusion of eGFP and firefly luciferase, which might allow the simultaneous determination of the expression levels and the spatial localization of the promoter under analysis.

A shortcoming of the present assay, however, is the transient expression of the constructs and, therefore, only short-term responses of promoters can be studied. For example, the adaptive immune response can not be studied with the assay since it develops after several weeks. On the other hand, we have found that normalization is absolutely required for the elimination of experimental variations. As we have found that the *Renilla* luciferase plasmid used for normalization can be induced by external stimuli, the choice of the normalization plasmid is critical. Thus, the CMV immediate-early promoter, which is commonly used for normalization in both *in vitro* and *in vivo* studies, is significantly induced by external stimuli such as endotoxin (LPS) and genomic DNA from bacteria, as previously reported in cell lines with LPS, cytokines and phorbol esters [Ramanathan *et al.*, 2005]. However, this limitation could be easily overcome using other commercial *Renilla* luciferase reporter vectors, such as those driven by the herpes simplex virus TK promoter (pRL-TK) or the early SV40 enhancer/promoter region (pRL-SV40).

We have developed a rapid and sensitive assay based on the classical dual-luciferase reporter technique which can be used as a new tool to characterize the minimum promoter region of a gene and the *in vivo* response of inducible promoters to different stimuli as well as in high throughput screening experiments. The flexibility of this assay is demonstrated by induction of the NF-κB-dependent promoters using simultaneous microinjection of different PAMPs as well as with the use of MO-gene mediated knockdown.

5. Annex I: Procedure

Microinjection

1- Prepare the microinjection mix containing 20 ng/µl of firefly luciferase and 2 ng/µl *Renilla* reporter plasmids. Add Buffer Tango 10× to a final concentration of 0.5×, and phenol red solution to a final concentration of 0.05%. When injecting morpholinos, they should be prepared to a final concentration of 1–10 µM.

CAUTION! When microinjecting exogenous molecules, such as PAMPs or drugs, check different *Renilla* reporter plasmids and select those with consistent expression.

2- Immediately after spawning, collect fertilized egg with a Pasteur pipette and place them in egg water on an agarose-modified Petri dish by means of the forceps.

CRITICAL STEP: It is very important to microinject the zebrafish embryos at early developmental stages (from one- to eight-cells) to ensure that the cytoplasmic flows introduce DNA into the cell.

3- Load glass capillaries with 1–5 µl of microinjection mix by using a 0.5–10-µl microloader tip.

4- Put the Petri dish with the fertilized eggs under a stereomicroscope at 40× magnifications and place the loaded needle toward the yolk sac, close to the embryo cell. By using the microinjector, insert the tip of the needle into the yolk and inject a 0.5–1 nl drop by setting the proper pressure (50–60 Psi) and time (10–100 ms).

5- Incubate the injected embryos for 24–48 h at 28.5°C in egg water.

Quantitative evaluation of the response with the Dual-Luciferase Reporter Assay System

6- The next day, collect live injected embryos and put three of them in a 1.5 ml microcentrifuge tube.

7- Remove the egg water, wash the embryos with PBS and remove it completely.

CAUTION! Take care during the wash because the eggs may break.

8- Incubate the embryos with 50 µl of passive lysis buffer (PLB) 1× for 30 min at room temperature, shaking at 150 rpm.

9- After incubation, homogenize the embryos with the pellet pestle.

CRITICAL STEP: From this point onwards, protect samples from light.

10- Spin the embryo extracts for 3 min at 13,000 rpm to remove cellular debris.

11- Measure firefly and *Renilla* luciferase activities according to the manufacturer.

Timing

• Step 1: 30 min. Preparation of microinjection mix.

• Step 2: 10 min. Preparation for injection of 100 zebrafish embryos.

• Steps 3–5: 15 min. Microinjection of 100 zebrafish embryos.

• Steps 6–11: 2 h. Quantitative evaluation of the response of 100 zebrafish embryos with the Dual-Luciferase Reporter Assay System.

Chapter II:

A non-canonical function of telomerase RNA in the regulation of developmental myelopoiesis in zebrafish

Abstract

Dyskeratosis congenita (DC) is an inherited disorder with mutations affecting telomerase or telomeric proteins. DC patients usually die of bone marrow failure. Here, genetic depletion of the telomerase RNA component (*TR*) in the zebrafish results in impaired myelopoiesis, despite normal development of hematopoietic stem cells (HSCs). The neutropenia caused by *TR* depletion is independent of telomere length and telomerase activity. Genetic analysis shows that *TR* modulates the myeloid-erythroid fate decision by controlling the levels of the master myeloid and erythroid transcription factors *spi1* and *gata1*, respectively. The alteration in levels occurs through stimulation of *gcsf* and *mcsf*. Our model of *TR* deficiency in the zebrafish illuminates the non-canonical roles of *TR*, and could establish therapeutic targets for DC.

1. Introduction

Telomerase is a RNA-dependent DNA polymerase that synthesizes telomeric repeats at the end of eukaryotic chromosomes [Blackburn, 2005]. This enzyme complex consists of a catalytic protein with a telomere-specific reverse transcriptase activity (TERT), an internal RNA template (*TR*) and a number of associated proteins [Hodes *et al.*, 2002]. Telomerase is essential for the lifelong maintenance of multiple cells, including hematopoietic stem cells (HSCs) [Allsopp *et al.*, 2002]. Traditionally, telomerase alterations have been associated to cancer and aging. TERT, *TR* or both components are also involved in some rare human diseases. For example, heterozygous mutations of human *TR* and *TERT* genes have been described in patients with acquired aplastic anemia and the autosomal dominant form of dyskeratosis congenita (DC) [Kirwan & Dokal, 2009; Trahan & Dragon, 2009] and in patients with idiopathic pulmonary fibrosis [Tsakiri *et al.*, 2007].

Dyskeratosis congenita (DC) is an inherited disorder characterized by a variety of phenotypes but patients usually die of bone marrow failure [Vulliamy & Dokal, 2008]. DC patients show signs of premature aging and they are more susceptible to develop cancers. All DC patients have some defects in telomere biology and that those defects affect the renewing capabilities of HSCs [Brummendorf & Balabanov, 2006; Drummond *et al.*, 2007]. All mutations identified to date in DC patients are found in telomerase components or in telomere stabilizing components [Vulliamy & Dokal, 2008]. Although mutations in both *TR* and *TERT* genes act as autosomal dominant due to an haploinsufficiency of telomerase and show disease anticipation associated with progressive telomere shortening [Vulliamy *et al.*, 2004], the presentation of the disease is more serious in patients with mutations affecting *TR* [Vulliamy & Dokal, 2008].

Besides its telomere lengthening function, there is increasing evidence that TERT can have physiological roles that are independent of this central function in both mammals [Choi *et al.*, 2008; Geserick & Blasco, 2006; Stewart *et al.*, 2002; Sarin *et al.*, 2005; Park *et al.*, 2009] and zebrafish [Imamura *et al.*, 2008]. Zebrafish telomerase promotes the development of hematopoietic cells through a non-canonical mechanism that is independent of the authentic telomerase activity of TERT and the role of this enzyme in telomere lengthening [Imamura *et al.*, 2008]. The cancer promoting activity of *TR* may occur independently of telomerase activity [Blasco *et al.*, 1996; Cayuela *et*

al., 2005; Fragnet *et al.*, 2003; Li *et al.*, 2005]. Although the mechanism involved in this activity of *TR* is largely unknown, a recent study identified 2198 *TR* binding sites in the genome using chromatin isolation by RNA purification (ChIRP), which represents a large resource to study potential non-canonical functions of *TR* RNA and telomerase [Chu *et al.*, 2011]. *TR* occupied multiple *Wnt* genes directly and several binding sites near the *MYC* gene, concordant with previously documented binding sites of *TERT* [Chu *et al.*, 2011].

In the present study, we have taken advantage of the easy genetic manipulation and transparency of zebrafish embryos, together with the availability of several transgenic lines with labeled blood cells, to identify a non-canonical role of *TR*. Genetic inhibition of *TR* demonstrated normal emergence of HSCs, but there was an alteration of cell fate. The change in developmental myelopoiesis occurred through the regulation of the master myeloid and erythroid transcription factors *spi1* and *gata1*. The alteration in levels of these transcription factors was controlled by stimulation of granulocyte- and macrophage-colony stimulating factors. Telomere length in the *TR* deficient animals was surprisingly normal. Our studies identify a cell fate change established by a non-canonical role for *TR*.

2. Materials and methods

2.1. Animals

Zebrafish (*Danio rerio* H., Cypriniformes, Cyprinidae) were obtained from the Zebrafish International Resource Center and mated, staged, raised and processed as described [Westerfield, 2000]. The *tert* mutant line (allele hu3430) was obtaining from the Sanger Institute and has been previously described [Anchelin *et al*., 2013; Henriques *et al*., 2013]. The *casper* mutant [White *et al.*, 2008] and Tg(*gata1*:DsRed) [Traver *et al.*, 2003] lines were previously described. The transgenics lines Tg(*lyz*::DsRed) [Hall *et al.*,2007], Tg(*mpx*::eGFP) [Renshaw *et al.*,2006], Tg(*mpeg1*::GAL4/*uas*::NTRmCherry) (*mpeg1*::mCherry was used throughout this manuscript for clarity) [Ellett *et al*., 2011] and Tg(*cd41*::eGFP) [Ma *et al*., 2011] were kindly provided by Drs. P. Crosier, S. Renshaw , G. Lieschke and RI Handin, respectively.

The experiments performed comply with the Guidelines of the European Union Council (86/609/EU). Experiments and procedures were performed as approved by the Bioethical Committee of the University Hospital "Virgen de la Arrixaca" (Spain) and by the Children's Hospital Boston institutional Animal Care and Use Committee (USA).

2.2. Morpholino and RNA microinjection

Specific morpholinos (MOs) (Gene Tools) were resuspended in nuclease-free water to 1mM (**Table I**). *In vitro*-transcribed RNA was obtained following manufacturer's instructions (mMESSAGE mMACHINE kit, Ambion). Both MOs and mRNA were mixed in microinjection buffer (0.5x Tango buffer and 0.05 % phenol red solution) and microinjected into the yolk sac of one- to eight-cell-stage embryos using a microinjector Narishige IM300 (0.5-1 nL per embryo). The amount of injected RNA is indicated in each figure. The same amount of MOs and RNA were used in all experimental groups.

Table I: Specific morpholinos used in this study.

Morpholino	Sequence (5'→3')	Recognized region	Supposed effect	Working dosis (ng/egg)	Reference
standard (stdMo)	CCTCTTACCTCA GTTACAATTTATA	None	Negative control.	variable	-
TRMo1	AAGAAGCGTTAG GGTTAGAGAAAGT	Recognizes the template region in the pseudoknot/template domain of *TR*.	Blocks the template region, preventing the telomerase activity.	0.5	This study
TRMo2	TCAAGTTAATCT GCTCAGTGTTGTG	Recognizes the Box H motif in the ScaRNA domain of *TR*.	Blocks the dyskerin recognition site, preventing the efficient *TR* stabilization and localization, and the telomerase activity.	1	This study
TRMo3	AGCCGAACTCTT GGCGGCAGTCAAA	Recognizes the P6 and P6.1 helices in the CR4/CR5 domain of *TR*.	Blocks the CR4/CR5 domain, preventing the efficient binding and assembly of *TR* to the TERT protein and the telomerase activity.	4.8	This study
gata1Mo	GTTTGGACTCAC CTGGACTGTGTCT	Recognizes the first exon/intron boundary of *gata1a* gene.	Blocks the splicing of *gata1a* mRNA.	3.4	Galloway *et al.*, 2005
spi1Mo	GATATACTGATA CTCCATTGGTGGT	Recognizes the start codon of *spi1* gene.	Blocks translation of *spi1*	8	Rhodes *et al.*, 2005

2.3. Analysis of development

The effect of MOs on development was evaluated as previously reported [Kimmel *et al.*, 1995]. Briefly, it was recorded the side-to-side flexures at 22 hours post-fertilization (hpf) (25-26 somites stage); heartbeat, red blood cells on yolk and early pigmentation in retina and skin at 24 hpf (Prim 5 stage); head trunk angle (HTA), retina pigmented, weak circulation, early touch reflect and straight tail and caudal artery halfway to end of tail at 30 hpf (Prim 15 stage); and early motility, tail pigmentation, strong circulation, and caudal artery ¾ of the way to the end of tail at 36 hpf (Prim 30 stage).

2.4. Neutrophil staining

Zebrafish embryos of different ages were fixed overnight at 4 ºC in 4% paraformadehyde (PFA). Fixed larvae were briefly washed twice in PBS. Larvae were incubated in 1:50 TSA Cyanine5 (TSA^{TM}-Plus Fluorescein kit, Perkin Elmer, UK) without light for 10 min at 28°C. Larvae were re-fixed for 20 minutes and endogenous peroxidase activity quenched with an hour incubation in 0.3% H_2O_2. Fluorescein-labeled neutrophils were then counted under an epifluorescence Lumar V12 stereomicroscope equipped with a digital camera (AxioCam MRm) (Zeiss).

2.5. Embryo blood collection and staining

Blood cells were collected by cardiac puncture on anesthetized embryos in a solution of 0.02% tricaine (Sigma), 1% bovine serum albumin (BSA) in phosphate buffered saline (PBS), pH 7.4. Collected cells were immediately spread on glass slides, allowed to air dry, fixed in methanol for 30 seconds and stained by the Wright-Giemsa method [Imamura *et al.* 2008].

2.6. o-dianisidine staining

Embryos were anesthetized with Tricaine at 2 dpf and stained with 1mg/ml o-dianisidine (Sigma) in staining buffer (40% ethanol, 10mM NaAc, 0.675% H_2O_2) for 15 minutes in the dark. Embryos were imaged using a Scope.A1 stereomicroscope equipped with a digital camera (AxioCam ICc 3, Zeiss).

2.7. Flow cytometry

Two- and three-day tg(*mpx*:eGFP) larvae (300-600) were anesthetized in tricaine, minced with a razor blade, incubated at 28°C for 30 min with 0.077 mg/mL Liberase (Roche) and the resulting cell suspension passed through a 40 µm cell strainer. eGFP^{+} cells were then sorted using a staff-operated Beckman Coulter MoFlo Legacy Cell Sorter at the Bauer Core of the University of Harvard.

2.8. Telomerase activity assay

A real-time quantitative telomeric repeat amplification protocol (Q-TRAP) analysis was performed as described [Herbert *et al.*, 2006] with slight modifications [Anchelin *et al.*, 2011]. Data were collected and converted into Relative Telomerase Activity units performing the calculation: RTA of sample $=10^{(Ct\ sample-\gamma int)/slope}$. The standard curve obtained was: y= -3.2295x + 23.802.

2.9. Q-FISH

A quantitative fluorescence *in situ* hybridization (Q-FISH) on interphasic blood cells collected as described above from 3 days post-fertilization (dpf) larvae was performed as described in Canela *et al.* (2007). Cy3 and DAPI images were captured with 100X and 60X objectives respectively using a Nikon Digital Camera DXM 1200C on a Nikon Direct Eclipse fluorescence microscope. Telomere fluorescence signals were quantified using the TFL-TELO program (from Peter Lansdorp, Vancouver, Canada).

2.10. Recruitment assay

At 3 dpf, *mpx*:eGFP larvae were anesthetized in tricaine and complete transection of the tail was performed with a disposable sterile scalpel. Then, they were mounted in 1% (wt/vol) low-melting-point agarose dissolved in egg water. The success of transection was confirmed immediately through an epifluorescence Lumar V12 stereomicroscope equipped with green fluorescent filters. Each larva/image was imaged at transection, which was established as time zero. Thereafter, images were captured at the selected times while animals were kept in their agar matrixes with the added medium at 28.5 °C. All images were acquired with the integrated camera on the stereomicroscope and were used for subsequently counting the number of neutrophils recruited to the wound area, established between the arterio-venous loop and the end of the tail.

2.11. Bacterial infection assay

Larvae were infected with ~10 CFU/larvae of wild type strain 12023 of *Salmonella enterica serovar Typhimurium* (*S. typhimurium*) kindly provided by Prof.

DW Holden. Briefly, bacteria were injected in the Duct of Cuvier of 2 dpf larvae and then monitored every 24 hours over a 5-day period for clinical signs of disease and mortality [van der Sar *et al.*, 2003].

2.12. Whole-mount RNA *in situ* hybridization

Transparent *Casper* embryos were used for this assay. Whole-mount RNA *in situ* hybridization (WISH) was carried out as described [Thisse *et al.*, 1993]. *TR, tert*, *lmo2*, *spi1* (*pu.1*), *gata1*, *gcsfr*, *cmyb*, *runx1* and *rag1* RNA probes were generated using the DIG RNA Labeling Kit (Roche Applied Science) from linearized plasmids. Embryos were imaged using a Scope.A1 stereomicroscope equipped with a digital camera (AxioCam ICc 3, Zeiss).

2.13. Analysis of gene expression

Total RNA was extracted from whole embryos/larvae or sorted cell suspensions with TRIzol reagent (Invitrogen) following the manufacturer's instructions and treated with DNase I, amplification grade (1 U/μg RNA; Invitrogen). SuperScript III RNase H Reverse Transcriptase (Invitrogen) was used to synthesize first-strand cDNA with oligo(dT)18 (for all genes but *TR*) or R1 (for *TR*) primers from 1 μg of total RNA at 50°C for 50 min. Real-time PCR was performed with a MyiQ™ instrument (BIO-RAD) using SYBR® Premix Ex Taq™ (Perfect Real Time) (Takara). Reaction mixtures were incubated for 10 min at 95°C, followed by 40 cycles of 15 s at 95°C, 1 min at 60°C, and finally 15 s at 95°C, 1 min at 60°C, and 15 s at 95°C. For each zebrafish mRNA, gene expression was normalized to the ribosomal protein S11 (*rps11*) content in each sample using the comparative *Ct* method ($2^{-\Delta\Delta}Ct$). The primers used are shown in **Table II**. In all cases, each PCR was performed with triplicate samples and repeated at least with two independent samples.

Table II: Gene accession numbers and primer sequences used for gene expression analysis.

Species	Gene	Accession number	Name	Sequence (5'-3')
Zebrafish				
	rps11	NM_213377	F1 R1	ACAGAAATGCCCCTTCACTG GCCTCTTCTCAAAACGGTTG
	TR	EF569636	F1 R2 R1	**GGTCTCACAGGTTTGGCTGT** **TGCAGGATCAGTGTTTGAGG** **GGCGTATTTGCAGGATCAGT**
	tert	NM_001083866	F2 R1	CGGTATGACGGCCTATCACT TAAACGGCCTCCACAGAGTT
	spi1	NM_198062	F1 R1	**TGTTACCCTCACAACGTCCA** **GCAGAAGGTCAAGCAGGAAC**
	gata1a	NM_131234	F1 R1	CGTTGGGTGTCCCCCGGTCT ACGAGGCTCGGCTCTGGACG
	gcsf (*csf3*)	FM174388	F1 R1	TGAAGCAACGACCCTGTCGCA CCGCGGCCTCAGTCTGGAAA
	mcsf (*csf1a*)	NM_001114480	F1 R1	AGCCCACAAAGCCAAGGTAA CTGACGCTCTGTGAAGGTGT
Human				
	GAPDH	NM_002046	QT01192646	*QuantiTect Primer Assay (QIAGEN)*
	TR	NR_001566	F3 R3	CCCTAACTGAGAAGGGCGTA GCTCTAGAATGAACGGTGGAA
	TERT	NM_003219	F1 R1	TGACACCTCACCTCACCCAC CACTGTCTTCCGCAAGTTCAC

2.14. Analysis of *gcsf* gene promoter activity

A 2Kb genomic DNA sequence upstream of *gcsf* +1 position was amplified using the following primers: forward 5´ CAGTGTTGTGGTTTTGGTCCAGGCG 3´ and reverse 5´ CCGGACACCGAGCACCGGCGAGCCGCC 3´. The DNA fragment was cloned in the SmaI site of the pGL3basic vector (Promega) driving the expression of firefly luciferase gene (*gcsf*::Luc). One-to-eight-cell-stage embryos were microinjected in the yolk with 0.5-1 nL of a mix containing 20 ng/µl of the firefly luciferase construct, 2 ng/µl of *Renilla* luciferase plasmid, 1 ng/egg of stdMo and TRMo2 morpholinos or 200 pg/egg of *in vitro*-transcribed *TR* RNA. After 48 hours, tail sections of at least 50 larvae were obtained, pooled and assayed for luciferase activity as previously described [Alcaraz-Pérez *et al.*, 2008].

2.15. Statistical analysis

Data were analyzed by analysis of variance (ANOVA). The differences between two samples were analyzed by the Student *t*-Test. A log rank test was used to calculate the statistical differences in the survival of the different experimental groups.

3. Results

3.1. *TR* deficiency impairs telomerase activity but does not alter development

To study the role of telomerase RNA component (*TR*) in hematopoiesis, we used antisense morpholino (MO)-mediated knockdown technology in zebrafish embryos. Three different MOs were designed, each one targeting a different domain of *TR*, namely the template, CR4/CR5 and ScaRNA domains (**Fig. 1, Table I**).

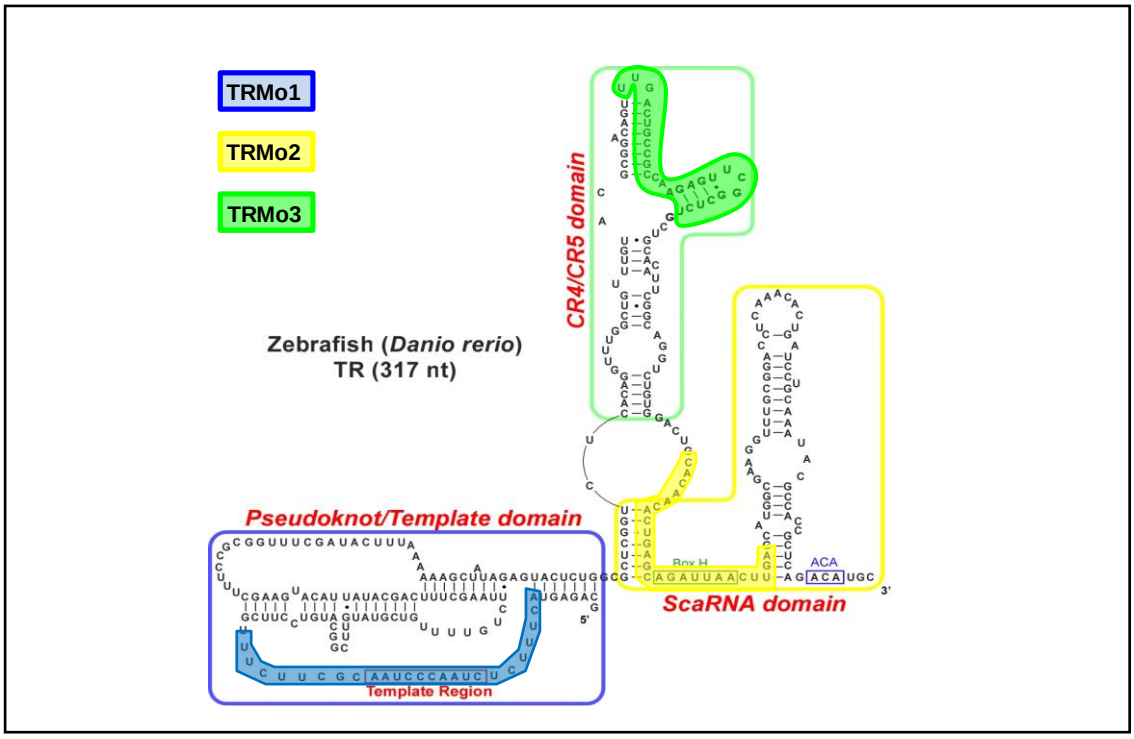

Figure 1: Scheme showing the location of the different MOs against *TR*. This figure is adapted from [Xie *et al.*, 2008].

The efficiency of these MOs was assayed by Q-TRAP, which has been reported to be a rapid and accurate assay for the quantification of telomerase activity [Herbert *et al.*, 2006]. In each case, there was impaired telomerase activity (**Fig. 2**), yet none of the MOs significantly affected zebrafish survival for up to 5 days (**Fig. 3**) nor altered development (**Table III**).

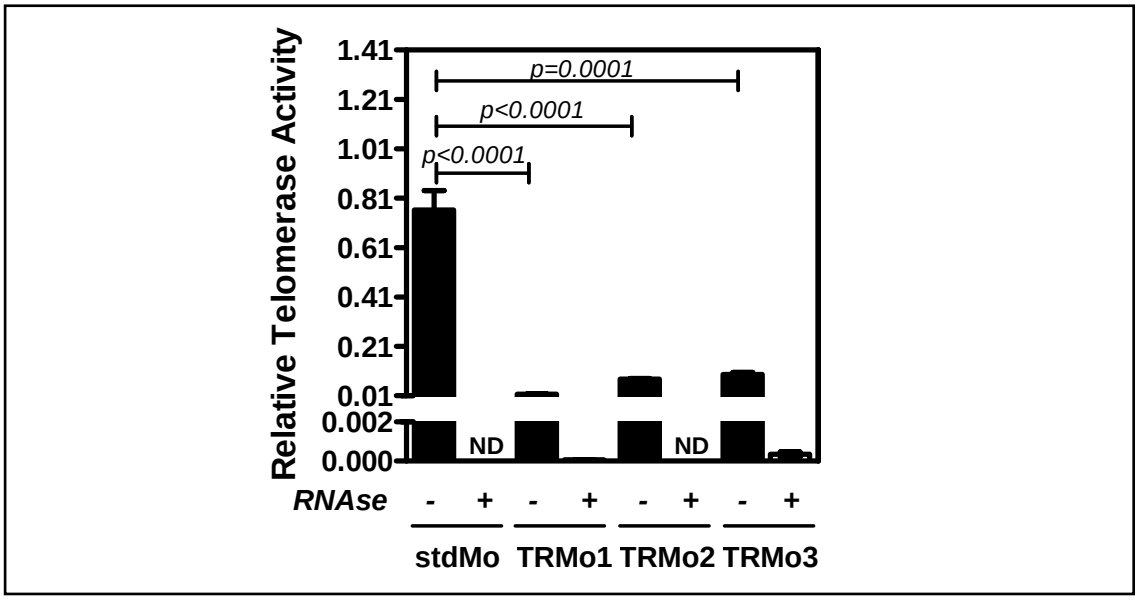

Figure 2: Assessment the efficiency of MOs by Q-TRAP. Zebrafish embryos were microinjected at the one-cell stage with stdMo or the three different MOs against *TR*. At 3 dpf, telomerase activity was measured in 100 pooled zebrafish larvae using 1 µg of protein extract. The specificity of the assay was confirmed using negative control samples that were treated with 1 µg of RNAse at 37 ºC for 20 min. Results are expressed as the mean ± SEM from triplicate samples. Statistical significance was assessed using the Student's *t*-Test ($p<0.05$). ND: not detected.

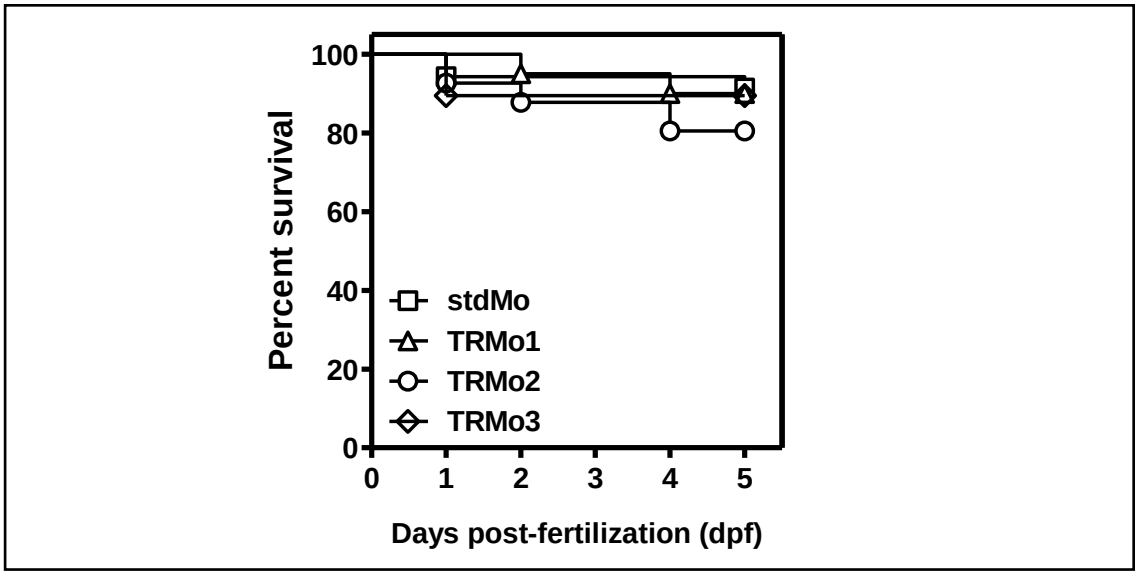

Figure 3: Study of the effect of MOs in survival. Kaplan-Meier representation of the survival of three genetic backgrounds. The survival curves were not statistically different, log rank test $p>0.05$. stdMo, n=35; TRMo1, n=20; TRMo2, n=41; TRMo3, n=38.

Table III: Study of the effect of MOs in development.

	Developmental stage			
Morphant	**Prim 3 (22 hpf)**	**Prim 5 (24 hpf)**	**Prim 15 (30 hpf)**	**Prim 30 (36 hpf)**
std (n=31)	Side-to-side flexures Yes Otoliths Yes	Heartbeat Yes Red blood cells on yolk Yes Pigmentation in retina/skin Yes	HTA 95° Early touch reflect Yes Straight tail Yes Retina pigmented Yes Weak circulation Yes Caudal artery halfway to end of tail Yes	Early motility Yes Tail pigmentation Yes Strong circulation Yes Caudal artery is ¾ of the way to the end of tail Yes
TR1 (n=25)	Side-to-side flexures Yes Otoliths Yes	Heartbeat Yes Red blood cells on yolk Yes Pigmentation in retina/skin Weak	HTA 95° Early touch reflect Yes Straight tail Yes Retina pigmented Yes Weak circulation Yes Caudal artery halfway to end of tail Yes	Early motility Yes Tail pigmentation Yes Strong circulation Yes Caudal artery is ¾ of the way to the end of tail Yes
TR2 (n=31)	Side-to-side flexures Yes Otoliths Yes	Heartbeat Yes Red blood cells on yolk Yes Pigmentation in retina/skin Yes	HTA 95° Early touch reflect Yes Straight tail Yes Retina pigmented Yes Weak circulation Yes Caudal artery halfway to end of tail Yes	Early motility Yes Tail pigmentation Yes Strong circulation Yes Caudal artery is ¾ of the way to the end of tail Yes
TR3 (n=22)	Side-to-side flexures Yes Otoliths Yes	Heartbeat Yes Red blood cells on yolk Yes Pigmentation in retina/skin Weak	HTA 95° Early touch reflect Yes Straight tail Yes Retina pigmented Yes Weak circulation Yes Caudal artery halfway to end of tail Yes	Early motility Yes Tail pigmentation Yes Strong circulation Yes Caudal artery is ¾ of the way to the end of tail Yes

3.2. *TR* deficiency induces neutropenia but does not compromise neutrophil functionality

Although *TR* knockdown with three different MOs had no obvious effect on development, blood cell formation and circulation, we analyzed in more detail the number of neutrophils of zebrafish larvae at 3 dpf using a Tyramide Signal Amplification (TSA) staining assay for detection of myeloperoxidase (Mpx) [Loynes *et al.*, 2010], which is a specific marker of zebrafish neutrophils [Renshaw *et al.*, 2006]. Interestingly, the three *TR* morphants showed a marked neutropenia compared with the control group (**Fig. 4**).

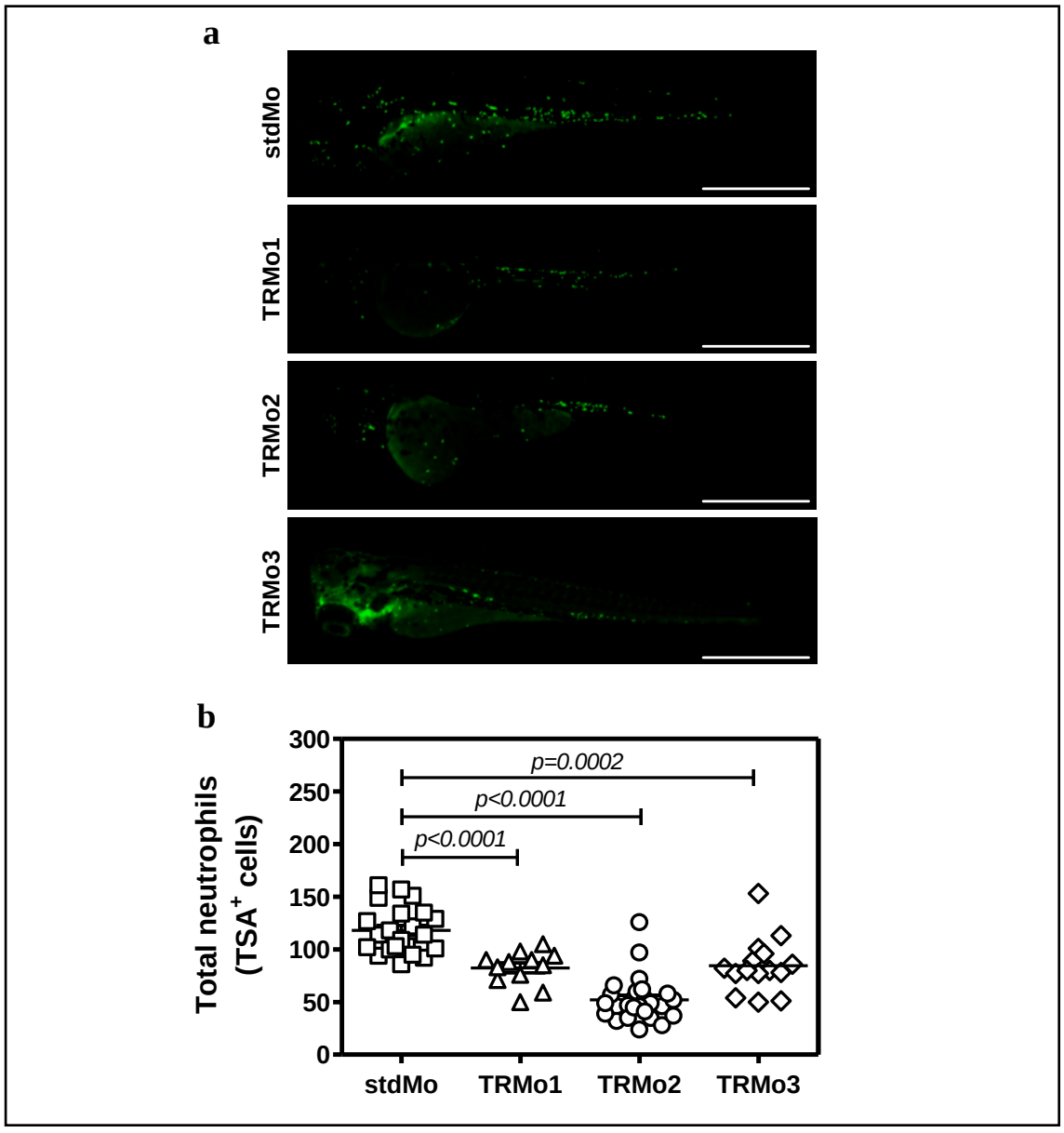

Figure 4: The three *TR* morphants showed neutropenia. Zebrafish embryos were microinjected at the one-cell stage with MOs. (**a**) At 3 dpf, neutrophils were stained using the TSA kit and visually quantified from high-quality pictures, scale bar: 1mm. (**b**) The three *TR* mophants showed a marked neutropenia compared with the control group. Each symbol in graph represents one larva and the mean ± SEM is also indicated. Statistical significance was assessed using the Student's *t*-Test ($p<0.05$).

From now on, once checked that the three MOs led to the same phenotype, we continued the study with the morpholino TRMo2, since it is similar to a *TR*-deficient animal because is directly implicated in the stabilization and location of *TR*, and we limited the counting area to the PBI or the CHT, depending on the age.

To rule out that *TR* deficiency directly affected the expression or activity of Mpx, rather than neutrophil development and maintenance, we directly counted the number of lysozyme (lyz) positive cells in the tg(*lyz*:DsRed) line, which has red fluorescent neutrophils [Hall *et al.*, 2007], and neutropenia was also evident (**Fig. 5**).

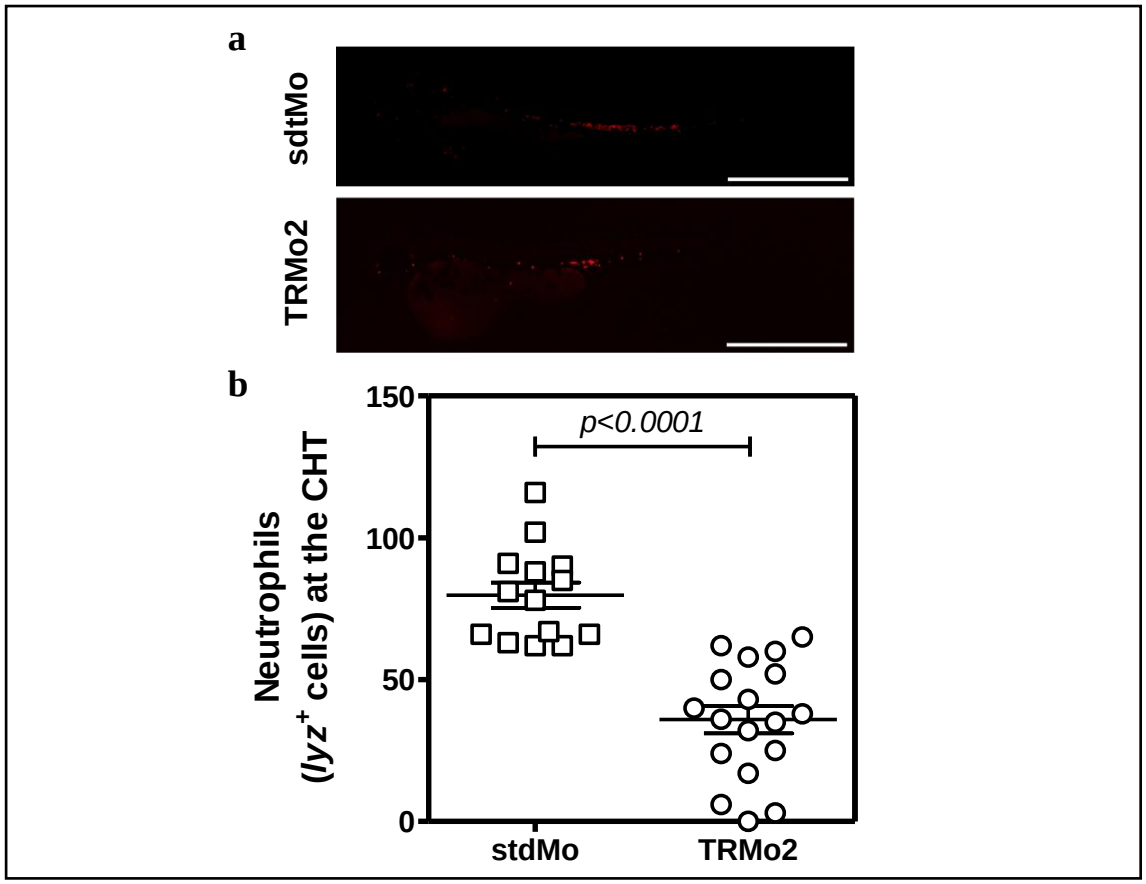

Figure 5: The absence of *TR* triggered neutropenia. Tg(*lyz*:DsRed) zebrafish embryos were microinjected at the one-cell stage with MOs. (**a**) At 3 dpf, neutrophils at the CHT were visually quantified from high-quality pictures, scale bar: 1mm. (**b**) The *TR* mophant showed a marked neutropenia compared with the control group. Each symbol in graph represents one larva and the mean ± SEM is also indicated. Statistical significance was assessed using the Student's *t*-Test ($p<0.05$).

To examine if macrophages were affected, a tg(*mpeg1*:mCherry) line was used that has red fluorescent macrophages [Ellett *et al.*, 2011]. The number of macrophages was also reduced in *TR*-deficient larvae (**Fig. 6**).

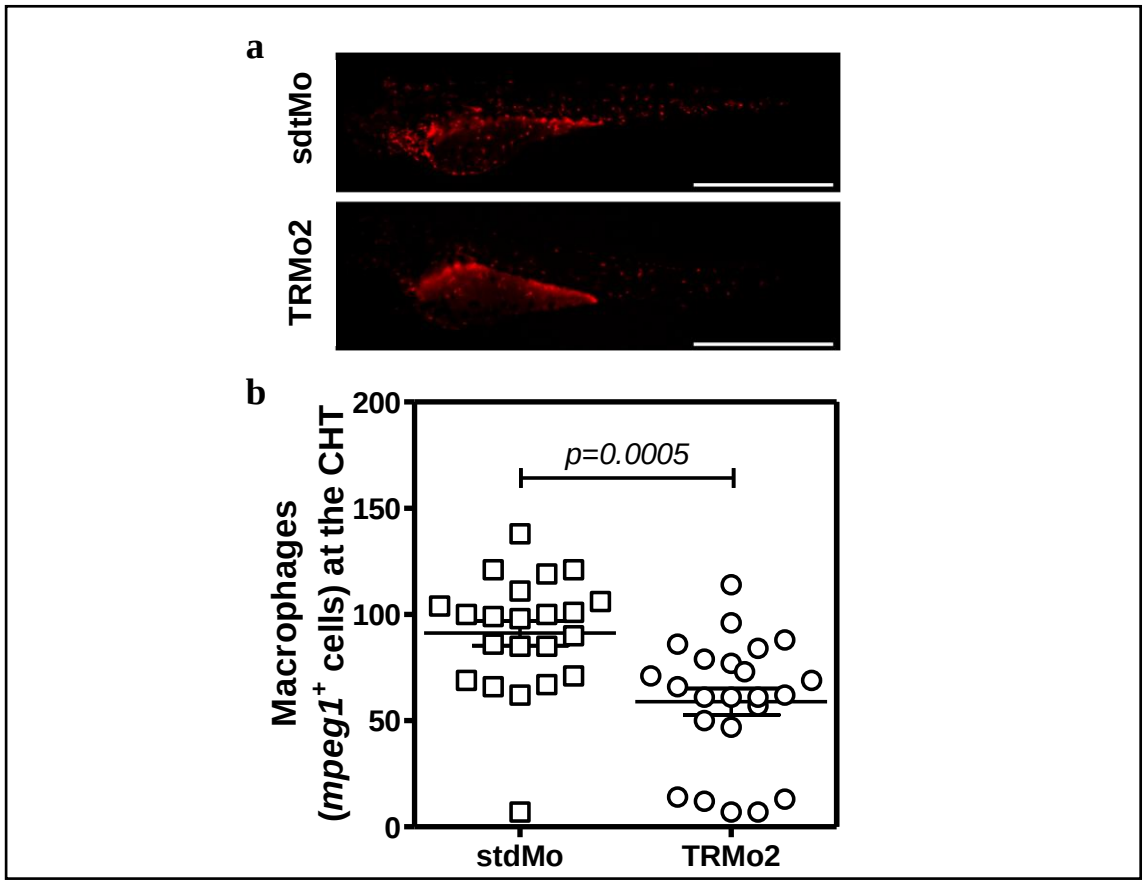

Figure 6: The absence of *TR* triggered monocytopenia. Tg(*mpeg1*:mCherry) zebrafish embryos were microinjected at the one-cell stage with MOs. (**a**) At 3 dpf, macrophages at the CHT were visually quantified from high-quality pictures, scale bar: 1mm. (**b**) Quantification of macrophage counts. Each symbol in graph represents one larva and the mean ± SEM is also indicated. Statistical significance was assessed using the Student's *t*-Test ($p<0.05$).

We next examined myeloid cell activity in *TR*-deficient larvae. First, we performed a recruitment assay to study neutrophil responses to an injury by tail fin transaction of 3 dpf tg(*mpx*:eGFP) zebrafish larvae. Although the neutrophil number at the injury site was lower at all time points analyzed in *TR*-deficient larvae, the kinetics of the recruitment was similar in both groups, being maximum at 6 hours post-wound (hpw) (**Fig. 7**), as previously described [Renshaw *et al.*, 2006].

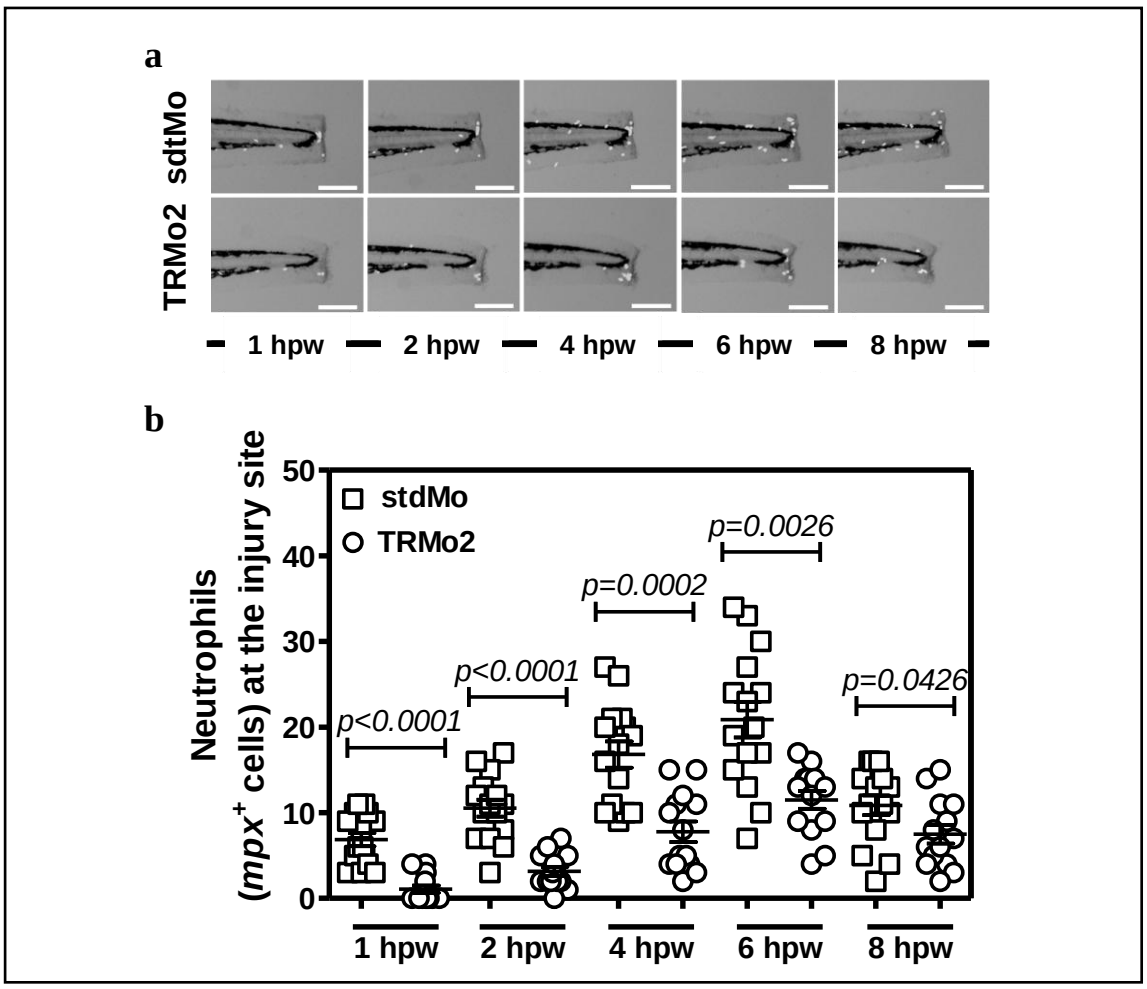

Figure 7: *TR* deficiency does not affect the neutrophil behavior against an injury. Tailfins of tg(*mpx*::eGFP) std and *TR* morphants were transected at 3 dpf and the number of fluorescent neutrophils visible in the tail was assessed by fluorescence microscopy. (**a**) Positive cells in animals from both groups were visually quantified from high-quality pictures from an 8 hour time series, scale bar: 0.2 mm. (**b**) Quantification of neutrophils at the injury site. Each symbol in graph represents one larva and the mean ± SEM is also indicated. Statistical significance was assessed using the Student's *t*-Test ($p<0.05$).

Next, we infected the larvae with the intracellular pathogenic bacterium *S. typhimurium* and found that the *TR* deficient embryos showed similar resistance to infection with this bacterium (**Fig. 8**). Depletion of myeloid cells, i.e. neutrophils and macrophages, using a MO against the master myeloid transcription factor *spi1* (also known as *pu.1*) [Rhodes *et al.*, 2005] rendered larvae hypersusceptible to *S. typhimurium* infection (**Fig. 8**). In addition, *TR*-deficient larvae were also able to respond to *S. typhimurium* infection by upregulating the expression of the genes encoding the powerful pro-inflammatory cytokines IL-1β and TNFα at 24 hours post-

infection (hpi), albeit at lower levels than their wild-type siblings (**Fig. 9**). Altogether, these observations establish that *TR*-deficient larvae have reduced number of neutrophils and macrophages, but that the cells that are present are fully functional.

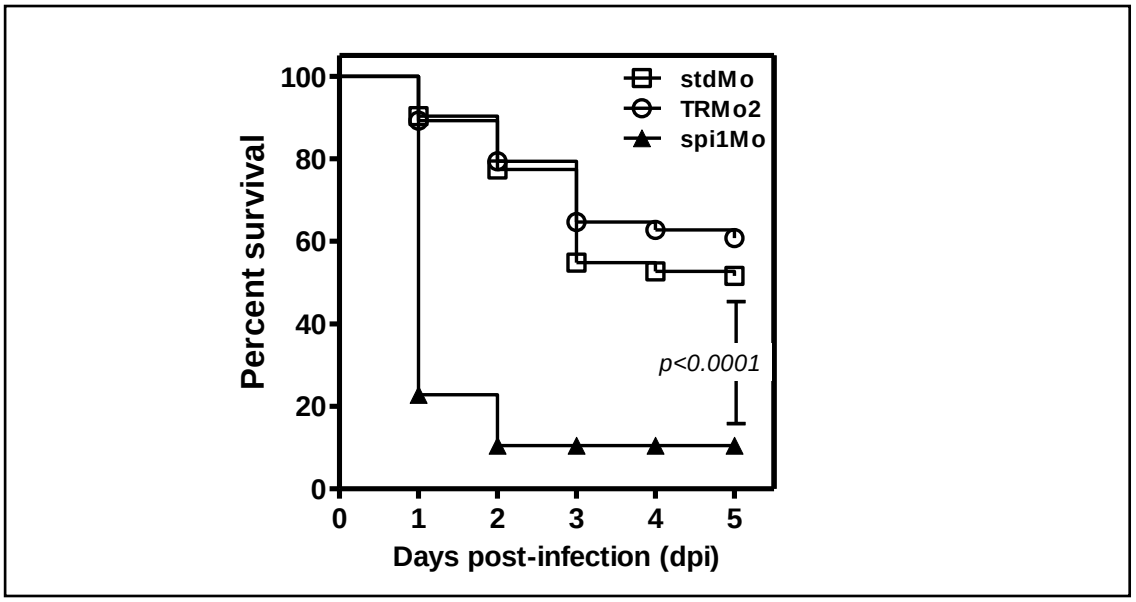

Figure 8: Kaplan-Meier representation of the survival of std and *TR* morphants infected with *S. typhimurium* at 2 dpf. There were no statistically significant differences between std and *TR* morphants, log rank test p>0.05. *spi1* morphants were more susceptible to infection than their std siblings, log rank test p<0.0001. No mortality was found in non-infected fish; these curves were omitted for clarity. stdMo, n=93; TRMo2, n=102; spi1Mo, n=56.

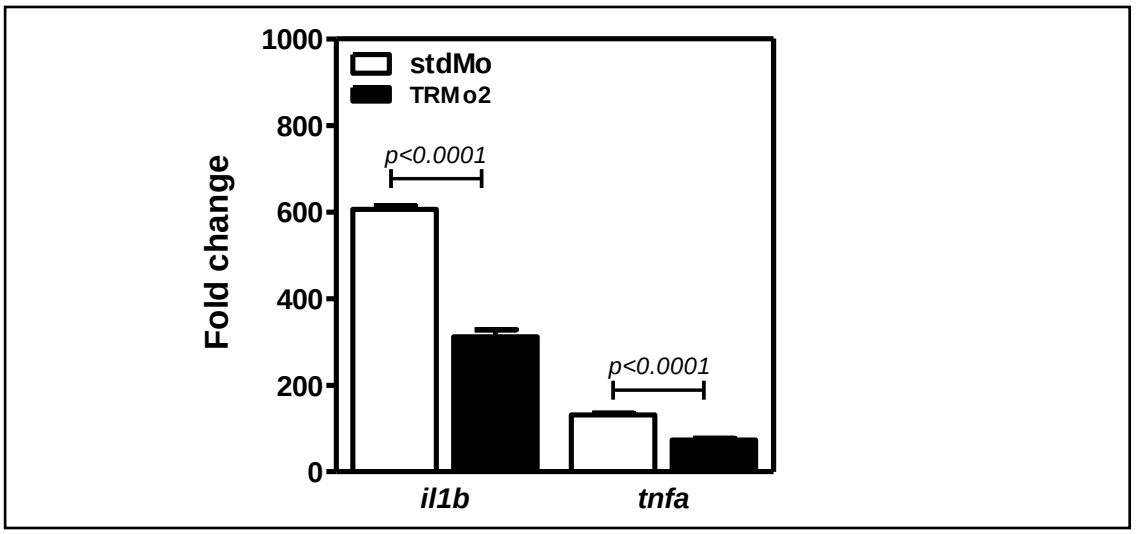

Figure 9: qRT-PCR assay (IL-1β and TNFα) of whole larvae at 24 hpi. Results are shown relative to non-infected larvae and are expressed as the mean ± SEM from triplicate samples. Statistical significance was assessed using the Student's *t*-Test (p<0.05).

3.3. The induction of neutropenia by *TR* depletion is independent of both telomere length and telomerase activity

As the knockdown of *TR* by MOs resulted in the lack of telomerase activity, we wondered whether the *TR* deficiency resulted in the shortening of telomere length, which may explain the observed phenotype. Telomere length was measured by Q-FISH in interphasic blood cells collected by cardiac puncture from 3 dpf larvae injected with stdMo and TRMo2. The results showed a similar telomere shortening, weak but significant, in *TR*- and *tert*-deficient larvae. In addition, the proportion of blood cells with short telomeres was similar in both groups of animals (**Fig. 10**).

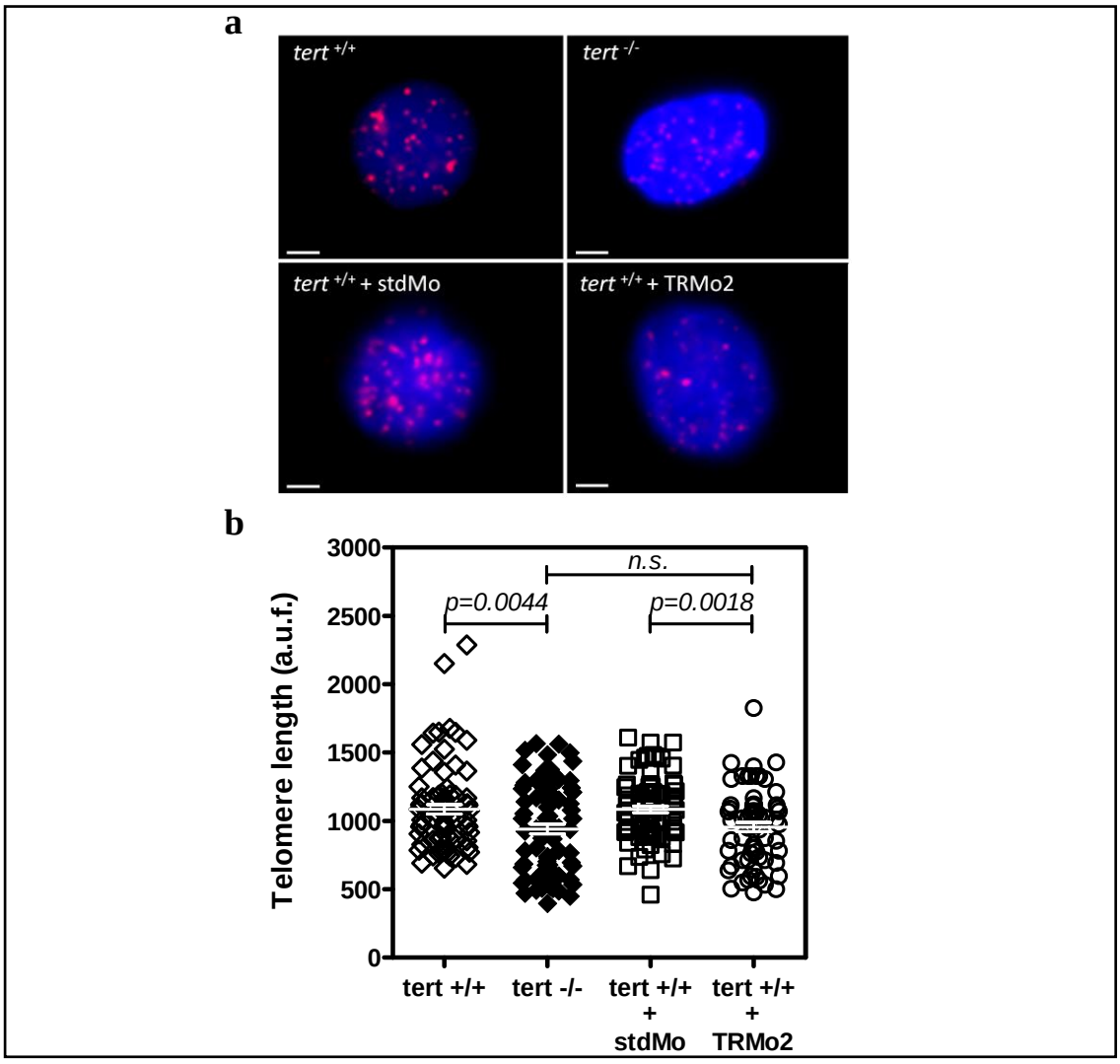

Figure 10: The absence of *TR* is not associated with telomere shortening. (**a**) Representative images of interphasic blood cells from 3 dpf larvae stained with a fluorescent telomeric probe. Nuclei were labelled with DAPI. Scale bar: 2 μm. (**b**) Telomere length was evaluated by Q-FISH in interphasic blood cells from 3 dpf larvae. Each symbol in graph represents one cell and

the mean ± SEM is also indicated. Statistical significance was assessed using the Student's *t*-Test ($p<0.05$).

Next, we wondered whether the neutropenia of *TR*-deficient larvae was related to the lack of telomerase activity. To accomplish this, we performed a TSA staining assay at 30 hpf using a *tert*$^{-/-}$ zebrafish line, which lack telomerase activity (Anchelin *et al.*, 2013), and their *tert*$^{+/+}$ siblings. Although *tert*-deficient embryos showed normal number of neutrophils, the deficiency of *TR* resulted in the reduction of neutrophils in both wild type and *tert*-deficient fish to a similar level, demonstrating that the loss of neutrophils was independent of telomerase activity (**Fig. 11**).

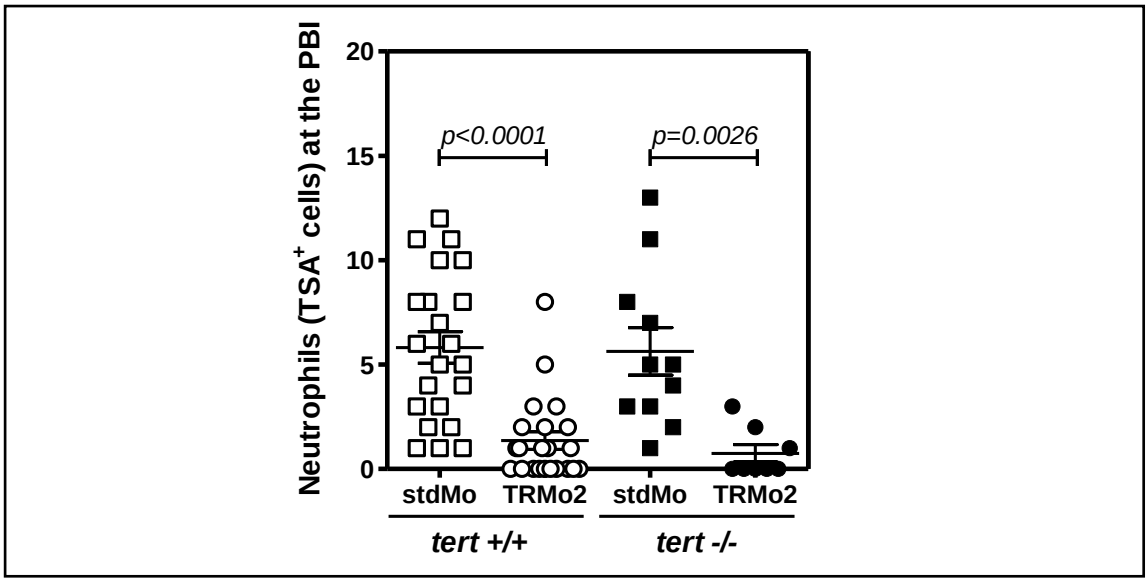

Figure 11: The induction of neutropenia by *TR* depletion is independent of telomerase activity. Neutrophils of *tert*$^{+/+}$ and *tert*$^{-/-}$ embryos were stained at 30 hpf, visualized by fluorescence microscopy and manually counted at the PBI. Each symbol represents one embryo and the mean ± SEM is also indicated. Statistical significance was assessed using the Student's *t*-Test ($p<0.05$).

The role plays by *TR* in myelopoiesis independently of telomerase activity prompted us to examine the expression of *TR* and *tert* genes in sorted neutrophils (mpx^{+} cells). *TR* RNA levels were strikingly higher in neutrophils than in unsorted cells, while *tert* mRNA was undetectable in neutrophils. Interestingly, the TRMo2 was able to

strongly reduce the RNA levels of *TR* in unsorted cells and neutrophils but had no effect on *tert* mRNA levels (**Fig. 12**).

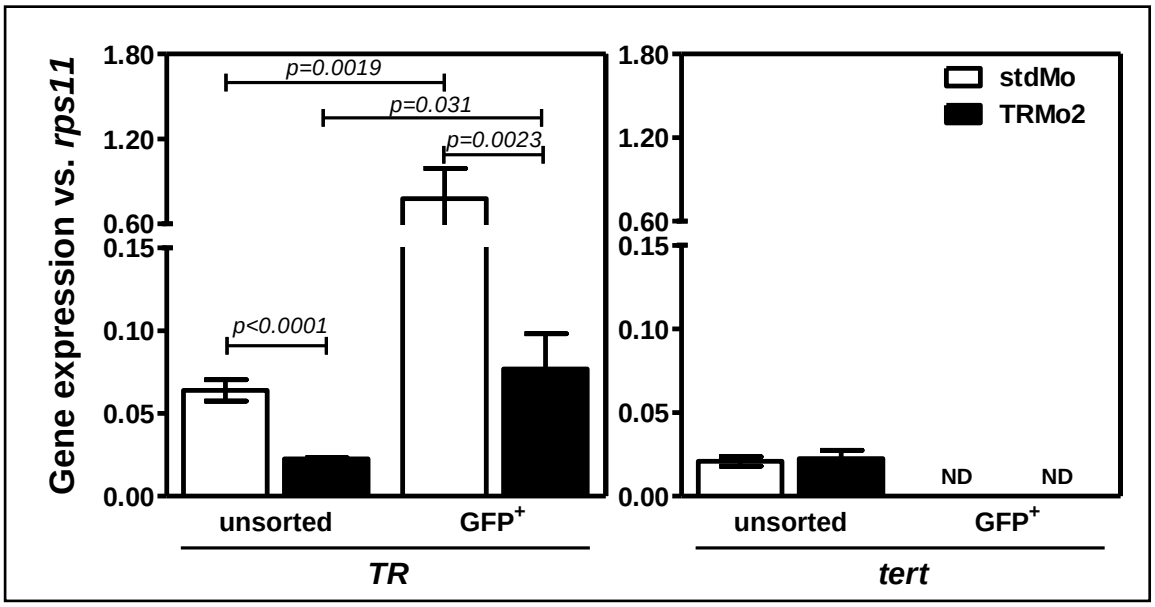

Figure 12: Neutrophil specific *TR* and tert expression. The mRNA levels of *TR* and *tert* was determined by RT-qPCR in unsorted vs. neutrophils (mpx^+) at 3 dpf. The graph shows the mean ± SEM of three independent experiments. Statistical significance was assessed using the Student's *t*-Test ($p<0.05$). ND, not detected.

As expected, *TR* and *tert* genes were ubiquitously expressed during development (**Fig. 13**), although *tert* was found to be expressed at higher levels by skin and neuromasts of 3 dpf larvae. These results further suggest a non-canonical role of *TR* in myelopoiesis.

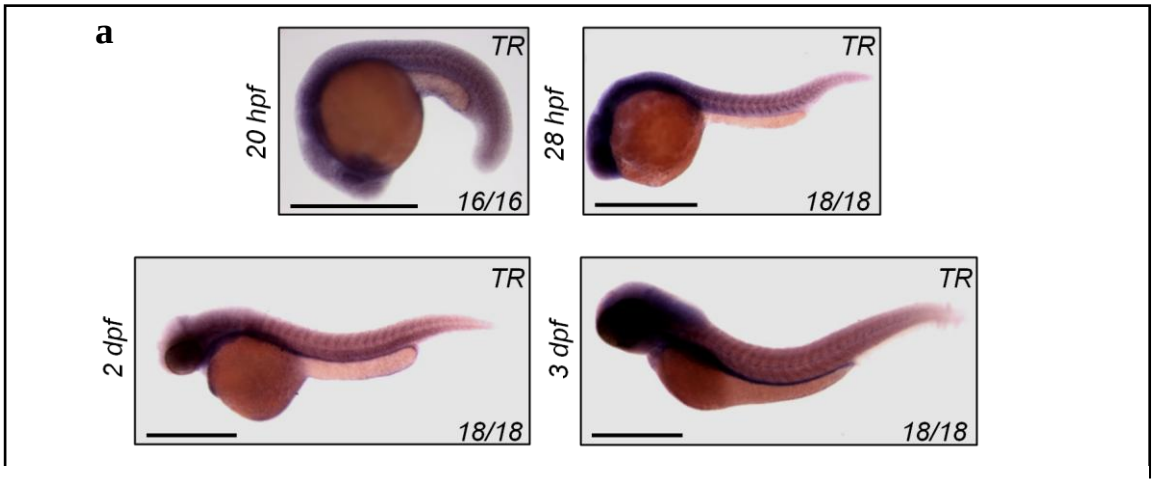

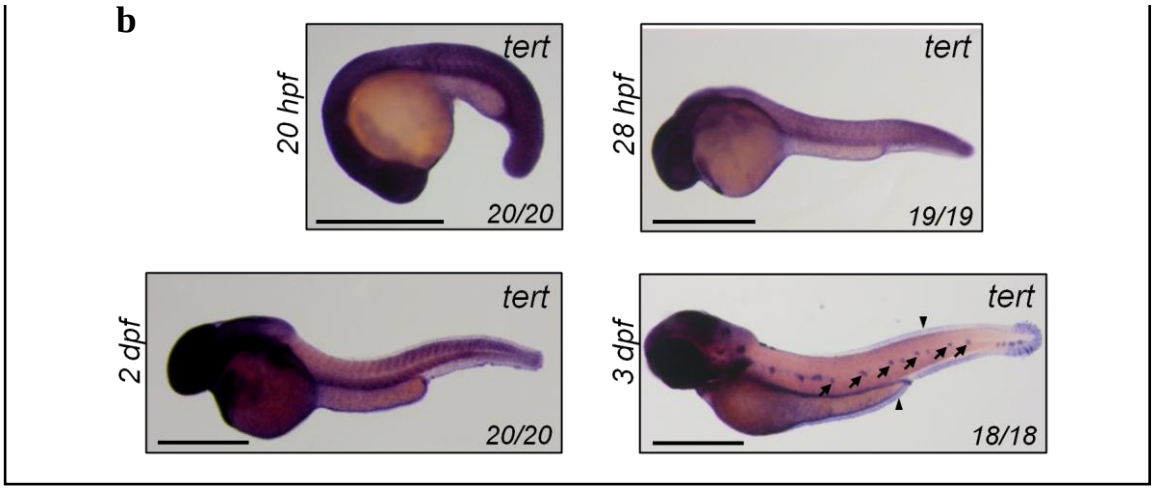

Figure 13: WISH for *TR* and *tert* during development. The expression of *TR* (**a**) and *tert* (**b**) genes was ubiquitous during development. Numbers in pictures represent the animals with the shown phenotype per total analyzed animals. Arrows: neuromasts. Arrow heads: skin. Scale bar: 1 mm.

3.4. *TR* is required for myelopoiesis but dispensable for the development of HSCs

To further determine the role of *TR* in zebrafish definitive hematopoiesis, we analyzed the expression of the specific hematopoietic genes *lmo2*, *gata1*, *spi1* (*pu.1*), *gcsfr*, *cmyb*, *runx1*, and *rag1* by using WISH at different time points. The expression of *lmo2* and *gata1*, which are markers of EMPs at 30 hpf and are expressed in the PBI [Bertrand *et al*., 2010], was unaffected by *TR* deficiency, whereas the expression of *spi1* and *gcsfr*, canonical markers of myeloid cells and neutrophils, respectively, was severely reduced at the PBI (**Fig. 14**). This result was further confirmed with a TSA staining assay at 30 hpf, which showed the reduction of neutrophils (mpx^+ cells) in *TR*-deficient embryos (**Fig. 15**).

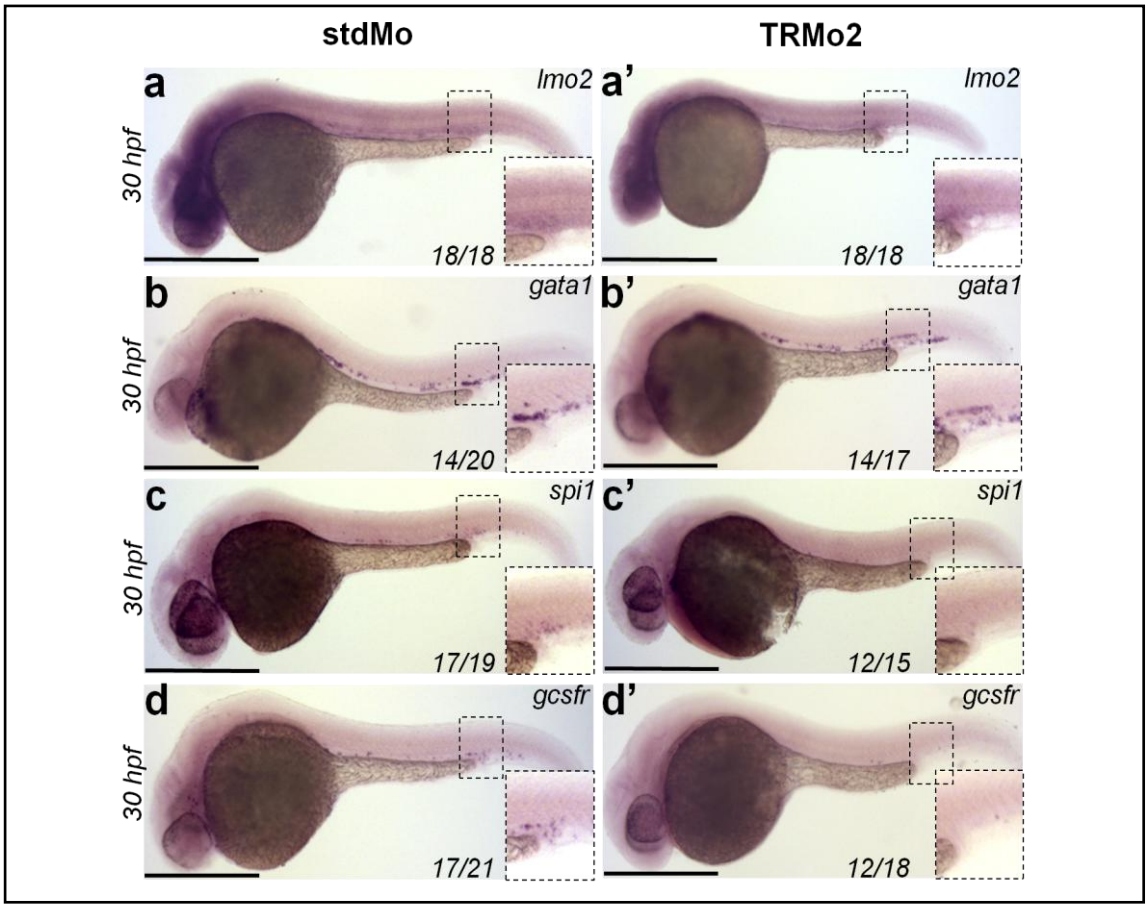

Figure 14: WISH of *lmo2*, *gata1*, *spi1* and *gcsfr* genes at 30 hpf. Zebrafish embryos were microinjected at the one-cell stage with stdMo or TRMo2. The expression of *lmo2* and *gata1*at 30 hpf was unaffected by *TR* deficiency (**a,b**), whereas the expression of *spi1* and *gcsfr* was severely reduced at the PBI (**c,d**). Numbers in pictures represent the animals with the shown phenotype per total analyzed animals. Scale bar: 0.5 mm.

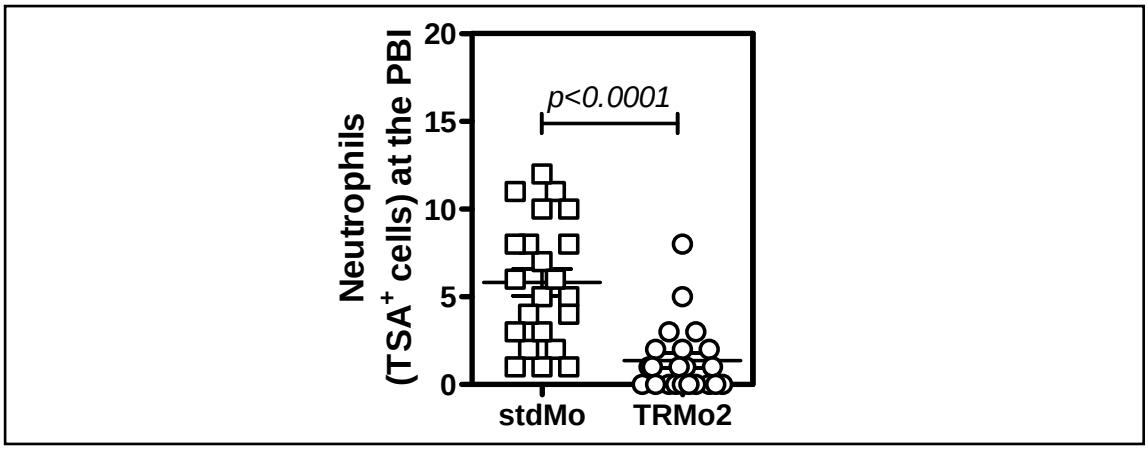

Figure 15: Reduction of neutrophils in *TR*-deficient embryos at 30 hpf. Zebrafish embryos were microinjected at the one-cell stage with stdMo or TRMo2. Then, neutrophils were stained at 30 hpf and visualized by fluorescence microscope and manually counted at the PBI. Each symbol represents one embryo and the mean ± SEM is also indicated. Statistical significance was assessed using the Student's *t*-Test ($p<0.05$).

The expression of *cmyb* and *runx1* begin by 36 hpf at the AGM and they mark emerging definitive hematopoietic stem and progenitor cells [Burns *et al.*, 2005]. Notably, the absence of *TR* did not affect the expression of *cmyb* and *runx1* (**Fig. 16**). This result was also verified using the tg(*cd41*::GFP) [Ma *et al.*, 2011], in which the number of cd41^{+} cells (HSCs and thrombocytes) at 3 dpf was independent of the presence of *TR* (**Fig. 17**).

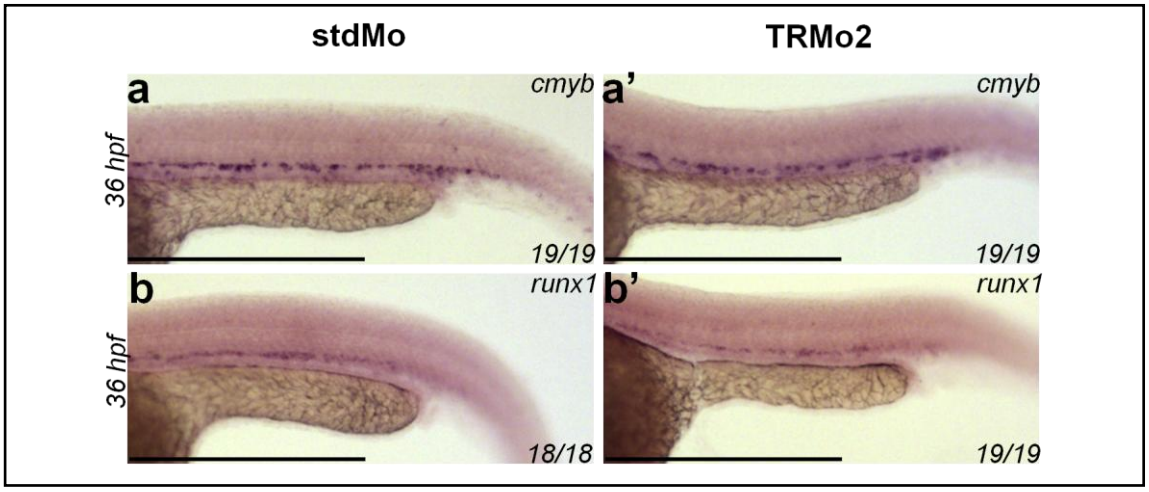

Figure 16: WISH of *cmyb* and *runx1* genes at 36 hpf. Zebrafish embryos were microinjected at the one-cell stage with stdMo or TRMo2. The expression of *cmyb* and *runx1* at 36 hpf was unaffected by *TR* deficiency at the AGM (**a,b**). Numbers in pictures represent the animals with the shown phenotype per total analyzed animals. Scale bar: 0.5 mm.

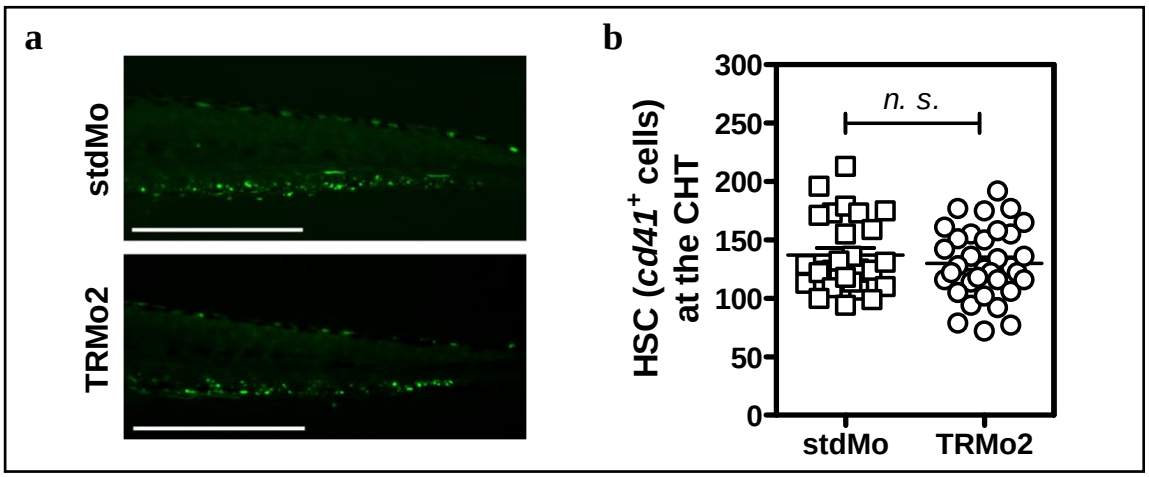

Figure 17: The number of *cd41*$^{+}$ cells (HSCs and thrombocytes) at 3 dpf is independent of the presence of *TR*. Tg(cd41::GFP) zebrafish embryos were microinjected at the one-cell stage with stdMo or TRMo2. Then, the number of *cd41+* cells were directly visualized by fluorescence microscopy at 3 dpf (**a**), scale bar: 0.5 mm, and manually counted at the CHT (**b**). Each symbol in graph represents one larva and the mean ± SEM is also indicated. Statistical significance was assessed using the Student's *t*-Test ($p<0.05$). n.s., not significant.

The expression of *gata1* and *rag1*, which are expressed in erythrocytes and differentiated thymic T cells, respectively, was apparently unaffected by *TR* deficiency. In sharp contrast, the expression of the myeloid markers *spi1* and *gcsfr* was significantly reduced at 36 hpf (**Fig. 18**).

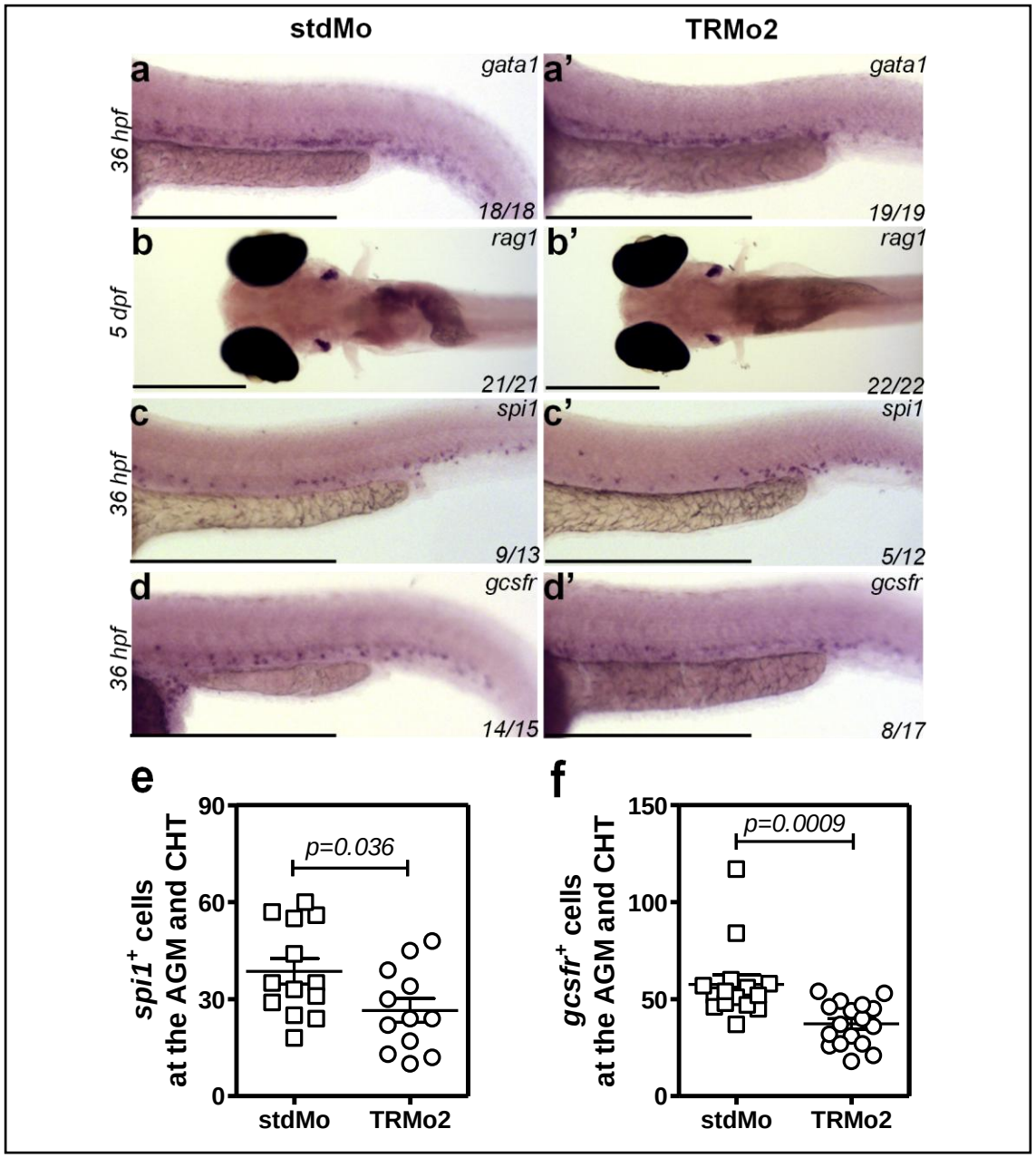

Figure 18: WISH of *gata1, rag1, spi1 and gcsfr* genes. Zebrafish embryos were microinjected at the one-cell stage with stdMo or TRMo2. The expression of both *gata1* at 36 hpf (**a**) and *rag1* at 5 dpf (**b**) was unaffected by *TR* deficiency, whereas the expression of *spi1* and *gcsfr* was significantly reduced at 36 hpf (**c,d**). Numbers in pictures represent the animals with the shown phenotype per total analyzed animals. Scale bar: 0.5 mm. Quantification of *spi1*$^+$ cells (**e**) and g*csfr*$^+$ cells (**f**) at the AGM and CHT. Each symbol in graphs represents one larva and the mean ± SEM is also indicated. Statistical significance was assessed using the Student's *t*-Test ($p<0.05$).

Collectively, these results suggest that although *TR* is dispensable for the emergence of EMPs and HSCs in zebrafish embryos, it is required for the differentiation of neutrophils, and likely macrophages, from EMPs and HSCs.

To study whether myeloid progenitor differentiation was altered in the absence of *TR*, we stained blood cells collected by cardiac puncture from 48 hpf embryos with Wright-Giemsa stain and observed alterations in blood cell morphology in *TR*-deficient embryos. Thus, the blood cells from *TR*-deficient embryos showed statistically significant lower radius and higher nucleus/cytoplasm ratio than their wild type siblings (**Fig. 19**). These findings are consistent with a delay in differentiation.

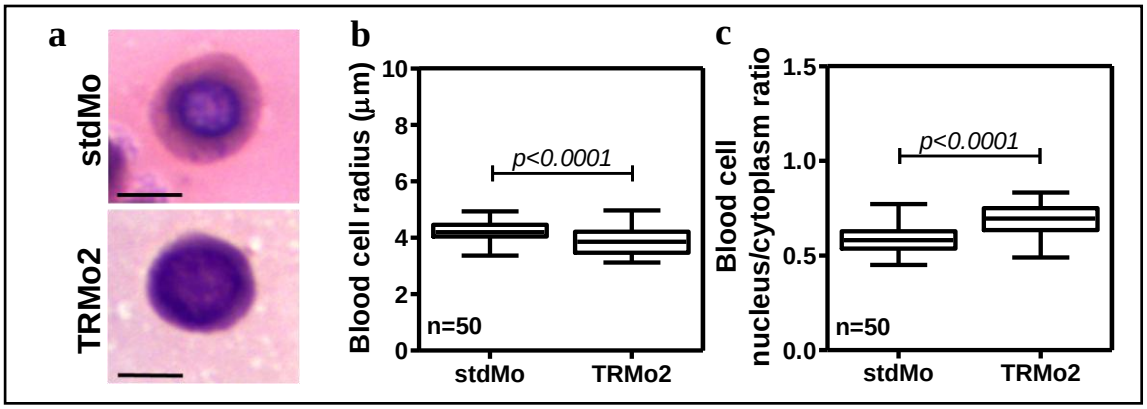

Figure 19: *TR* deficiency impairs blood cell differentiation. Zebrafish embryos were microinjected at the one-cell stage with stdMo or TRMo2. At 2 dpf, circulating embryonic red blood cells were obtained and stained with Wright-Giemsa (**a**), scale bar: 5 µm. Cells obtained from *TR*-deficient embryos are smaller (**b**) and shows a higher nucleo/cytoplasm ratio (**c**) compared with wild type cells. The results are shown as the mean ± SEM of 50 blood cells.

3.5. *TR* deficiency alters the *spi1*/*gata1a* balance in blood cells

spi1 and *gata1* are both transcriptional factors essential for the differentiation of HSCs to myeloid and erythroid cells, respectively. The expression of *TR*, *spi1* and *gata1a* was analyzed in the CHT of 2 dpf embryos. The *spi1*/*gata1a* ratio was significantly reduced when *TR* was depleted, usually because *spi1* transcript levels decreased and those of *gata1a* increased (**Fig. 20**).

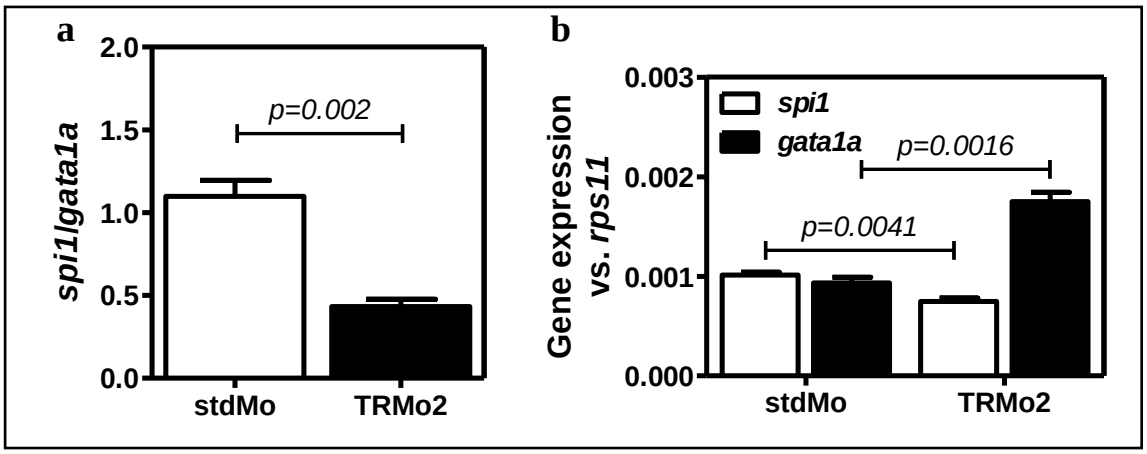

Figure 20: *TR* deficiency alters the *spi1*/*gata1a* balance in the CHT. Zebrafish embryos were microinjected at the one-cell stage with stdMo or TRMo2. At 2 dpf, the expression of *spi1* and *gata1a* was analyzed in the CHT from tail sections. (**a**) *spi1/gata1a* expression ratio and (**b**) mRNA levels determined by qRT-PCR. Statistical significance was assessed using the Student's *t*-Test ($p<0.05$).

These results prompted us to investigate the impact of *TR* overexpression in developmental myelopoiesis. The results showed that an *in vitro* transcribed and capped *TR* RNA was able to rescue the number of neutrophils in *TR* morphants at 3 dpf, despite it failed to significantly rescue the *spi1*/*gata1a* ratio (**Fig. 21**).

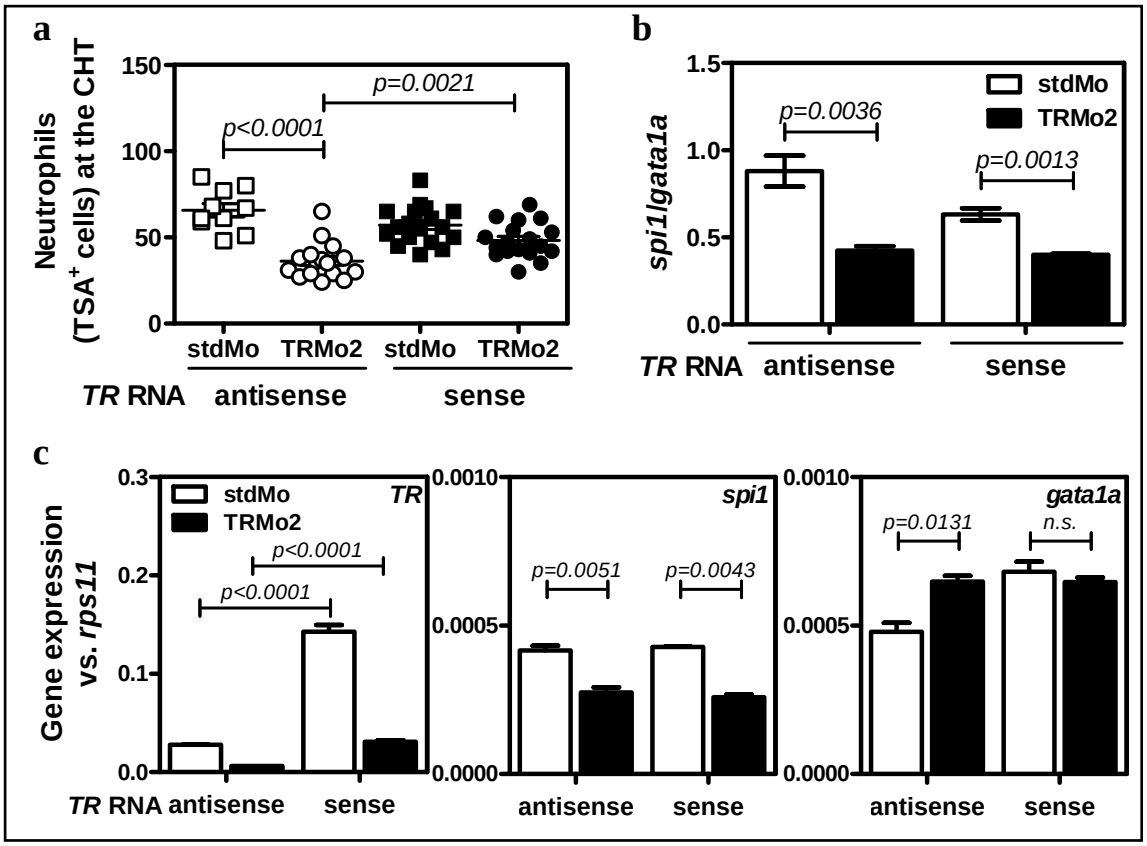

Figure 21: *TR* overexpression is able to rescue the neutropenia in *TR* morphants at 3 dpf. Zebrafish embryos were microinjected at the one-cell stage with stdMo or TRMo2 in combination with 200 pg/egg of *in vitro* transcribed and CAP-modified antisense and *TR* RNA. (**a**) Neutrophils were stained at 3 dpf and visualized by fluorescence microscope and manually counted at the CHT. Each symbol in graph represents one larva and the mean ± SEM is also indicated. (**b**) *spi1/gata1a* expression ratio and (**c**) mRNA levels determined by qRT-PCR in tail sections of 2 dpf larvae. Statistical significance was assessed using the Student's *t*-Test ($p<0.05$). n.s., not significant.

We next studied the epistatic relationships between *TR* and *spi1*. Overexpression of *spi1* RNA was also able to rescue the number of neutrophils and the *spi1*/*gata1a* balance (**Fig. 22**).

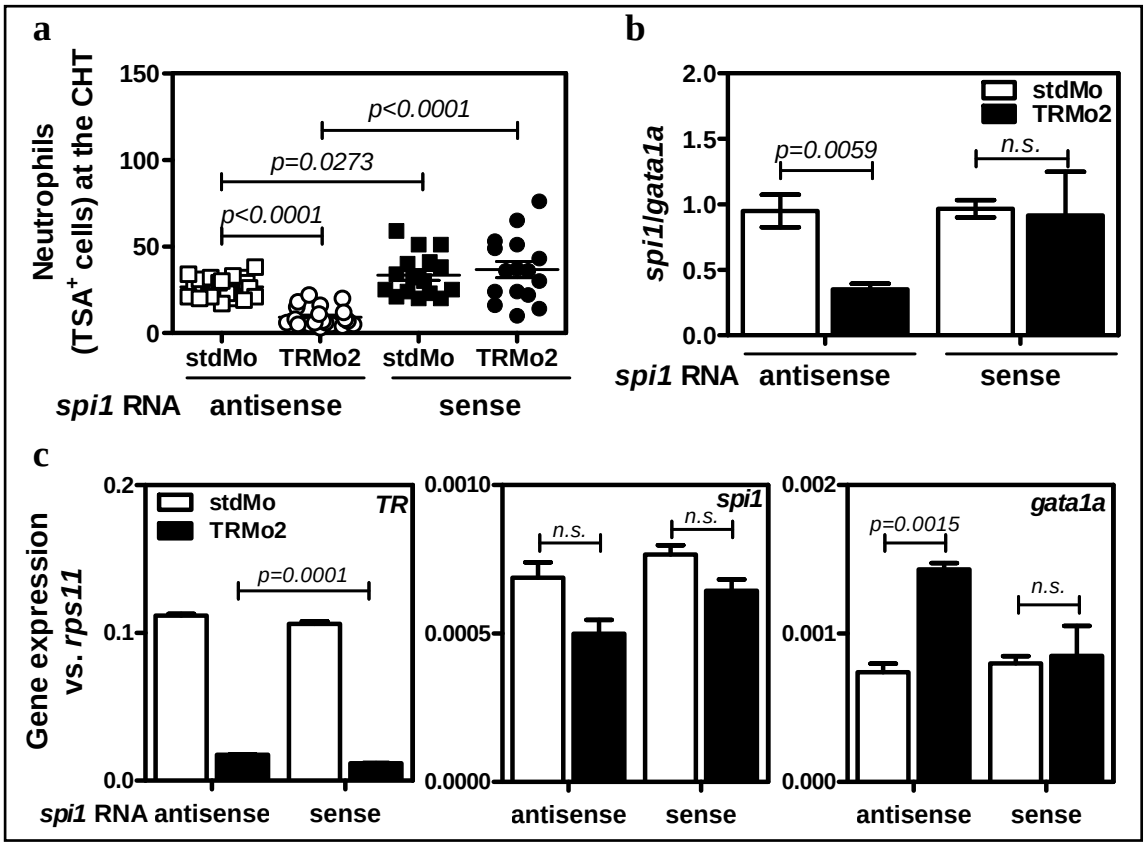

Figure 22: *spi1* overexpression is able to rescue the neutropenia in *TR* morphants at 3 dpf. Zebrafish embryos were microinjected at the one-cell stage with stdMo or TRMo2 in combination with 50 pg/egg of *in vitro* transcribed and CAP-modified antisense and *spi1* RNA. (**a**) Neutrophils were stained at 3 dpf and visualized by fluorescence microscope and manually counted at the CHT. Each symbol in graph represents one larva and the mean ± SEM is also indicated. (**b**) *spi1/gata1a* expression ratio and (**c**) mRNA levels determined by qRT-PCR in tail sections of 2 dpf larvae. Statistical significance was assessed using the Student's *t*-Test ($p<0.05$). n.s., not significant.

Similarly, depletion of *gata1a* using a specific MO was also able to rescue the number of neutrophils and the *spi1*/*gata1a* balance (**Fig. 23**).

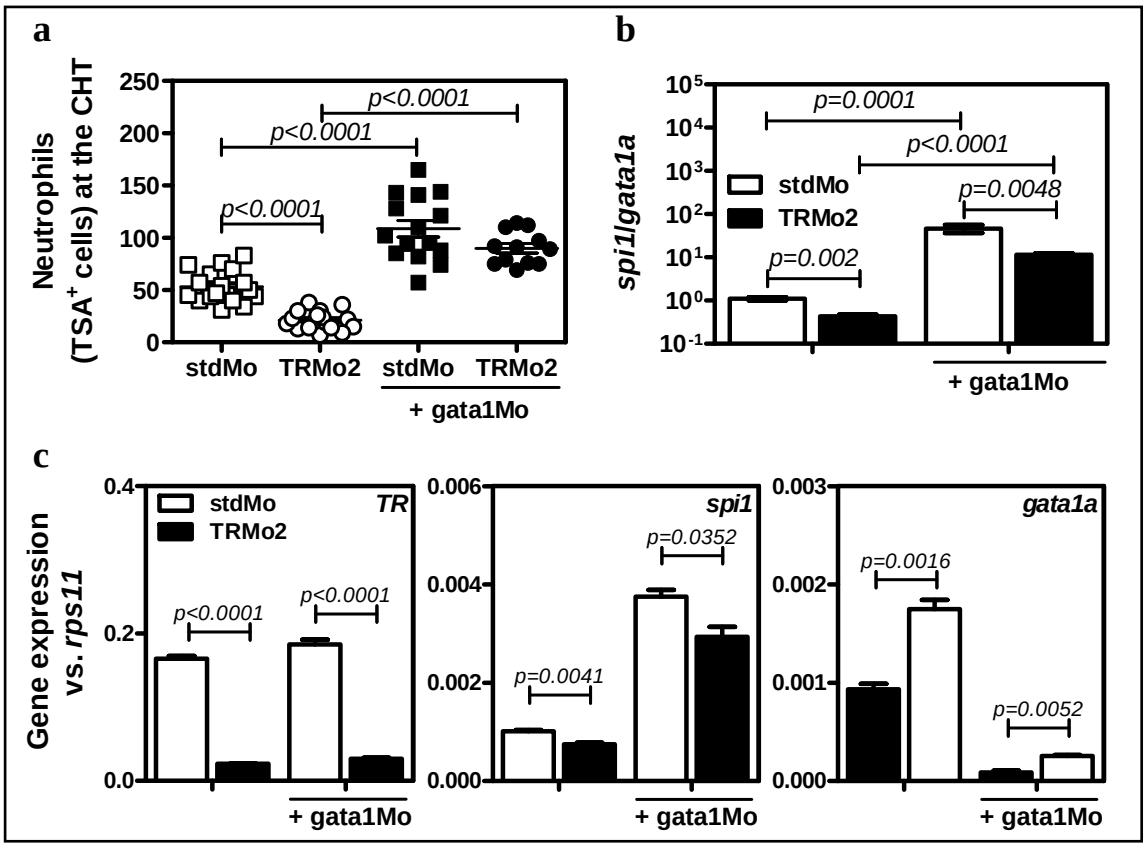

Figure 23: *gata1a* depletion is able to rescue the neutropenia in *TR* morphants at 3 dpf. Zebrafish embryos were microinjected at the one-cell stage with stdMo or TRMo2 alone or in combination with gata1Mo. (**a**) Neutrophils were stained at 3 dpf and visualized by fluorescence microscope and manually counted at the CHT. Each symbol in graph represents one larva and the mean ± SEM is also indicated. (**b**) *spi1/gata1a* expression ratio and (**c**) mRNA levels determined by qRT-PCR in tail sections of 2 dpf larvae. Statistical significance was assessed using the Student's *t*-Test ($p<0.05$).

Our studies define a crucial role of *TR* in maintaining a critical balance between the major myeloid (*spi1*) and erythroid (*gata1a*) transcription factors.

3.6. *TR* regulates the expression of *gcsf* and *mcsf*

It has recently been identified 2198 *TR* binding sites in the human genome, which represents a large resource to study potential non-canonical functions of *TR* RNA and telomerase [Chu *et al.*, 2011]. Strikingly, *TR* occupied binding sites near *CSF1* and *CSF2* genes, which encodes macrophage colony-stimulating factor (MCSF) and granulocyte-macrophage colony-stimulating factor (GMCSF), respectively. Although no orthologues for *CSF2* gene have been identified to date in zebrafish, true orthologues for *CSF1* and *CSF3*, which encodes (GCSF), have been found and shown to stimulate the survival, proliferation and differentiation of neutrophil and macrophages, respectively [Herbomel *et al.*, 2001; Liongue *et al.*, 2009]. We sought to determine whether *TR* was able to regulate the expression of these important cytokines. *TR*-deficient larvae showed reduced mRNA levels of both *gcsf* and *mcsf* compared with wild-type siblings. And conversely, overexpression of *TR* RNA increased the transcript levels of both genes (**Fig. 24**).

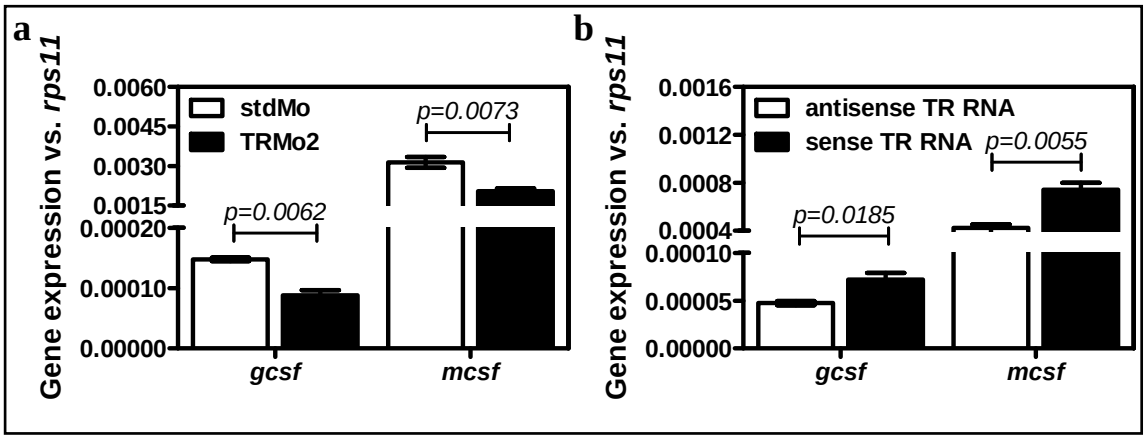

Figure 24: *TR* regulates the expression of *gcsf* and *mcsf* in the CHT. Zebrafish embryos were microinjected at the one-cell stage with stdMo or TRMo2 alone (**a**) or in combination with 200 pg/egg of *in vitro* transcribed and CAP-modified antisense and *TR* RNA (**b**). *gcsf* and *mcsf* expression was analyzed by RT-qPCR in tail sections of 2 dpf larvae. Statistical significance was assessed using the Student's *t*-Test ($p<0.05$).

On the other hand, overexpression of *gcsf* and *mcsf* mRNAs rescued the number of neutrophils and macrophages, respectively. In addition, *gcsf* overexpression, and to some extend *mcsf*, increased *spi1* expression levels while they did not affect *TR* levels (**Fig. 25**).

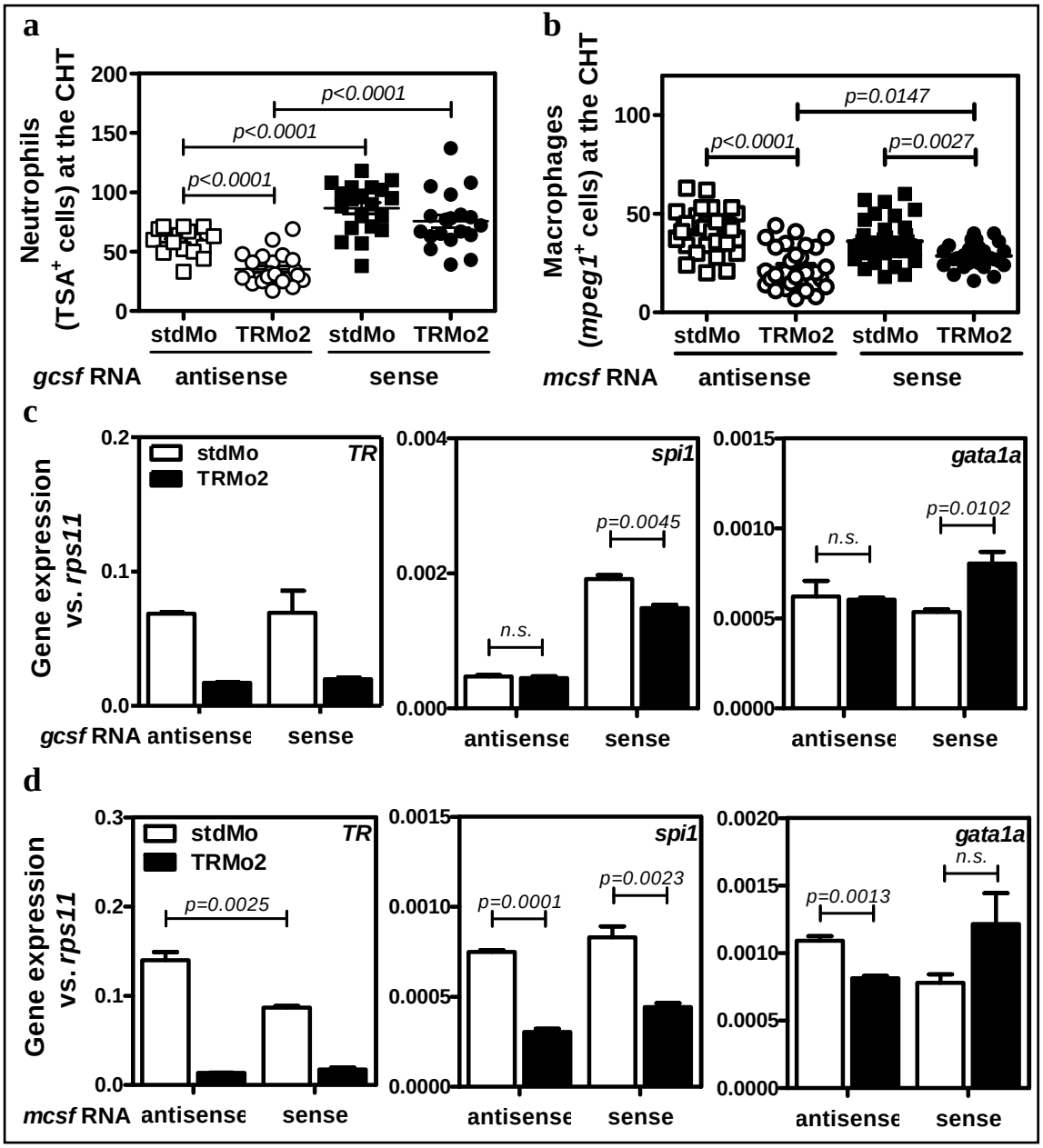

Figure 25: Overexpression of both *gcsf* and *mcsf* is able to rescue the neutropenia in *TR* morphants at 3 dpf. Zebrafish embryos were microinjected at the one-cell stage with stdMo or TRMo2 in combination with 100 pg/egg (**a,c**) or 200 pg/egg (**b,d**) of *in vitro* transcribed and CAP-modified antisense, *gcsf* (**a,c**) or *mcsf* RNA (**b,d**), respectively. (**a,b**) At 3 dpf, neutrophils and macrophages were visualized by fluorescence microscope and manually counted at the CHT. Each symbol in graph represents one larva and the mean ± SEM is also indicated. (**c,d**)

mRNA levels were determined by qRT-PCR in tail sections of 2 dpf larvae. Statistical significance was assessed using the Student's *t*-Test ($p<0.05$). n.s., not significant.

We next decided to use a luciferase reporter assay in whole zebrafish embryos, as we have previously described [Alcaraz-Pérez *et al.*, 2008]. The results showed that *TR* deficiency inhibited, while *TR* overexpression activated, *gcsf* promoter activity (**Fig. 26**).

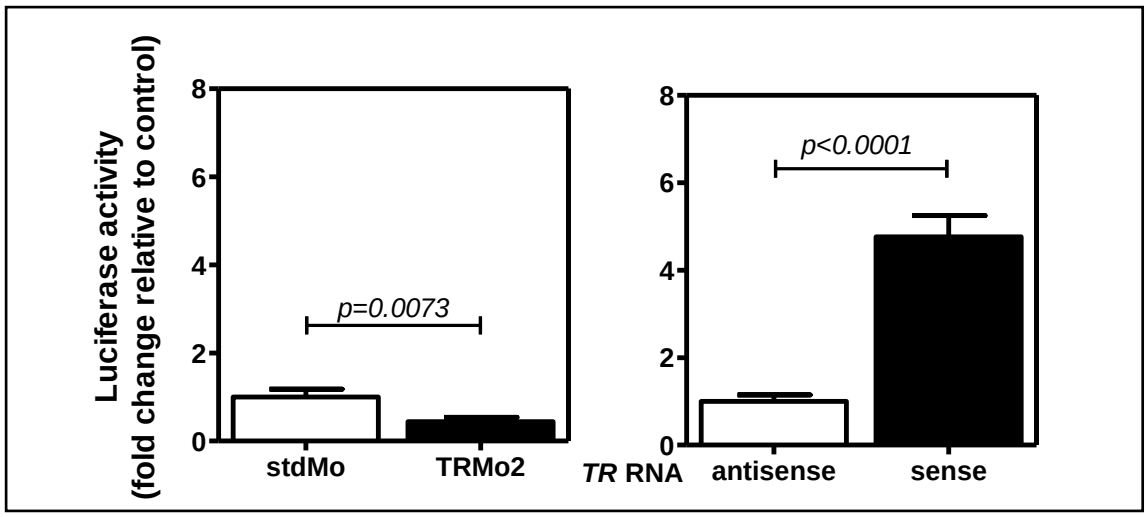

Figure 26: *TR* regulates the *gcsf* promoter activity. Luciferase activity in tail sections of 2 dpf larvae. Statistical significance was assessed using the Student's *t*-Test ($p<0.05$).

Collectively, these results strongly suggest that *TR* regulate the expression of *gcsf* and *mcsf* genes which maintain a critical balance between the major myeloid (*spi1*) and erythroid (*gata1a*) transcription factors.

4. Discussion

DC is an inherited disorder with mutations affecting telomerase components or telomere stabilizing components, which is characterized by a variety of phenotypes [Vulliamy & Dokal, 2008]. However, DC patients usually die of bone marrow failure due to a deficient renewing capability of HSCs [Brummendorf & Balabanov, 2006; Drummond *et al.*, 2007]. Curiously, the presentation of the disease is more serious in patients with mutations affecting *TR* [Vulliamy & Dokal, 2008] and some mutations, such as 58G→A, are not associated with impaired telomerase activity *in vitro* [Chen & Greider, 2003]. In addition, various evidences have shown the cancer promoting activity of *TR* independently of telomerase activity [Blasco *et al.*, 1996; Cayuela *et al.*, 2005; Fragnet *et al.*, 2003; Li *et al*., 2005]. All these observations, together with the ability of *TR* to specifically bind 2198 sites in the human genome [Chu *et al.*, 2011], led us to hypothesized that *TR* plays a non-canonical role in hematopoiesis through the regulation of gene expression. We found that genetic depletion of *TR* in zebrafish embryos with three different MOs resulted in a strong neutropenia and monocytopenia, which was fully rescued by overexpression of *TR* RNA, confirming the specificity of the observed phenotype. Strikingly, the effect of *TR* in developmental myelopoiesis is independent of telomerase activity and telomere length, since (1) *tert* mutant larvae showed normal number of neutrophils; (2) *TR* depletion also led to neutropenia in *tert* mutant larvae; (3) telomere length was weakly affected and to similar levels in *TR*- and *tert*-deficient larvae; and (4) *TR* was expressed at very high levels in zebrafish neutrophils, while *TERT* was undetectable in these cells. These results point to a non-canonical role of *TR* in myelopoiesis and suggest its probable involvement in the regulation of neutrophil function.

TR-deficient neutrophils were recruited to wounds similarly to wild types. *TR*-deficient larvae did not show higher susceptibility to *S. typhimurium* and were able to upregulate *il1b* and *tnfa* genes at similar levels as wild types upon the infection. To the best of our knowledge, there is a single study on neutrophil function from DC patients [Rochowski *et al.*, 2011]. This study showed that there was no significant difference in the degree of phorbol 12-myristate acetate (PMA) and N-formyl-methyonyl-leucyl-phenylalanine (fMLP)-triggered respiratory burst activity between 18 DC patients and their respective healthy family members. Unfortunately, the gene mutated in these patients was unknown and it is likely that there was a pool of patients with mutations

affecting genes encoding different telomerase and/or telomere components. Our studies suggest that more DC patients should be examined for neutrophil defects.

One of the most interesting observations of our study is that definitive hematopoiesis was not affected in *TR*-deficient embryos. Thus, the expression of canonical markers for EMPs and HSCs seemed to be normal, as the number of $CD41^{+}$ cells at the CHT. Erythropoiesis and lymphopoiesis proceeded normally, further confirming that emergence, maintenance and differentiation of HSCs was unaffected in *TR*-deficient embryos. In contrast, *TR*-deficient embryos/larvae showed lower number of $spi1^{+}$ and $gcsfr^{+}$ cells, confirming that *TR* is specifically required for the differentiation of myeloid cells, i.e. neutrophils and macrophages. These results may explain the persistant neutropenia and altered myelopoiesis observed in DC children who showed normal erythropoiesis, megakaryopoiesis and normal lymphocyte subgroups and antibody levels [Yel *et al.*, 1996; Yilmaz *et al.*, 2002]. We speculate that the critical role played by *TR* in telomere maintenance might have masked its non-canonical role in myelopoiesis, since the majority of DC patients are examined at later stages of the disease when critically short telomeres severely impair HSC renewal and bone marrow failure is imminent.

Our *in vivo* genetic analysis provides the first experimental evidence to our knowledge that *TR* modulates a critical gene regulatory network required for myelopoiesis, probably by regulating the expression of the two main growth factors involved in the differentiation of neutrophils (gcsf) and macrophages (mcsf). This is not unexpected since human *TR* binds direct to both the *CSF1* and *CSF2* gene promoters [Chu *et al.*, 2011] and there is a complex crosstalk between mouse *GCSF*/*GMCSF* and *SPI1* [Berclaz *et al.*, 2007; Berclaz *et al.*, 2002; Dahl *et al.*, 2003]. Therefore, *TR* could act as a positive transcription factor for these genes. Although the direct binding of *TR* to *gcsf* and *mcsf* upstream regulatory sequences requires to be demonstrated, the subtle regulation of the zebrafish *gcsf* gene promoter by *TR* levels, assayed by a luciferase reporter assay in whole zebrafish larvae, supports this conclusion.

The regulation of *spi1* and *gata1* genes in zebrafish has been shown to be critical for the differentiation of myeloid and erythroid cells. Reciprocal regulation of *spi1* and *gata1* determine myeloid vs. erythroid fate [Rhodes *et al.*, 2005]. In addition, loss of gata1 transforms primitive blood precursors into myeloid cells, resulting in a massive

expansion of granulocytic neutrophils and macrophages at the expense of red blood cells [Galloway *et al.*, 2005]. Our results demonstrate that *TR* modulates the myeloid vs. erythroid fate outcomes from HSCs by differentially controlling the levels of *spi1* and *gata1* via upregulation of *gcsf* and *mcsf*. Intriguingly, transcription intermediate factor-1γ (*tif1g*, *trim33*) also plays a similar role by differentially controlling the levels of *spi1* and *gata1* [Monteiro *et al.*, 2011].

The regulation of *CSF* genes by *TR* might have important clinical implications, since GCSF and GMCSF therapy has been used in DC patients to treat neutropenia [Solder *et al.*, 1998]. It is tempting to speculate, therefore, that this therapy might be specifically efficient in DC patients carrying mutations in the *TR* gene before telomeres are critically shorted in HSCs. While GCSF/GMCSF treatment was been found to be relatively effective in children [Yel *et al.*, 1996; Yilmaz *et al.*, 2002; Erduran *et al.*, 2003] and young adults with DC [Alter *et al.*, 1997; Oehler *et al.*, 1994], in other cases the treatment was only moderately effective in improving neutropoiesis [Putterman *et al.*, 1993; Russo *et al.*, 1990]. Unfortunately, the mutation responsible for DC in all these clinical trials was unknown. The different efficiency of GSCF/GMCSF therapy may be related to the mutated gene and the telomere length of the patients. This speculation is supported by the ability of $CD34^+$ cells from DC patients with a *TR* mutation to produce the different lineages of mature cells in normal numbers *in vitro* in response to growth factors, despite the HSC compartment of these patients was profoundly reduced [Goldman *et al.*, 2008]. Taken together, these results further indicate that telomere dysfunction of HSCs from DC patients or knockout mice might unmask the non-canonical role of *TR*.

In conclusion, this study provides experimental evidence that *TR* plays a non-canonical role in the regulation of myelopoiesis by fine-tuning the expression of *spi1* and *gata1* transcription factors in developing zebrafish embryos through the regulation of *gcsf* and *mcsf*. The *in vivo* model developed here is a powerful tool to illuminate the non-canonical functions of *TR* in HSC emergence, maintenance and differentiation. In this way, further studies with this model could elaborate signaling pathways that are perturbed in DC patients and could represent therapeutic targets.

Conclusions

The results obtained in this work lead to the following conclusions:

1. We have developed a rapid and sensitive assay based on the classical dual-luciferase reporter technique that can be used as a new tool to study both constitutive and inducible promoters in the context of a whole organism. This assay may be used in high throughput screening experiments.

2. MO-mediated genetic depletion of the telomerase RNA component (*TR)* impairs telomerase activity but does not alter zebrafish development.

3. *TR* deficiency induces neutropenia and monocytopenia but does not compromise neutrophil functionality.

4. The induction of neutropenia by *TR* depletion is independent of both telomere length and telomerase activity, suggesting a non-canonical role of *TR* in myelopoiesis.

5. *TR* regulates the expression of *gcsf* and *mcsf*. Hence, *TR* deficiency results in reduced *gcsf* and *mcsf* levels, leading to alter *spi1*/*gata1a* balance in blood cells and impaired myelopoiesis. However, neither HSC emergence nor erythropoiesis is affected by *TR* deficiency.

References

Abad JP, De Pablos B, Osoegawa K, De Jong PJ, Martín-Gallardo A, Villasante A. **Genomic analysis of *Drosophila melanogaster* telomeres: full-length copies of HeT-A and TART elements at telomeres.** *Mol Biol Evol* **21**(9):1613-9 (2004).

Alcaraz-Pérez F, Mulero V, Cayuela ML. **Application of the dual-luciferase reporter assay to the analysis of promoter activity in Zebrafish embryos.** *BMC Biotechnology* **8**:81 (2008).

Allsopp RC, Cheshier S, Weissman IL. **Telomerase activation and rejuvenation of telomere length in stimulated T cells derived from serially transplanted hematopoietic stem cells.** *J Exp Med* **196**, 1427-1433 (2002).

Alter BP, Baerlocher GM, Savage SA, Chanock SJ, Weksler BB, Willner JP, Peters JA, Giri N, Lansdorp PM. **Very short telomere length by flow FISH identifies patients with Dyskeratosis Congenita.** *Blood* **110**(5):1439-47 (2007).

Alter BP, Gardner FH, Hall RE. **Treatment of dyskeratosis congenita with granulocyte colony-stimulating factor and erythropoietin.** *Br J Haematol* **97**, 309-311 (1997).

Anchelin M, Alcaraz-Pérez F, Martínez CM, Bernabé-GarcíaM, Mulero V, Cayuela ML. **Premature aging in telomerase-deficient zebrafish.** *Dis Model Mech* **6**, 1101-1112 (2013).

Anchelin M, Murcia L, Alcaraz-Pérez F, García-Navarro EM, Cayuela ML. **Behaviour of telomere and telomerase during aging and regeneration in zebrafish.** *PLoS One* **6**, e16955 (2011).

Arenzana-Seisdedos F, Fernández B, Domínguez I, Jacqué JM, Thomas D, Díaz-Meco MT, Moscat J, Virelizier JL. **Phosphatidylcholine hydrolysis activates NF-kappa B and increases human immunodeficiency virus replication in human monocytes and T lymphocytes.** *J Virol* **67**:6596-6604 (1993).

Armanios M. **Syndromes of telomere shortening.** *Annu Rev Genomics Hum Genet* **10**:45-61 (2009).

Armanios M. **Telomerase and idiopathic pulmonary fibrosis.** *Mutat Res* **730**:52-58 (2012).

Armanios M, Chen JL, Chang YP, Brodsky RA, Hawkins A, Griffin CA, Eshleman JR, Cohen AR, Chakravarti A, Hamosh A, Greider CW. **Haploinsufficiency of telomerase reverse transcriptase leads to anticipation in autosomal dominant dyskeratosis congenita.** *Proc Natl Acad Sci USA* **102**, 15960-15964 (2005).

Azzalin CM, Reichenbach P, Khoriauli L, Giulotto E, Lingner J. **Telomeric repeat containing RNA and RNA surveillance factors at mammalian chromosome ends.** *Science* **318**(5851):798-801 (2007).

Berclaz PY, Carey B, Fillipi MD, Wernke-Dollries K, Geraci N, Cush S, Richardson T, Kitzmiller J, O'connor M, Hermoyian C, Korfhagen T, Whitsett JA, Trapnell BC. **GM-CSF regulates a PU.1-dependent transcriptional program determining the pulmonary response to LPS.** *Am J Respir Cell Mol Biol* **36**, 114-121 (2007).

Berclaz PY, Shibata Y, Whitsett JA, Trapnell BC. **GM-CSF, via PU.1, regulates alveolar macrophage Fcgamma R-mediated phagocytosis and the IL-18/IFN-gamma -mediated molecular connection between innate and adaptive immunity in the lung.** *Blood* **100**, 4193-4200 (2002).

Bertrand JY, Cisson JL, Stachura DL, Traver D. **Notch signaling distinguishes 2 waves of definitive hematopoiesis in the zebrafish embryo.** *Blood* **115**, 2777-2783 (2010).

Bertrand JY, Chi NC, Santoso B, Teng S, Stainier DY, Traver D. **Haematopoietic stem cells derive directly from aortic endothelium during development.** *Nature* **464**(7285):108-11 (2010).

Bertrand JY, Kim AD, Violette EP, Stachura DL, Cisson JL, Traver D. **Definitive hematopoiesis initiates through a committed erythromyeloid progenitor in the zebrafish embryo.** *Development* **134**(23):4147-56 (2007).

Blackburn EH. **Structure and function of telomeres.** *Nature* **350**:569-573 (1991).

Blackburn EH. **Telomeres and telomerase: their mechanisms of action and the effects of altering their functions.** *FEBS Lett* **579**, 859-862 (2005).

Blackburn EH, Greider CW, Szostak JW. **Telomeres and telomerase: the path from maize, Tetrahymena and yeast to human cancer and aging.** *Nat Med* **12**(10):1133-8 (2006).

Blasco MA. **Telomeres and human disease: ageing, cancer and beyond.** *Nat Rev Genet* **6**(8):611-22 (2005).

Blasco MA. **Telomere length, stem cells and aging.** *Nat Chem Biol* **3**:640-649 (2007).

Blasco MA, Funk W, Villeponteau B, Greider CW. **Functional characterization and developmental regulation of mouse telomerase RNA.** *Science* **269**:1267-1270 (1996).

Blasco MA, Lee HW, Hande MP, Samper E, Lansdorp PM, DePinho RA, Greider CW. **Telomere shortening and tumor formation by mouse cells lacking telomerase RNA.** *Cell* **91**, 25-34 (1997).

Blasco MA, Rizen M, Greider CW, Hanahan D. **Differential regulation of telomerase activity and telomerase RNA during multi-stage tumorigenesis.** *Nat Genet* **12**, 200-204 (1996).

Brummendorf TH & Balabanov S. **Telomere length dynamics in normal hematopoiesis and in disease states characterized by increased stem cell turnover.** *Leukemia* **20**, 1706-1716 (2006).

Burns CE, Traver D, Mayhall E, Shepard JL, Zon LI. **Hematopoietic stem cell fate is established by the Notch-Runx pathway.** *Genes Dev* **19**, 2331-2342 (2005).

Cairney CJ & Keith WN. **Telomerase redefined: integrated regulation of hTR and TERT for telomere maintenance and telomerase activity.** *Biochimie* **90**:13-23 (2008).

Canela A, Vera E, Klatt P, Blasco MA. **High-throughput telomere length quantification by FISH and its application to human population studies.** *Proc Natl Acad Sci USA* **104**:5300-5305 (2007).

Cayuela ML, Flores JM, Blasco MA. **The telomerase RNA component Terc is required for the tumour-promoting effects of Tert overexpression.** *EMBO Rep* **6**, 268-274 (2005).

Cesare AJ & Reddel RR. **Alternative lengthening of telomeres: models, mechanisms and implications.** *Nat Rev Genet* **11**(5):319-30 (2010).

Chen JL, Blasco MA, Greider CW. **Secondary structure of vertebrate telomerase RNA.** *Cell* **100**:503-514 (2000).

Chen JL & Greider CW. **Determinants in mammalian telomerase RNA that mediate enzyme processivity and cross-species incompatibility.** *EMBO J* **22**, 304-314 (2003).

Choi J, Southworth LK, Sarin KY, Venteicher AS, Ma W, Chang W, Cheung P, Jun S, Artandi MK, Shah N, Kim SK, Artandi SE. **TERT promotes epithelial proliferation through transcriptional control of a Myc- and Wnt-related developmental program.** *PLoS Genet* **4**(1):e10 (2008).

Chu C, Qu K, Zhong FL, Artandi SE, Chang HY. **Genomic maps of long noncoding RNA occupancy reveal principles of RNA-chromatin interactions.** *Mol Cell* **44**, 667-678 (2011).

Cohen SB, Graham ME, Lovrecz GO, Bache N, Robinson PJ, Red del RR. **Protein composition of catalytically active human telomerase from immortal cells.** *Science* **30**:1850-1853 (2007).

Cong Y & Shay JW. **Actions of human telomerase beyond telomeres.** *Cell Res* **18**:725-732 (2008).

Cong YS, Wright WE, Shay JW. **Human telomerase and its regulation.** *Microbiol Mol Biol Rev* **66**:407-425 (2002).

Curado S, Anderson RM, Jungblut B, Mumm J, Schroeter E, Stainier DY. **Conditional targeted cell ablation in zebrafish: a new tool for regeneration studies.** *Dev Dyn* **236**(4):1025-35 (2007).

d'Adda di Fagagna F, Reaper PM, Clay-Farrace L, Fiegler H, Carr P, Von Zglinicki T, Saretzki G, Carter NP, Jackson SP. **A DNA damage checkpoint response in telomere initiated senescence.** *Nature* **426**(6963):194-8 (2003).

Dahl R, Walsh JC, Lancki D, Laslo P, Iyer SR, Singh H, Simon MC. **Regulation of macrophage and neutrophil cell fates by the PU.1:C/EBPalpha ratio and granulocyte colony-stimulating factor.** *Nat Immunol* **4**, 1029-1036 (2003).

Darzacq X, Kittur N, Roy S, Shav-Tal Y, Singer RH, Meier UT. **Stepwise RNP assembly at the site of H/ACA RNA transcription in human cells.** *J Cell Biol* **173**:207-218 (2006).

de Jong JL & Zon LI. **Use of the zebrafish system to study primitive and definitive hematopoiesis.** *Annu Rev Genet* **39**:481-501 (2005).

de Lange T. **Shelterin: The protein complex that shapes and safeguards human telomeres.** *Genes Dev* **19**:2100-2110 (2005).

Detrich HW 3rd. **Fluorescent proteins in zebrafish cell and developmental biology.** *Methods Cell Biol* **85**:219-241 (2008).

Diotti R, Loayza D. **Shelterin complex and associated factors at human telomeres.** *Nucleus* **2**(2):119-35 (2011).

Dokal I, Bungey J, Williamson P, Oscier D, Hows J, Luzzatto L. **Dyskeratosis congenita fibroblasts are abnormal and have unbalanced chromosomal rearrangements.** *Blood* **80**, 3090-3096 (1992).

Donate LE & Blasco MA. **Telomeres in cancer and ageing.** *Philos Trans R Soc Lond B Biol Sci* **366**(1561):76-84 (2011).

Drachtman RA & Alter BP. **Dyskeratosis congenita.** *Dermatol Clin* **13**, 33-39 (1995)

Drummond MW, Balabanov S, Holyoake TL, Brummendorf TH. **Concise review: Telomere biology in normal and leukemic hematopoietic stem cells.** *Stem Cells* **25**, 1853-1861 (2007).

Egan ED & Collins K. **Biogenesis of telomerase ribonucleoproteins**. *RNA* **18**(10):1747-59 (2012).

Ekker SC & Larson JD. **Morphant technology in novel developmental systems.** *Genesis* **30**:89-93 (2001).

Ekker SC. **Nonconventional antisense in zebrafish for functional genomics applications.** *Methods Cell Biol* **77**:121-136 (2004).

Ellett F, Pase L, Hayman JW, Andrianopoulos A, Lieschke GJ. **mpeg1 promoter transgenes direct macrophage-lineage expression in zebrafish.** *Blood* **117**, e49-56 (2011).

Else T. **Telomeres and telomerase in adrenocortical tissue maintenance, carcinogenesis, and aging.** *J Mol Endocrinol* **43**(4):131-41 (2009).

Entringer S, Epel ES, Lin J, Buss C, Shahbaba B, Blackburn EH, Simhan HN, Wadhwa PD. **Maternal psychosocial stress during pregnancy is associated with newborn leukocyte telomere length.** *Am J Obstet Gynecol* **208**(2):134.e1-7 (2013).

Erduran E, Hacisalihoglu S, Ozoran Y. **Treatment of dyskeratosis congenita with granulocyte-macrophage colony-stimulating factor and erythropoietin.** *J Pediatr Hematol Oncol* **25**, 333-335 (2003).

Evans CJ, Hartenstein V, Banerjee U. **Thicker than blood: conserved mechanisms in *Drosophila* and vertebrate hematopoiesis.** *Dev Cell* **5**(5):673-90 (2003).

Feldser DM, Hackett JA, Greider CW. **Telomere dysfunction and the initiation of genome instability.** *Nature Reviews Cancer* **3**, 623-627 (2003).

Feng J, Funk WD, Wang S, Weinrich SL, Avilion AA, Chiu C, Adams RR, Chang E, Allsopp RC, Yu J, Le S, West M, Harley CB, Andrews WH, Greider CW, Villeponteau B. **The RNA component of human telomerase.** *Science* **269**:1236-1241 (1995).

Flynn RL, Centore RC, O'Sullivan RJ, Rai R, Tse A, Songyang Z, Chang S, Karlseder J, Zou L. **TERRA and hnRNPA1 orchestrate an RPA-to-POT1 switch on telomeric single-stranded DNA.** *Nature* **471**(7339):532-6 (2011).

Fragnet L, Blasco MA, Klapper W, Rasschaert D. **The RNA subunit of telomerase is encoded by Marek's disease virus.** *J Virol* **77**, 5985-5996 (2003).

Fu D & Collins K. **Distinct biogenesis pathways for human telomerase RNA and H/ACA small nucleolar RNAs.** *Mol Cell* **11**:1361-1372 (2003).

Fu D & Collins K. **Human telomerase and Cajal body ribonucleoproteins share a unique specificity of Sm protein association.** *Genes Dev* **20**:531-536 (2006).

Fu D & Collins K. **Purification of human telomerase complexes identifies factors involved in telomerase biogenesis and telomere length regulation.** *Mol Cell* **28**:773-785 (2007).

Galati A, Micheli E, Cacchione S. **Chromatin structure in telomere dynamics.** *Front Oncol* **3**:46 (2013).

Galloway JL, Wingert RA, Thisse C, Thisse B, Zon LI. **Loss of gata1 but not gata2 converts erythropoiesis to myelopoiesis in zebrafish embryos.** *Dev Cell* **8**, 109-116 (2005).

Galloway JL & Zon LI. **Ontogeny of hematopoiesis: examining the emergence of hematopoietic cells in the vertebrate embryo.** *Curr Top Dev Biol* **53**:139-58 (2003).

García CK, Wright WE, Shay JW. **Human diseases** of **telomerase dysfunction**: **insights into tissue aging**. *Nucleic Acids Res* **35**(22):7406-16 (2007). Review.

Geserick C & Blasco MA. **Novel roles for telomerase in aging.** *Mech Ageing Dev* **127**, 579-583 (2006).

Goldman FD, Aubert G, Klingelhutz AJ, Hills M, Cooper SR, Hamilton WS, Schlueter AJ, Lambie K, Eaves CJ, Lansdorp PM. **Characterization of primitive hematopoietic cells from patients with dyskeratosis congenita.** *Blood* **111**, 4523-4531 (2008).

Goldman F, Bouarich R, Kulkarni S, Freeman S, Du HY, Harrington L, Mason PJ, Londono-Vallejo A, Bessler M. **The effect of TERC haploinsufficiency on the inheritance of telomere length.** *Proc Natl Acad Sci USA* **102**, 17119-17124 (2005).

Gomez DE, Armando RG, Farina HG, Menna PL, Cerrudo CS, Ghiringhelli PD, Alonso DF. **Telomere structure and telomerase in health and disease (review).** *Int J Oncol* **41**(5):1561-9 (2012).

Gore AV, Monzo K, Cha YR, Pan W, Weinstein BM. **Vascular development in the zebrafish.** Cold Spring Harb Perspect Med **2**(5):a006684 (2012).

Greider CW. **Telomeres and senescence: the history, the experiment, the future.** *Curr Biol* **8**(5):178-81 (1998).

Greider CW. **Telomere length regulation.** *Annu Rev Biochem* **65**:337-365 (1996). Review.

Griffith JD, Comeau L, Rosenfield S, Stansel RM, Bianchi A, Moss H, de Lange T. **Mammalian telomeres end in a large duplex loop.** *Cell* **97**(4):503-14 (1999).

Hall C, Flores MV, Storm T, Crosier K, Crosier P. **The zebrafish lysozyme C promoter drives myeloid-specific expression in transgenic fish.** *BMC Dev Biol* **7**, 42 (2007).

Harley CB, Futcher AB, Greider CW. **Telomeres shorten during ageing of human fibroblasts.** *Nature* **345**(6274):458-60 (1990).

Hartenstein V & Mandal L. **The blood/vascular system in a phylogenetic perspective.** *Bioessays* **28**(12):1203-10 (2006).

Heiss NS, Knight SW, Vulliamy TJ, Klauck SM, Wiemann S, Mason PJ, Poustka A, Dokal I. **X-linked dyskeratosis congenita is caused by mutations in a highly conserved gene with putative nucleolar functions.** *Nat Genet* **19**, 32-38 (1998).

Henriques CM, Carneiro MC, Tenente IM, Jacinto A, Ferreira MG. **Telomerase is required for zebrafish lifespan.** *PLoS Genet* **9**, e1003214 (2013).

Henriques CM & Ferreira MG. **Consequences of telomere shortening during lifespan.** *Curr Opin Cell Biol* **24**(6):804-8 (2012).

Herbert BS, Hochreiter AE, Wright WE, Shay JW. **Nonradioactive detection of telomerase activity using the telomeric repeat amplification protocol.** *Nat Protoc* **1**, 1583-1590 (2006).

Herbomel P, Thisse B, Thisse C. **Zebrafish early macrophages colonize cephalic mesenchyme and developing brain, retina, and epidermis through a M-CSF receptor-dependent invasive process.** *Dev Biol* **238**, 274-288 (2001).

Hockemeyer D, Palm W, Wang RC, Couto SS, de Lange T. **Engineered telomere degradation models dyskeratosis congenita.** *Genes & Dev* **22**:1773-1785 (2008).

Hodes RJ, Hathcock KS, Weng NP. **Telomeres in T and B cells.** *Nat Rev Immunol* **2**, 699-706 (2002).

Imamura S, Uchiyama J, Koshimizu E, Hanai J, Raftopoulou C, Murphey RD, Bayliss PE, Imai Y, Burns CE, Masutomi K, Gagos S, Zon LI, Roberts TM, Kishi S. **A non-canonical function of zebrafish telomerase reverse transcriptase is required for developmental hematopoiesis.** *PLoS One* **3**, e3364 (2008).

Isogai S, Hitomi J, Yaniv K, Weinstein BM. **Zebrafish as a new animal model to study lymphangiogenesis.** Anat Sci Int **84**(3):102-11 (2009).

Jády BE, Bertrand E, Kiss T. **Human telomerase RNA and box H/ACA scaRNAs share a common Cajal body-specific localization signal.** *J Cell Biol* **164**:647-652 (2004).

Kamachi Y, Okuda Y, Kondoh H. **Quantitative assessment of knockdown efficiency of morpholino antisense oligonucleotides in zebrafish embryos using a luciferase assay.** *Genesis* **46**:1-7 (2007).

Kawai T & Akira S. **Signaling to NF-κB by Toll-like receptors.** *Trends Mol Med* **13**:460-469 (2007).

Kawakami K. **Transgenesis and gene trap methods in zebrafish by using the Tol2 transposable element.** *Methods Cell Biol* **77**:201-22 (2004).

Kimmel CB, Ballard WW, Kimmel SR, Ullmann B, Schilling TF. **Stages of embryonic development of the zebrafish.** *Dev Dyn* **203**, 253-310 (1995).

Kirwan M & Dokal I. **Dyskeratosis congenita, stem cells and telomeres.** *Biochim Biophys Acta* **1792**, 371-379 (2009).

Langheinrich U. **Zebrafish: a new model on the pharmaceutical catwalk.** *BioEssays* **25**:904-912 (2003).

Lau BW, Wong AO, Tsao GS, So KF, Yip HK. **Molecular cloning and characterization of the zebrafish (*Danio rerio*) telomerase catalytic subunit (telomerase reverse transcriptase, TERT).** *J Mol Neurosci* **34**(1):63-75 (2008).

Lee HW, Blasco MA, Gottlieb GJ, Horner JWII, Greider CW, DePinho RA. **Essential role of mouse telomerase in highly proliferative organs.** *Nature* **392**, 569-574 (1998).

Leong IU, Lai D, Lan CC, Johnson R, Love DR, Johnson R, Love DR. **Targeted mutagenesis of zebrafish: use of zinc finger nucleases.** *Birth Defects Res C Embryo Today* **93**(3):249-55 (2011). Review.

Li S, Crothers J, Haqq CM, Blackburn EH. **Cellular and gene expression responses involved in the rapid growth inhibition of human cancer cells by RNA interference-mediated depletion of telomerase RNA.** *J Biol Chem* **280**, 23709-23717 (2005).

Liongue C, Hall CJ, O'Connell BA, Crosier P, Ward AC. **Zebrafish granulocyte colony-stimulating factor receptor signaling promotes myelopoiesis and myeloid cell migration.** *Blood* **113**, 2535-2546 (2009).

Loynes CA, Martin JS, Robertson A, Trushell DM, Ingham PW, Whyte MK, Renshaw SA. **Pivotal Advance: Pharmacological manipulation of inflammation resolution during spontaneously resolving tissue neutrophilia in the zebrafish.** *J Leukoc Biol* **87**, 203-212 (2010).

Lundblad V & Blackburn EH. **An alternative pathway for yeast telomere maintenance rescues est1- senescence.** *Cell* **73**(2):347-60 (1993).

Ma D, Zhang J, Lin HF, Italiano J, Handin RI. **The identification and characterization of zebrafish hematopoietic stem cells.** *Blood* **118**, 289-297 (2011).

Maida Y, Yasukawa M, Furuuchi M, Lassmann T, Possemato R, Okamoto N, Kasim V, Hayashizaki Y, Hahn WC, Masutomi K. **RNA-dependent RNA polymerase formed by TERT and the RMRP RNA.** *Nature* **4610**:230-235 (2009).

Makarov VL, Hirose Y, Langmore JP. **Long G tails at both ends of human chromosomes suggest a C strand degradation mechanism for telomere shortening.** *Cell* **88**(5):657-66 (1997).

Marciniak R & Guarente L. **Human genetics: Testing telomerase.** *Nature* **413**, 370-373 (2001).

Marsh JC, Will AJ, Hows JM, Sartori P, Darbyshire PJ, Williamson PJ, Oscier DG, Dexter TM, Testa NG. **''Stem cell'' origin of the hematopoietic defect in dyskeratosis congenita.** *Blood* **79**, 3138-3144 (1992).

Martin CS, Moriyama A, Zon LI. **Hematopoietic stem cells, hematopoiesis and disease: lessons from the zebrafish model.** *Genome Med* **3**(12):83 (2011).

Martin-Rivera L, Herrera E, Albar JP, Blasco MA. **Expression of mouse telomerase catalytic subunit in embryos and adult tissues.** *Proc Natl Acad Sci USA* **95**, 10471-10476 (1998).

Meng X, Noyes MB, Zhu LJ, Lawson ND, Wolfe SA. **Targeted gene inactivation in zebrafish using engineered zinc-finger nucleases.** *Nat Biotechnol* **26**(6):695-701 (2008).

Mione MC & Trede NS. **The zebrafish as a model for cancer.** *Dis Model Mech* **3**(9-10):517-23 (2010).

Mitchell JR, Wood E, Collins K. **A telomerase component is defective in the human disease dyskeratosis congenita.** *Nature* **402**, 551-555 (1999).

Miyake Y, Nakamura M, Nabetani A, Shimamura S, Tamura M, Yonehara S, Saito M, Ishikawa F. **RPA-like mammalian Ctc1-Stn1-Ten1 complex binds to single-stranded DNA and protects telomeres independently of the Pot1 pathway.** *Mol Cell* **36**(2):193-206 (2009).

Monteiro R, Pouget C, Patient R. **The gata1/pu.1 lineage fate paradigm varies between blood populations and is modulated by tif1gamma.** *EMBO J* **30**, 1093-1103 (2011).

Morin GB. **The human telomere terminal transferase enzyme is a ribonucleoprotein that synthesizes TTAGGG repeats.** *Cell* **59**:521-529 (1989).

Murphey RD & Zon LI. **Small molecule screening in the zebrafish.** *Methods* **39**:255-261 (2006).

Nasevicius A & Ekker SC. **Effective targeted gene "knockdown" in zebrafish.** *Nat. Genet* **26**:216-220 (2000).

Nicoli S & Presta M. **The zebrafish/tumor xenograft angiogenesis assay.** *Nat Protoc* **2**:2918-2923 (2007).

Nishio N & Kojima S. **Recent progress in dyskeratosis congenita.** *Int J Hematol* **92**:419-424 (2010).

Oehler L, Reiter E, Friedl J, Kabrna E, Haas OA, Rosenkranz A, Lechner K, Geissler K. **Effective stimulation of neutropoiesis with rh G-CSF in dyskeratosis congenita: a case report.** *Ann Hematol* **69**, 325-327 (1994).

Ogami M, Ikura Y, Ohsawa M, Matsuo T, Kayo S, Yoshimi N, Hai E, Shirai N, Ehara S, Komatsu R, Naruko T, Ueda M. **Telomere shortening in human coronary artery diseases.** *Arterioscler Thromb Vasc Biol* **24**(3):546-50 (2004).

Olovnikov AM. **A theory of marginotomy. The incomplete copying of template margin in enzymic synthesis of polynucleotides and biological significance of the phenomenon.** *J Theor Biol* **41**(1):181-90 (1973).

O'neill LA & Bowie AG. **The family of five: TIR-domain-containing adaptors in Toll-like receptor signaling.** *Nat Rev Immunol* **7**:353-364 (2007).

Paik EJ & Zon LI. **Hematopoietic development in the zebrafish.** *Int J Dev Biol* **54**(6-7):1127-37 (2010).

Park JI, Venteicher AS, Hong JY, Choi J, Jun S, Shkreli M, Chang W, Meng Z, Cheung P, Ji H, McLaughlin M, Veenstra TD, Nusse R, McCrea PD, Artandi SE. **Telomerase modulates Wnt signalling by association with target gene chromatin.** *Nature* **460**, 66-72 (2009).

Patton EE & Zon LI. **The art and design of genetic screens: zebrafish.** *Nat Rev Genet* **2**:956–966 (2001).

Pereboom TC, van Weele LJ, Bondt A, MacInnes AW. **A zebrafish model of dyskeratosis congenita reveals hematopoietic stem cell formation failure resulting from ribosomal protein-mediated p53 stabilization.** *Blood* **118**(20):5458-65 (2011).

Porro A, Feuerhahn S, Reichenbach P, Lingner J. **Molecular dissection of telomeric repeat-containing RNA biogenesis unveils the presence of distinct and multiple regulatory pathways.** *Mol Cell Biol* **30**(20):4808-17 (2010).

Prescott J, Wentzensen IM, Savage SA, De Vivo I. **Epidemiologic evidence for a role of telomere dysfunction in cancer etiology.** *Mutat Res* **730**(1-2):75-84 (2012).

Prowse KR & Greider CW. **Developmental and tissue specific regulation of mouse telomerase and telomere length.** *Proc Natl Acad Sci USA* **92**, 4818-4822 (1995).

Putterman C, Safadi R, Zlotogora J, Banura R, Eldor A. **Treatment of the hematological manifestations of dyskeratosis congenita.** *Ann Hematol* **66**, 209-212 (1993).

Pyati UJ, Look AT, Hammerschmidt M. **Zebrafish as a powerful vertebrate model system for in vivo studies of cell death.** *Sem Cancer Biol* **17**:154-165 (2007).

Quaife NM, Watson O, Chico TJ. **Zebrafish: an emerging model of vascular development and remodelling.** *Curr Opin Pharmacol* **12**(5):608-14 (2012).

Ramanathan M, Haskó G, Leibovich SJ. **Analysis of signal transduction pathways in macrofages using expression vectors with CMV promoters: a cautionary tale**. *Inflammation* **29**:94-102 (2005).

Redon S, Reichenbach P, Lingner J. **The non-coding RNA TERRA is a natural ligand and direct inhibitor of human telomerase.** *Nucleic Acids Res* **38**(17):5797-806 (2010).

Renshaw SA & Trede NS. **A model 450 million years in the making: zebrafish and vertebrate immunity.** *Dis Model Mech* **5**(1):38-47 (2012).

Renshaw SA, Loynes CA, Trushell DM, Elworthy S, Ingham PW, Whyte MK. **A transgenic zebrafish model of neutrophilic inflammation.** *Blood* **108**, 3976-3978 (2006).

Rhodes J, Hagen A, Hsu K, Deng M, Liu TX, Look AT, Kanki JP. **Interplay of pu.1 and gata1 determines myelo-erythroid progenitor cell fate in zebrafish.** *Dev Cell* **8**, 97-108 (2005).

Richard P, Darzacq X, Bertrand E, Jády BE, Verheggen C, Kiss T. **A common sequence motif determines the Cajal bodyspecific localization of box H/ACA scaRNAs.** *EMBO J* **22**:4283-4293 (2003).

Rochowski A, Sun C, Glogauer M, Alter BP. **Neutrophil functions in patients with inherited bone marrow failure syndromes.** *Pediatr Blood Cancer* **57**, 306-309 (2011).

Rohner N, Perathoner S, Frohnhöfer HG, Harris MP. **Enhancing the efficiency of N-ethyl-N-nitrosourea-induced mutagenesis in the zebrafish.** *Zebrafish* **8**(3):119-23 (2011).

Royle NJ, Méndez-Bermúdez A, Gravani A, Novo C, Foxon J, Williams J, Cotton V, Hidalgo A. **The role of recombination in telomere length maintenance.** *Biochem Soc Trans* **37**(Pt 3):589-95 (2009).

Russo CL, Glader BE, Israel RJ, Galasso F. **Treatment of neutropenia associated with dyskeratosis congenita with granulocyte-macrophage colony-stimulating factor.** *Lancet* **336**, 751-752 (1990).

Santos JH, Meyer JN, Skorvaga M, Annab LA, Van Houten B. **Mitochondrial hTERT exacerbates free-radical-mediated mtDNA damage.** *Aging Cell* **6**:399-411 (2004).

Santos JH, Meyer JN, Van Houten B. **Mitochondrial localization of telomerase as a determinant for hydrogen peroxide-induced mitochondrial DNA damage and apoptosis.** *Hum Mol Genet* **15**:1757-1768 (2006).

Sarin KY, Cheung P, Gilison D, Lee E, Tennen RI, Wang E, Artandi MK, Oro AE, Artandi SE. **Conditional telomerase induction causes proliferation of hair follicle stem cells.** *Nature* **436**, 1048-1052 (2005).

Savage SA, Giri N, Baerlocher GM, Orr N, Lansdorp PM, Alter BP. **TINF2, a component of the shelterin telomere protection complex, is mutated in dyskeratosis congenita.** *Am J Hum Genet* **82**:501-509 (2008).

Schmidt R, Strahle U, Scholpp S. **Neurogenesis in zebrafish - from embryo to adult.** *Neural Dev* **8**:3 (2003).

Sepulcre MP, Alcaraz-Pérez F, López-Muñoz MA, Roca FJ, Meseguer J, Cayuela ML, Mulero V. **Fish TLR4 does not recognize bacterial LPS and negatively regulates MyD88 signaling pathway.** *J Immunol* **182**:1836-45 (2009).

Sfeir A. **Telomeres at a glance.** *J Cell Sci* **125**:4173-8 (2012).

Shay JW. **Molecular pathogenesis of aging and cancer: are telomeres and telomerase the connection?** *J Clin Pathol* **50**(10):799-800 (1997).

Sherr CJ & McCormick F. **The RB and p53 pathways in cancer.** *Cancer Cell* **2**(2):103-12 (2002).

Silvestre DC & Londoño-Vallejo A. **Telomere dynamics in mammals.** *Genome Dyn* **7**:29-45 (2010).

Solder B, Weiss M, Jager A, Belohradsky BH. **Dyskeratosis congenita: multisystemic disorder with special consideration of immunologic aspects. A review of the literature.** *Clin Pediatr (Phila)* **37**, 521-530 (1998).

Starr JM, McGurn B, Harris SE, Whalley LJ, Deary IJ, Shiels PG. **Association between telomere length and heart disease in a narrow age cohort of older people.** *Exp Gerontol* **42**(6):571-3 (2007).

Steffens JP, Masi S, D'Aiuto F, Spolidorio LC. **Telomere length and its relationship with chronic diseases - New perspectives for periodontal research.** *Arch Oral Biol* **58**(2):111-117 (2012).

Stewart JA, Chaiken MF, Wang F, Price CM. **Maintaining the end: roles of telomere proteins in end-protection, telomere replication and length regulation.** *Mutat Res* **730**(1-2):12-9 (2012).

Stewart SA, Hahn WC, O'Connor BF, Banner EN, Lundberg AS, Modha P, Mizuno H, Brooks MW, Fleming M, Zimonjic DB, Popescu NC, Weinberg RA. **Telomerase contributes to tumorigenesis by a telomere length-independent mechanism.** *Proc Natl Acad Sci USA* **99**, 12606-12611 (2002).

Sumanas S & Larson JD. **Morpholino phosphorodiamidate oligonucleotides in zebrafish: a recipe for functional genomics?** *Brief Functional Genomics Proteomics* **1**:239-256 (2002).

Teng SC, Chang J, McCowan B, Zakian VA. **Telomerase-independent lengthening of yeast telomeres occurs by an abrupt Rad50p-dependent, Rif-inhibited recombinational process.** *Mol Cell* **6**(4):947-52 (2000).

Teng SC & Zakian VA. **Telomere-telomere recombination is an efficient bypass pathway for telomere maintenance in *Saccharomyces cerevisiae*.** *Mol Cell Biol* **19**(12):8083-93 (1999).

Theimer CA & Feigon J. **Structure and function of telomerase RNA.** *Curr Opin Struct Biol* **16**:307-318 (2006).

Thisse C, Thisse B, Schilling TF, Postlethwait JH. **Structure of the zebrafish snail1 gene and its expression in wild-type, spadetail and no tail mutant embryos.** *Development* **119**, 1203-1215 (1993).

Trahan C & Dragon F. **Dyskeratosis congenita mutations in the H/ACA domain of human telomerase RNA affect its assembly into a pre-RNP.** *RNA* **15**, 235-243 (2009).

Traver D, Paw BH, Poss KD, Penberthy WT, Lin S, Zon LI. **Transplantation and *in vivo* imaging of multilineage engraftment in zebrafish bloodless mutants.** *Nat Immunol* **4**, 1238-1246 (2003).

Tsakiri KD, Cronkhite JT, Kuan PJ, Xing C, Raghu G, Weissler JC, Rosenblatt RL, Shay JW, García CK. **Adult-onset pulmonary fibrosis caused by mutations in telomerase.** *Proc Natl Acad Sci USA* **104**, 7552-7557 (2007).

Tsao DA, Wu CW, Lin YS. **Molecular cloning of bovine telomerase RNA.** *Gene* **221**:51-58 (1998).

Tycowski KT, Shu MD, Kukoyi A, Steitz JA. **A conserved WD40 protein binds the Cajal body localization signal of scaRNP particles.** *Mol Cell* **34**:47-57 (2009).

Ulaner GA, Giudice LC. **Developmental regulation of telomerase activity in human fetal tissues during gestation.** *Mol Hum Reprod* **3**(9):769-73 (1997).

van der Sar AM, Musters RJ, van Eeden FJ, Appelmelk BJ, Vandenbroucke-Grauls CM, Bitter W. **Zebrafish embryos as a model host for the real time analysis of *Salmonella typhimurium* infections.** *Cell Microbiol* **5**, 601-611 (2003).

van der Sar AM, Stockhammer OW, Laan C van der, Spaink HP, Bitter W, Meijer AH. **MyD88 innate immune function in a zebrafish embryo infection model.** *Infect Immun* **74**:2436-2441 (2006).

Venteicher AS, Abreu EB, Meng Z, McCann KE, Terns RM, Veenstra TD, Terns MP, Artandi SE. **A human telomerase holoenzyme protein required for Cajal body localization and telomere synthesis.** *Science* **323**:644-648 (2009).

Veinteicher AS, Meng Z, Mason PJ, Veenstra TD, Artandi SE. **Identification of ATPases pontin and reptin as telomerase components essential for holenzyme activity.** *Cell* **132**:945-957 (2008).

Vercammen E, Staal J, Beyaert R. **Sensing of viral infection and activation of innate immunity by toll-like receptor 3.** *Clin Microbiol Rev* **21**:13-25 (2008).

Vulliamy T, Beswick R, Kirwan M, Marrone A, Digweed M, Walne A, Dokal I. **Mutations in the telomerase component NHP2 cause the premature ageing syndrome dyskeratosis congenita.** *Proc Natl Acad Sci USA* **105**:8073-8078 (2008)

Vulliamy TJ & Dokal I. **Dyskeratosis congenita: the diverse clinical presentation of mutations in the telomerase complex.** *Biochimie* **90**, 122-130 (2008).

Vulliamy TJ, Knight SW, Mason PJ, Dokal I. **Very short telomeres in the peripheral blood of patients with X-linked and autosomal dyskeratosis congenita.** *Blood Cells Mol Dis* **27**, 353-357 (2001).

Vulliamy T, Marrone A, Dokal I, Mason PJ. **Association between aplastic anaemia and mutations in telomerase RNA.** *Lancet* **22**:2168-2170 (2002).

Vulliamy T, Marrone A, Goldman F, Dearlove A, Bessler M, Mason PJ, Dokal I. **The RNA component of telomerase is mutated in autosomal dominant dyskeratosis congenita.** *Nature* **413**, 432-435 (2001).

Vulliamy TJ, Marrone A, Knight SW, Walne A, Mason PJ, Dokal I. **Mutations in dyskeratosis congenita: their impact on telomere length and the diversity of clinical presentation.** *Blood* **107**, 2680-2685 (2006).

Vulliamy T, Marrone A, Szydlo R, Walne A, Mason PJ, Dokal I. **Disease anticipation is associated with progressive telomere shortening in families with dyskeratosis congenita due to mutations in TERC.** *Nat Genet* **36**, 447-449 (2004).

Walne AJ & Dokal I. **Dyskeratosis Congenita: a historical perspective.** *Mech Ageing Dev* **129**:48-59 (2008).

Walne AJ, Vulliamy T, Marrone A, Beswick R, Kirwan M, Masunari Y, Al-Qurashi FH, Aljurf M, Dokal I. **Genetic heterogeneity in autosomal recessive dyskeratosis congenita with one subtype due to mutations in the telomerase associated protein NOP10.** *Hum Mol Genet* **16**, 1619-1629 (2007).

Watson JD. **Origin of concatemeric T7 DNA.** *Nat New Biol* **239**(94):197-201 (1972).

Westerfield, M. **The Zebrafish Book. A Guide for the Laboratory Use of Zebrafish *Danio* (Brachydanio) rerio.** Eugene, OR.: University of Oregon Press (2000).

Wellinger RJ, Ethier K, Labrecque P, Zakian VA. **Evidence for a new step in telomere maintenance.** *Cell* **85**(3):423-33 (1996).

White RM, Sessa A, Burke C, Bowman T, LeBlanc J, Ceol C, Bourque C, Dovey M, Goessling W, Burns CE, Zon LI. **Transparent adult zebrafish as a tool for *in vivo* transplantation analysis.** *Cell Stem Cell* **2**, 183-189 (2008).

Wright WE & Shay JW. **Telomere dynamics in cancer progression and prevention: fundamental differences in human and mouse telomere biology.** *Nat Med* **6**, 849-851 (2000).

Wyatt HDM, West SC, Beattie TL. **InTERTpreting telomerase structure and function.** *Nucleic Acids Res* **38**:5609-5612 (2010).

Xie M, Mosig A, Qi X, Li Y, Stadler PF, Chen JJ. **Structure and function of the smallest vertebrate telomerase RNA from teleost fish.** *J Biol Chem* **283**, 2049-2059 (2008).

Yel L, Tezcan I, Sanal O, Ersoy F, Berkel AI. **Dyskeratosis congenita: unusual onset with isolated neutropenia at an early age.** *Acta Paediatr Jpn* **38**, 288-290 (1996).

Yilmaz K, Inaloz HS, Unal B, Guler E. **Dyskeratosis congenita with isolated neutropenia and granulocyte colony-stimulating factor treatment.** *Int J Dermatol* **41**, 170-172 (2002).

Zhang Y, Morimoto K, Danilova N, Zhang B, Lin S. **Zebrafish models for dyskeratosis congenita reveal critical roles of p53 activation contributing to hematopoietic defects through RNA processing.** *PLoS One* **7**(1):e30188 (2012).

Zhong F, Savage SA, Shkreli M, Giri N, Jessop L, Myers T, Chen R, Alter BP, Artandi SE. **Disruption of telomerase trafficking by TCAB1 mutation causes dyskeratosis congenita.** *Genes Dev* **25**:11-16 (2011).

Zijlmans JM, Martens UM, Poon SS, Raap AK, Tanke HJ, Ward RK, Lansdorp PM. **Telomeres in the mouse have large inter-chromosomal variations in the number of T2AG3 repeats.** *Proc Natl Acad Sci USA* **94**, 7423-7428 (1997).

Zon LI & Peterson R. ***In vivo* drug discovery in the zebrafish.** *Nat Rev Drug Discov* **41**:35-44 (2005).

Publications

Alcaraz-Pérez F, Mulero V, Cayuela ML (2008). Application of the dual-luciferase reporter assay to the analysis of promoter activity in zebrafish embryos. *BMC Biotechnol.* 8, pp. 81 - 81.

Sepulcre MP, **Alcaraz-Pérez F**, López-Muñoz A, Roca FJ, Meseguer J, Cayuela ML, Mulero V (2009). Evolution of lipopolysaccharide (LPS) recognition and signaling: fish TLR4 does not recognize LPS and negatively regulates NF-kappaB activation. *J Immunol.* 182 - 4, pp. 1836 - 45.

Jelassi B, Chantôme A, **Alcaraz-Pérez F**, Baroja-Mazo A, Cayuela ML, Pelegrín P, Surprenant A, Roger S (2011). P2X(7) receptor activation enhances SK3 channels- and cystein cathepsin-dependent cancer cells invasiveness. *Oncogene.* 30 - 18, pp. 2108 - 22.

Anchelin M, Murcia L, **Alcaraz-Pérez F**, García-Navarro EM, Cayuela ML (2011). Behaviour of telomere and telomerase during aging and regeneration in zebrafish. *PLoS One.* 6 - 2, pp. e16955 - e16955.

Espín R, Roca FJ, Candel S, Sepulcre MP, González-Rosa JM, **Alcaraz-Pérez F**, Meseguer J, Cayuela ML, Mercader N, Mulero V (2013). TNF receptors regulate vascular homeostasis through a caspase-8, caspase-2 and P53 apoptotic program that bypasses caspase-3. *Dis Model Mech.* 6, 383-396.

Anchelin M, **Alcaraz-Pérez F**, Martínez CM, Bernabé-García M, Mulero V, Cayuela ML (2013). Premature aging in telomerase-deficient zebrafish. *Dis Model Mech.* doi: 10.1242/dmm.011635.

Angosto D, Montero J, Lopez-Muñoz A, **Alcaraz-Pérez F**, Bird S, Sarropoulou E, Abellán E, Meseguer J, Sepulcre MP, Mulero V (2013). Identification and functional characterization of a new IL-1 family member, IL-1Fm2, in most evolutionarily advanced fish. *Innate Immun*.

Alcaraz-Pérez F, García-Castillo J, García-Moreno D, López-Muñoz A, Anchelin M, Angosto D, Zon LI, Mulero V, Cayuela ML. (2014). A non-canonical function of telomerase RNA in the regulation of developmental myelopoiesis in zebrafish. *Nat Commun*. 5:3228. doi: 10.1038/ncomms4228.

Crottès D, **Alcaraz-Pérez F**, Tichet M, Gariano G, Martial S, Guizouarn H, Pellissier B, Loubat A, Presta M, Tartare-Deckert S, Cayuela ML, Martin P, Borgese F and Soriani O (2014). Sig1R potentiates chronic myeloid leukemic cell invasiveness potency by shaping membrane cell electrical activity in response to ECM stimulation. *PLoS Biol*. (*Under review*).

Resumen en español

1. Introducción

Los cromosomas eucariotas consisten en grandes moléculas de ADN lineal y proteínas asociadas que almacenan la información genética en los organismos vivos. En los extremos, los cromosomas tienen una estructura nucleoproteica especial llamada **telómero** que "camufla" los extremos libres, evitando que sean reconocidos por los mecanismos celulares que monitorizan daño en el ADN, y asegurando así la integridad de los cromosomas [Greider, 1996].

El principal problema de los telómeros es el conocido como "problema de la replicación de los extremos". Este problema surge como consecuencia de que todas las ADN polimerasas funcionan en la dirección 5'→3' y requieren la presencia de un oligonucleótido de ARN como punto de partida. Como resultado, los cromosomas lineales se acortan con cada ronda de replicación [Watson, 1972; Olovnikov, 1973]. En ausencia de un mecanismo compensatorio, tras un número de divisiones celulares las células acabarían perdiendo material génico y desembocando en la muerte celular prematura, lo que pondría en peligro la supervivencia no sólo del individuo sino también de las especies.

Los organismos eucariotas han solventado este problema mediante la **telomerasa**, que es una DNA polimerasa dependiente de RNA con actividad retrotranscriptasa que añade repeticiones teloméricas al final de los cromosomas, haciendo posible que la longitud de los telómeros se mantenga constante [Blackburn, 2005]. La telomerasa es un complejo ribonucleoproteico compuesto por una subunidad catalítica (TERT), un componente de RNA (*TR*) que actúa como molde para la síntesis de telómeros y una serie de proteínas accesorias específicas de especie encargadas de regular la biogénesis, de la localización subcelular y de otra funciones *in vivo* de la telomerasa [Wyatt *et al.*, 2010]. En humanos, se han identificado 7 proteínas: Dyskerin, NHP2, NOP10, Pontin, Reptin, GAR1 y TCAB1 [Fu & Collins, 2007].

Una longitud telomérica por encima de un límite es un prerrequisito para que haya replicación celular [Blackburn *et al.*, 2006]. La telomerasa es activa durante la embriogénesis y el desarrollo mientras que, en adultos, está limitada a los tipos celulares con una alta tasa de proliferación (piel, intestino, linfocitos activados), a la línea germinal y a las células madre [Ulaner *et al.*, 1997]. En el resto de tipos celulares, los

telómeros se acortan de manera progresiva con cada división hasta que alcanzan una longitud crítica y, entonces, se activan los mecanismos de respuesta de daño en el ADN y las células entran en senescencia, o bien sufren apoptosis [Blasco, 2005; Galati *et al.*, 2013]. Sin embargo, a veces las células pueden sufrir daños en los mecanismos de control de daño en el ADN y, en vez de entrar en senescencia, continúan proliferando de manera ilimitada, dando lugar a la aparición de tumores que, en combinación con otras mutaciones, pueden acabar desarrollando un cáncer. En estos casos, las células re-establecen la estabilidad genómica y también la longitud telomérica ya sea mediante la re-expresión de la telomerasa o por un mecanismo de mantenimiento de los telómeros independiente de la telomerasa y basado en la recombinación homóloga, el denominado "mecanismo ALT" (por sus siglas en inglés, *alternative lengthening of telomeres*) [Lundblad & Blackburn, 1993; Teng &. Zakian, 1999; Teng *et al*., 2000].

Al margen de su función en la síntesis de los telómeros, se han descrito otras funciones del complejo de la telomerasa que se han denominado **funciones "extracurriculares"**. Por ejemplo, en humanos, TERT puede funcionar como un modulador transcripcional de la ruta de señalización de Wnt-β-catenina [Park *et al.*, 2009]. También se sabe que forma un complejo con un ARN distinto de *TR*, funcionando como una ARN polimerasa dependiente de ARN [Maida et al., 2009]. La telomerasa también está implicada en la regulación de la apoptosis de manera independiente al mantenimiento de los telómeros [Cong & Shay, 2008] y a través de la mitocondria [Santos *et al*., 2006]. Y, es más, se sabe que la contribución de TERT a la proliferación epitelial, a la tumorogénesis y al envejecimiento también está mediada por un mecanismo independiente del alargamiento telomérico [Choi *et al.*, 2008; Sarin *et al.*, 2005; Stewart *et al.*, 2002; Geserick & Blasco, 2006]. En contraste con TERT, cuya transcripción está reprimida en la mayoría de células somáticas, *TR* se expresa de manera constitutiva en las células humanas, y se ensambla como un complejo ribonucleoproteico estable de manera ubicua [Cong *et al.*, 2002; Cairney & Keith, 2007], lo que sugiere una función "extracurricular" también para *TR*. Por ejemplo, se sabe que *TR* contribuye a la promoción del cáncer de manera independiente a la actividad telomerasa [Blasco *et al.*, 1996; Cayuela *et al.*, 2005; Fragnet *et al.*, 2003; Li *et al*., 2005]. Y, en un estudio reciente, se han identificado 2198 sitios de unión de *TR* en el genoma, lo que respalda la teoría de que *TR* pudiera actuar como un modulador transcripcional de otros genes [Chu *et al*., 2011].

Los telómeros están implicados directamente en la senescencia celular, jugando un papel fundamental en los procesos de envejecimiento. A las enfermedades asociadas con el acortamiento de los telómeros se les conoce como **enfermedades teloméricas**. Se han descrito múltiples mutaciones en distintos componentes del complejo de la telomerasa en el contexto de varios síndromes de envejecimiento prematuro, como son la diskeratosis congénita [Walne & Dokal, 2008], la anemia aplásica [Vulliamy *et al.*, 2002], el síndrome de Hoyeraal-Hreidarsson [Nishio & Kojima, 2010] y la fibrosis pulmonar idiopática [Armanios, 2012]. El denominador común en todas estas enfermedades es el acortamiento telomérico [Armanios, 2009]. La **diskeratosis congénita** (DC) fue la primera enfermedad asociada con mutaciones en la telomerasa [Walne & Dokal, 2008]. Se trata de un síndrome de envejecimiento prematuro con una incidencia de 1 de cada 100.000 aproximadamente. Las manifestaciones clínicas generalmente aparecen en la infancia, incluyendo pigmentación anormal de la piel, distrofia de las uñas y leucoplaquia oral. A estos síntomas característicos, les acompañan retraso en el desarrollo, pérdida de pelo y fallo de órganos. El fallo de la médula ósea es la principal causa de muerte, a la edad media de 16 años, seguida por la fibrosis pulmonar y el cáncer [Marciniak & Guarente, 2001]. Existen tres modos de herencia de la DC: recesiva asociada al cromosoma X (con mutaciones en diskerin) [Heiss *et al*., 1998], autosómica dominante (con mutaciones en TERT, *TR* y TIN2) [Vulliamy *et al.*, 2001; Vulliamy *et al.*, 2004] y autosómica recesiva (con mutaciones en NOP10) [Walne *et al*., 2007]. Independientemente del modo de herencia genética, todos los pacientes de DC tienen en común el acortamiento telomérico [Mitchell *et al.*, 1999; Vulliamy *et al*., 2004; Armanios *et al*., 2005; Vulliamy *et al*., 2001], siendo la severidad del fenotipo inversamente proporcional a la longitud telomérica [Vulliamy *et al.*, 2006]. Sólo cuando las mutaciones afectan a TERT o a *TR*, se da el *fenómeno de anticipación*, es decir, la enfermedad se presenta y se agrava cada vez más temprano en las sucesivas generaciones [Vulliamy *et al*., 2004; Armanios *et al*., 2005].

El acortamiento telomérico debido a la disfunción de la telomerasa tiene una gran relevancia en el proceso fisiológico del envejecimiento, como sugiere el fenotipo de los modelos de ratón deficientes en telomerasa [Blasco *et al.*, 1997; Lee *et al.*, 1998]. Tras sucesivas generaciones de ratones deficientes en *TR*, una vez que se alcanza una longitud telomérica crítica, estos ratones muestran un fenotipo de envejecimiento prematuro: menor esperanza de vida, alopecia, disminución de la viabilidad celular de

tejidos altamente proliferativos, disminución de la capacidad de reparación de heridas y un ligero incremento en la indidencia de cáncer. Sin embargo, los modelos de ratón deficientes en telomerasa no reproducen con fidelidad los síntomas de las enfermedades teloméricas humanas, presumiblemente porque su longitud telomérica de partida es mucho mayor que la de humanos [Blasco *et al.*, 1997; Zijlmans *et al.*, 1997], presentan actividad telomerasa en la mayoría de sus tejidos [Prowse & Greider, 1995; Martin-Rivera *et al.*, 1998], y porque el acortamiento telomérico no juega un papel clave en la senescencia celular [Wright & Shay, 2000]. Por todo ello, se necesita un modelo animal alternativo al de ratón que sea capaz de reproducir la sintomatología de las enfermedades teloméricas humanas para poder estudiarlas con más detalle.

El **pez cebra** es un excelente modelo vertebrado para el estudio tanto de la ciencia básica como la aplicada. Hasta la fecha, el pez cebra ha sido propuesto como un excelente modelo vertebrado para el estudio del sistema inmunitario [Renshaw & Trede, 2012], la hematopoyesis [Martin *et al.*, 2011], el desarrollo vascular [Isogai *et al.*, 2009; Quaife *et al.*, 2012; Gore *et al.*, 2012], la neurogénesis [Schmidt *et al.*, 2013] y el cáncer [Mione & Trede, 2010], entre otros.

La hematopoyesis del pez cebra es similar a la de humanos, y tiene distintas fases durante la embriogénesis [de Jong & Zon, 2005; Galloway & Zon, 2003; Chen & Zon, 2009]. Tal es así, que el pez cebra ha sido validado por numerosos trabajos para el estudio de la regulación de la biología de las células madre hematopoyéticas y de la diferenciación de los distintos linajes, lo cual es necesario para mejorar el diagnóstico y el tratamiento de enfermedades hematopoyéticas humanas y las terapias de trasplante de médula ósea.

En 2011, Anchelin y colaboradores publicaron un estudio sobre el comportamiento de los telómeros y la telomerasa durante los procesos de envejecimiento y regeneración en el pez cebra, concluyendo que la longitud telomérica y la expresión de la telomerasa están estrechamente relacionadas a lo largo del ciclo de vida del pez y son limitantes para la duración de la vida, por lo que ambos parámetros pueden usarse como biomarcadores de envejecimiento del pez cebra [Anchelin *et al.*, 2011].

El pez cebra tiene una longitud telomérica similar a la de humanos y, como en ellos, constituye un factor limitante del número de divisiones celulares. De hecho, en

dos estudios recientes, se ha caracterizado un modelo de pez cebra deficiente en telomerasa que muestra síntomas de envejecimiento prematuro desde la primera generación y también reproduce el fenómeno de anticipación observado en humanos con DC [Anchelin *et al*., 2013; Henriques *et al*., 2013]. Por tanto, el pez cebra es un modelo complementario al de ratón para estudiar las enfermedades teloméricas. Tal es así, que en los últimos dos años se han desarrollado tres modelos de pez cebra para el estudio de la DC que tienen afectado el complejo de la telomerasa, dos con con mutaciones en los genes *nop10* y nola1, y el tercero, deficiente para *dkc1* [Pereboom *et al.*, 2011; Zhang *et al.*, 2012]. Los tres modelos presentan defectos hematopoyéticos mediados por p53 debido a un procesamiento defectuoso del ARN ribosómico 18S, pero sin que se vean afectados ni la longitud telomérica ni la actividad telomerasa en los estadíos tempranos de la enfermedad, sugiriendo que su papel en el mantenimiento telomérico no contribuye a la DC hasta fases más tardías. La presencia de telomerasa en distintos tejidos puede estar asociada al crecimiento indeterminado de los teleósteos. Sin embargo, *tert* también se expresa en las neuronas de la retina [Lau *et al*., 2008], que son células post-mitóticas que no se dividen en condiciones normales, lo que sugiere que, como en humanos, la telomerasa tiene otras funciones "extracurriculares" en el pez cebra. Por ejemplo, se sabe que zfTERT promueve el desarrollo de las células hematopoyéticas a través de un mecanismo no canónico que es independiente de la actividad telomerasa y de su papel en el mantenimiento de los telómeros [Imamura *et al*., 2008].

2. Objetivos

En el presente trabajo se proponen los siguientes objetivos concretos:

1. Desarrollo de un nuevo sistema chivato basado en la luciferasa para el estudio de promotores tanto constitutivos como inducibles en el contexto de un organismo completo.

2. Estudio del papel extracurricular del componente de ARN de la telomerasa (*TR*) en la hematopoyesis usando el pez cebra como modelo.

3. Materiales y Métodos

Animales

Peces cebra (*Danio rerio*) fueron cedidos por el centro internacional de recursos del pez cebra (ZIRC, Oregón, EEUU) y mantenidos como se describe en el manual del pez cebra [Westerfield, 2000]. La línea mutante para *tert* (alelo hu3430) fue obtenida del Instituto Sanger y ha sido previamente descrita [Anchelin *et al.*, 2013; Henriques *et al.*, 2013]. La línea mutante *casper* [White *et al.*, 2008] y la línea transgénica Tg(*gata1*:DsRed) [Traver *et al.*, 2003] también fueron descritas previamente. Las líneas transgénicas Tg(*lyz*::DsRed) [Hall *et al.*,2007], Tg(*mpx*::eGFP) [Renshaw *et al.*,2006], Tg(*mpeg1*::GAL4/*uas*::NTRmCherry) (en el texto se usa *mpeg1*::mCherry para mayor simplicidad) [Ellett *et al.*, 2011] y Tg(*cd41*::eGFP) [Ma *et al.*, 2011] fueron amablemente proporcionadas por los Drs. P. Crosier, SA. Renshaw , G. Lieschke y RI. Handin, respectivamente.

Los experimentos desarrollados cumplen con la directiva de la Unión Europea (86/609/EU) y han sido aprobados por el Comité de Bioética del Hospital Clínico Universitario "Virgen de la Arrixaca" (España) y por el Comité Institucional del Cuidado y Uso Animal del Hospital Infantil de Boston (EEUU).

Microinyección

ADN, ARN, PAMPs o morfolinos, solos o en combinación, se prepararon en la mezcla de microinyección (0.5x de tampón Tango y rojo fenol al 0.05 %) y se microinyectaron en el saco vitelino de embriones de pez cebra en el estadío de desarrollo de 1-8 células usando un microinyector Narishige IM300 (0.5-1 nL por embrión). Una vez microinyectados, los embriones se incubaron en *egg water* a 28.5 ºC.

Dual-luciferase reporter assay

Transcurridas 24-48 horas después de la microinyección, se seleccionaron los embriones vivos y se distribuyeron de tres en tres en tubos de microcentrífuga de 1.5 mL. El *egg water* se retiró y los embriones se lavaron con PBS, que también fue retirado. Los embriones se incubaron en 50 μL de PLB 1x [del *kit Dual-Luciferase*

Reporter Assay System (Promega, Cat.# E1910)], durante 30 min a temperatura ambiente y agitando a 150 rpm. Después de la incubación, los embriones se homogenizaron mecánicamente y el extracto fue centrifugado durante 3 min a 13,000 rpm para quitar los debris celulares. Finalmente se procedió a medir las actividades luciferasa de luciérnaga y de *Renilla* según las instrucciones del fabricante.

Análisis del desarrollo

El efecto de los morfolinos en el desarrollo fue evaluado como se publicó anteriormente [Kimmel *et al.*, 1995]. Brevemente, se analizó la presencia de flexiones de lado a lado a las 22 horas de vida (estadío de 25-26 somitos); el latido cardiaco, la presencia de células rojas en el saco vitelino y la pigmentación primaria de la retina y de la piel a las 24 horas (estadío Prim 5); el ángulo formado por la cabeza y el tronco (HTA), la pigmentación de la retina, el inicio de la circulación, el reflejo al tacto, la completa extensión de la cola y el desarrollo de la arteria caudal hasta la mitad de la cola a las 30 horas (estadío Prim 15); y el inicio de la movilidad, la pigmentación de la cola, la circulación fuerte, y el desarrollo de la arteria caudal hasta las ¾ de la cola a las 36 horas (estadío Prim 30).

Marcaje de neutrófilos

Embriones de pez cebra de diferentes edades fueron fijados durante toda la noche en paraformaldehído al 4% en PBS a 4 ºC. Una vez fijadas, las larvas fueron lavadas brevemente en PBS dos veces y entonces fueron incubadas en una dilución 1:50 de *TSA Cyanine5* (*TSA*^{TM}*-Plus Fluorescein* kit, Perkin Elmer, Reino Unido) protegidas de la luz durante 10 min a 28°C. Entonces, las larvas fueron re-fijadas durante 20 min y la actividad peroxidasa endógena fue enmascarada con 1 hora de incubación en H_2O_2 al 0.3%. Finalmente, los neutrófilos marcados con fluoresceína fueron contados manualmente usando un estereomicroscopio de fluorescencia Lumar V12 equipado con una cámara digital (AxioCam MRm) (Zeiss).

Obtención y tinción de células sanguíneas

Embriones de pez cebra de diferentes edades fueron anestesiados en una disolución de tricaína al 0.02% (Sigma) y BSA al 1% en PBS, con pH 7.4. Las células

sanguíneas se obtuvieron mediante punción cardiaca sobre un portaobjetos, en el que inmediatamente se hizo un frotis. Una vez seco, las células fueron fijadas en methanol durante 30 segundos y teñidas según el método Wright-Giemsa [Imamura *et al.* 2008].

Tinción con o-dianisidina

Para la tinción específica de eritrocitos, embriones de pez cebra de 2 días de edad fueron anestesiados con tricaína al 0.02% en *egg water* e incubados con o-dianisidina (Sigma) a 1mg/ml en tampón de tinción (etanol al 40%, NaAc 10mM y H_2O_2 al 0.675%) durante 15 minutos en oscuridad. Las imágenes de los embriones se obtuvieron con un estereomicroscopio Scope.A1 equipado con una cámara digital (AxioCam ICc 3, Zeiss).

Citometría de flujo

Entre 300 y 600 larvas de pez cebra de la línea transgénica tg(*mpx*:eGFP) de 2 y 3 días de edad fueron anestesiadas con tricaína al 0.02% en *egg water*, troceadas con un bisturí e incubadas con liberasa (Roche) a 0.077 mg/mL durante 30 minutos a 28°C. La suspensión celular resultante se pasó por un filtro de 40 µm y las células $eGFP^+$ fueron separadas usando un citómetro Beckman Coulter MoFlo Legacy Cell Sorter en el Bauer Core de la Universidad de Harvard.

Ensayo de la actividad telomerasa

El análisis de la actividad telomerasa se llevó a cabo mediante el protocol de amplificación de las repeticiones teloméricas cuantitativo (Q-TRAP) que fue descrito por Herbert y colaboradores en 2006 con ligeras modificaciones [Anchelin *et al.*, 2011]. Los datos fueron convertidos a unidades de actividad telomerase relativa (RTA) con el siguiente cálculo: RTA de la muestra=$10^{(Ct\ \text{muestra}-\gamma\text{int})/\text{pendiente}}$. La curva estándar obtenida fue: y= -3.2295x + 23.802.

Q-FISH

La longitud telomérica de células sanguíneas en interfase, obtenidas como se describe anteriormente, fue analizada de manera cuantitativa mediante una hibridación

in situ con una sonda fluorescente, como describieron Canela y colaboradores en 2007. Las imágenes de fluorescencia de Cy3 y DAPI fueron capturadas con un microscopio de fluorescencia Nikon Direct Eclipse equipado con una cámara digital Nikon DXM 1200C. La señal de fluorescencia de los telómeros fue cuantificada usando el programa TFL-TELO de Peter Lansdorp (Vancouver, Canada).

Ensayo de reclutamiento

Larvas de pez cebra de la línea transgénica tg(*mpx*:eGFP) de 3 días de edad fueron anestesiadas con tricaína al 0.02% en *egg water* y se hizo una transección completa de la cola con un bisturí estéril. Entonces, las larvas fueron montadas en agarosa de bajo punto de fusión al 1% (wt/vol) en *egg water*. El éxito de la transección fue confirmado inmediatamente mediante un estereomicroscopio de epifluorescencia Lumar V12 equipado con filtros de fluorescencia verde, con el que se tomaron imágenes que fueron establecidas como tiempo cero. A partir de entonces, se fueron tomando imágenes a distintos tiempos experimentales mientras las larvas continuaban a 28.5 ºC, montadas en la matriz de agarosa empapada con *egg water*. Todas las imágenes fueron adquiridas con la cámara integrada en el estereomicroscopio y posteriormente fueron usadas para contar el número de neutrófilos reclutados a la zona de la herida, establecida entre el bucle arterio-venoso y el final de la cola.

Ensayo de infección bacteriana

Las larvas de pez cebra fueron infectadas con ~10 CFU/larva de la estirpe salvaje 12023 de *Salmonella enterica serovar Typhimurium* (*S. typhimurium*), amablemente cedida por el Prof. DW Holden. Brevemente, las bacterias fueron inyectadas en el conducto de Cuvier de larvas de 2 días de edad, y la aparición de signos de enfermedad y la supervivencia fueron monitorizadas cada 24 horas durante 5 días [van der Sar *et al.*, 2003].

Hibridación *in situ*

Para este ensayo se utilizaron embriones transparentes de la línea mutante *casper*. El análisis de la expresión génica mediante hibridación *in situ* con sondas de ARN se

llevó a cabo según describieron Thisse y colaboradores en 1993. Las sondas de ARN para *TR*, *tert*, *lmo2*, *spi1* (*pu.1*), *gata1*, *gcsfr*, *cmyb*, *runx1* y *rag1* RNA se generaron a partir de plásmidos linealizados según las instrucciones del kit *DIG RNA Labeling Kit* (Roche Applied Science). Las imágenes de los embriones fueron tomadas con un estereomicroscopio Scope.A1 equipado con una cámara digital (AxioCam ICc 3, Zeiss).

Análisis de la expression génica

El ARN total fue extraído de embriones/larvas o de suspensions celulares con TRIzol (Invitrogen) siguiendo las instrucciones del fabricante y posteriormente fue tratado con DNasa I libre de RNasa (Invitrogen). La retrotranscriptasa Superscript III RNasa H^- (Invitrogen) se usó para sintetizar el cDNA con un cebador oligo-dT_{18} (para todos los genes, excepto para *TR*) o R1 (para *TR*) a partir de 1 μg de RNA total a 50ºC durante 50 minutos. La PCR a tiempo real fue realizada en un aparato MyiQ™ (BIO-RAD) usando SYBR® Premix Ex Taq™ (Perfect Real Time) (Takara). Las mezclas de reacción fueron incubadas durante 10 min a 95°C, seguido de 40 ciclos de 15 s a 95°C, 1 min a 60°C, y finalmente 15 s a 95°C, 1 min a 60°C, y 15 s a 95°C. Para cada ARN, la expression génica fue corregida por la protein ribosónica S11 (*rps11*) contenida en cada muestra usando el método *Ct* comparativo ($2^{-\Delta\Delta}$*Ct*). En todos los casos, cada PCR se llevó a cabo con cada muestra por triplicado y fue repetida al menos con dos muestras independientes.

Análisis de la actividad promotora del gen *gcsf*

Una secuencia de ADN genómico de 2 Kb aguas arriba de la posición +1 del gen *gcsf* fue amplificada usando los siguientes oligos: directo 5´ CAGTGTTGTGGTTTTGG TCCAGGCG 3´ y reverso 5´ CCGGACACCGAGCACCGGCGAGCCGCC 3´. El fragment de ADN fue clonado en el sitio SmaI del vector pGL3basic (Promega) dirigiendo la expression del gen de la luciferasa de luciérnaga (*gcsf*::Luc). Embriones en el estadío de desarrollo de 1-8 células fueron microinyectados en el saco vitelino con 0.5-1 nL de una mezcla conteniendo 20 ng/μL de la construcción con la luciferasa de luciérnada, 2 ng/μL del plásmido con la luciferasa de *Renilla*, y 1 ng/huevo de los morfolinos stdMo y TRMo2 solos o en combinación con 200 pg/huevo del ARN de *TR*

transcrito *in vitro*. Pasadas 48 horas, se obtuvieron secciones de colas de al menos 50 larvas y se midió la actividad luciferasa como se ha descrito anteriormente.

Análisis estadístico

Los datos fueron analizados mediante el análisis de la varianza (ANOVA). Las diferencias entre dos muestras se analizaron mediante el Test-*t* de Student. El Test Log-Rank fue usado para determinar las diferencias estadísticas en las curvas de supervivencia de distintos grupos experimentales.

4. Resultados y discusión

4.1. Desarrollo de un nuevo sistema chivato basado en la luciferasa para el estudio de promotores tanto constitutivos como inducibles en el contexto de un organismo completo

En este capítulo se combinaron las ventajas que tiene el ensayo clásico de la doble luciferasa con las que tiene el pez cebra como modelo vertebrado para desarrollar una técnica que permita analizar la actividad promotora y la función génica en el contexto de un organismo completo.

En primer lugar, se ilustró la utilidad de este nuevo sistema para la caracterización del promotor constitutivo de la telomerasa en el contexto de un organismo completo. En sólo 24 horas, se pudo determinar de manera cuantitativa la actividad promotora relativa de dos fragmentos de distinta longitud aguas arriba del sitio de inicio de la transcripción de la telomerasa. El resultado fue que un fragmento de 3 Kb fue capaz de dirigir la expresión de la luciferasa, mientras que un fragmento de sólo 1 Kb no pudo incrementar de manera significativa la expresión basal.

Otra aplicación de este sistema es la caracterización de la respuesta de promotores inducibles por diferentes estímulos. Para abordar este objetivo, en primer lugar hay que elegir el promotor óptimo para la normalización de las medidas, ya que está descrito que los promotores que clásicamente se usan para dirigir la expresión de la luciferasa de *Renilla* se ven afectados por distintos estímulos externos [Ramanathan *et al.*, 2005]. En este caso concreto, se analizó el efecto de los PAMPs clásicos LPS y ADN bacterianos sobre cuatro construcciones portadoras de la luciferasa de *Renilla* bajo el control de los promotores CMV, TK, SV40 y EF1α. El promotor CMV resultó ser inducido por ambos PAMPs, mientras que el promotor EF1α fue inhibido. Por este motivo, ambas construcciones fueron descartadas, ya que el uso de la primera resultaría en una subestimación de la respuesta del promotor inducible a estos estímulos, mientras que el uso de la segunda daría lugar a una sobreestimación de la misma. Por el contrario, los promotores TK y sobre todo el SV40 mostraron una expresión más constante, siendo éste último el seleccionado para el estudio del promotor inducible NF-κB que, como era de esperar, resultó ser inducido por ambos PAMPs.

Finalmente, también validamos el uso de esta técnica para el estudio de un gen de interés combinándola con la tecnología de inhibición génica mediante el uso de morfolinos. En concreto, estudiamos el papel que juega la proteína adaptadora MyD88 en la respuesta del promotor inducible NF-κB al ADN bacteriano. Para ello, combinamos la construcción del promotor inducible con el PAMP y con un morfolino específico para MyD88 [van der Sar *et al.*, 2006], resultando en una disminución significativa de la activación de NF-κB. La especificidad del ensayo se comprobó mediante el uso de un morfolino para el TLR3, que se sabe que no está implicado en la ruta de señalización del ADN bacteriano.

El nuevo sistema chivato basado en la luciferasa resultó ser una técnica rápida y sensible que puede ser utilizada como una nueva herramienta para caracterizar *in vivo* la mínima región promotora de un gen, la respuesta de promotores inducibles ante distintos estímulos, la validación de construcciones genéticas y la función de un gen de interés. Un pequeño inconveniente de la técnica es la necesidad de utilizar una segunda luciferasa para normalizar las medidas y eliminar las variaciones experimentales. Especialmente para el estudio de promotores inducibles, donde ya hemos visto que algunos promotores usados habitualmente como control interno pueden ser afectados por los estímulos externos [Ramanathan *et al.*, 2005], se hace necesario un estudio previo para elegir correctamente el plásmido de normalización. Otra limitación de la técnica es que sólo permite el estudio de promotores de respuesta corta, debido a que la expresión de los plásmidos es transitoria. Además, esta técnica tampoco proporciona información espacial de la expresión génica, para lo que debería complementarse con técnicas de hibridación *in situ* y de microscopía de fluorescencia. Sin embargo, a pesar de estas carencias, la técnica resulta muy valiosa cuando se combina con las ventajas que ofrece el pez cebra para hacer escrutinios a gran escala basados en el fenotipo [Patton & Zon, 2001], convirtiéndose en un sistema muy prometedor para la identificación y la validación de drogas o genes que lo corrijan, por ejemplo.

4.2. Estudio del papel extracurricular del componente de ARN de la telomerasa (*TR*) en la hematopoyesis usando el pez cebra como modelo

Tradicionalmente, las alteraciones en la telomerasa se han asociado al cáncer y al envejecimiento. Sin embargo, también se ha demostrado que la disfunción del complejo de la telomerasa está implicada en algunas enfermedades humanas raras como la anemia aplásica, la diskeratosis congénita [Kirwan & Dokal, 2009; Trahan & Dragon, 2009] y la fibrosis pulmonar [Tsakiri *et al.*, 2007]. La diskeratosis congénita (DC) es una enfermedad genética debida a mutaciones que afectan a los componentes de la telomerasa o a las proteínas estabilizadoras de los telómeros. La principal causa de muerte de esta enfermedad es el fallo en la médula ósea debido a una deficiente capacidad de regeneración de las células madre hematopoyéticas [Brummendorf & Balabanov, 2006; Drummond *et al.*, 2007]. Curiosamente, la enfermedad se presenta de manera más agresiva cuando las mutaciones afectan al componente de ARN de la telomerasa, *TR* [Vulliamy & Dokal, 2008], y algunas de esas mutaciones no están asociadas con la pérdida de actividad telomerasa *in vitro* [Chen & Greider, 2003]. Por otra parte, varios studios han demostrado actividad promotora del cáncer por parte de *TR* de manera independiente a la actividad telomerasa [Blasco *et al.*, 1996; Cayuela *et al.*, 2005; Fragnet *et al.*, 2003; Li *et al.*, 2005]. Estas observaciones, junto con la capacidad de *TR* para unirse específicamente a más de 2000 sitios del genoma humano [Chu *et al.*, 2011] nos llevaron a la hipótesis de que *TR* tiene un papel extracurricular en la hematopoyesis a través de la regulación de la expression de genes.

La inhibición genética de *TR* en embriones de pez cebra con tres morfolinos diferentes resultó en una fuerte neutropenia y monocitopenia. La neutropenia fue rescatada mediante la sobreexpresión del ARN de *TR*, confirmando la especificidad del fenotipo observado. Sorprendentemente, el efecto de *TR* en la mielopoyesis resultó ser independiente de la actividad telomerasa y de la longitud telomérica ya que (1) las larvas mutantes en *tert* mostraron un número normal de neutrófilos; (2) la ausencia de *TR* produjo neutropenia también en las larvas mutantes en *tert*; (3) la longitud telomérica fue ligeramente más corta y similar tanto en larvas deficientes en *TR* como en *tert*; y (4) la expression de *TR* fue muy alta en los neutrófilos aislados, mientras que la de *tert* fue indeterminada. Estos resultados apoyaron la hipótesis del papel extracurricular de *TR* en la mielopoyesis, sugiriendo su posible implicación en la regulación de la función de los neutrófilos. Estudios funcionales mostraron que los

neutrófilos de larvas de pez cebra deficientes en *TR* eran capaces de reclutarse a las heridas de manera similar al grupo control. De la misma manera, las larvas deficientes en *TR* no fueron más susceptibles a *S. typhimurium* que las larvas control y, como éstas, sobreexpresaron los genes proinflamatorios *il1β* y *tnfα* en respuesta a la infección. Por tanto, la ausencia de *TR* afecta al número de neutrófilos pero no a su funcionalidad. Hasta donde sabemos, existe un único estudio sobre la función de los neutrófilos de pacientes de DC en el que no hay diferencia en el nivel de producción de radicales libres de oxígeno en respuesta a la activación de la NADPH oxidasa entre los pacientes y sus respectivos familiares sanos [Rochowski *et al.*, 2011].

Una de las observaciones más interesantes de nuestro estudio es que la hematopoyesis definitiva no está afectada en las larvas deficientes en *TR*. De todos los genes analizados, los únicos cuya expresión fue afectada por la ausencia de *TR* fueron los específicos de la mielopoyesis: *spi1* y *gcsfr*. Colectivamente, los resultados sugirieron que *TR* no era necesario para la aparición ni de las células madre ni de las progenitoras de la hematopoyesis, pero sí que lo era para la diferenciación de éstas en neutrófilos y macrófagos. Para comprobar esta hipótesis, hicimos un estudio morfológico de las células sanguíneas en ausencia de *TR*, observando una alteración de la morfología consistente con un retraso en la diferenciación de las células progenitoras. Estos resultados podrían explicar la neutropenia persistente y la mielopoyesis alterada que se observa en niños con DC, que sí que muestran una eritropoyesis, megacariopoyesis y linfopoyesis normales [Yel *et al.*, 1996; Yilmaz *et al.*, 2002]. Nosotros especulamos que la función clásica de *TR* en el mantenimiento de los telómeros podría enmascarar su papel extracurricular en la mielopoyesis, puesto que muchos pacientes de DC se examinan en estadíos tardíos de la enfermedad, cuando los telómeros ya son críticamente cortos y afectan de manera severa a la renovación de las células madre hematopoyéticas, haciendo inminente el fallo de la medulla ósea.

Los factores transcripcionales *spi1* y *gata1* son esenciales para la diferenciación de las células madre hematopoyéticas en células mieloides y eritroides, respectivamente. La regulación recíproca de *spi1* y *gata1* determina el destino mieloide vs. el eritroide [Rhodes *et al.*, 2005]. Además, la pérdida de gata1 transforma los precursores sanguíneos primitivos en células mieloides, dando lugar a una expansión masiva de neutrófilos y macrófagos a expensas de la serie roja [Galloway *et al.*, 2005]. Nuestros resultados demostraron que *TR* modula el destino mieloide vs. el eritroide de las células

madre hematopoyéticas mediante el control diferencial de los niveles de *spi1* y *gata1*, probablemente regulando la expresión de los principales factores de crecimiento implicados en la diferenciación de los neutrófilos (gcsf) y los macrófagos (mcsf). Esto no es nada raro ya que, en humanos, *TR* se une directamente a los promotores de los genes de los factores de estimulación de colonias *CSF1* y *CSF2* [Chu *et al.*, 2011], y en ratón, hay una compleja relación entre los factores de estimulación de colonias de granulocitos y de macrófagos *GCSF*/*GMCSF* y *SPI* [Berclaz *et al.*, 2007; Berclaz *et al.*, 2002; Dahl *et al.*, 2003]. Por tanto, *TR* podría actuar como un factor de transcripción positivo para estos genes. Aunque la unión de *TR* a las secuencias reguladoras aguas arriba de los genes *gcsf* y *mcsf* está por demostrar, la sutil regulación del promotor del gen *gcsf* en pez cebra mediante los niveles de *TR*, según demostramos con un ensayo de luciferasa en el contexto de una larva completa, apoya esta hipótesis.

En conclusión, este estudio aporta pruebas experimentales de que *TR* juega un papel extracurricular en la regulación de la mielopoyesis mediante la puesta a punto de la expresión de los factores de transcripción *spi1* y *gata1* durante el desarrollo embrionario del pez cebra a través de la regulación de *gcsf* y *mcsf*. El modelo *in vivo* desarrollado es una herramienta muy poderosa para ilustrar las funciones extracurriculares de *TR* en la aparición, mantenimiento y diferenciación de las células madre hematopoyéticas. En este sentido, más estudios con este modelo podrían ayudar a esclarecer las vías de señalización afectadas en los pacientes de DC y que podrían representar dianas terapéuticas.

5. Conclusiones

Los resultados de este trabajo conducen a las siguientes conclusiones:

1. Hemos desarrollado un ensayo rápido y sensible basado en la técnica clásica de la doble luciferasa que puede utilizarse como nueva herramienta para el estudio de promotores constitutivos e inducibles en el contexto de un organism completo. Este ensayo podría usarse para hacer escrutinios a gran escala.

2. La inhibición genética del componente de ARN de la telomerasa (*TR)* mediante el uso de morfolinos afecta a la actividad telomerasa pero no altera el desarrollo del pez cebra.

3. La deficiencia de *TR* induce neutropenia y monocitopenia pero no compromete la funcionalidad de los neutrófilos.

4. La neutropenia inducida en ausencia de *TR* es independiente de la longitud telomérica y de la actividad telomerasa, lo cual sugiere un papel extracurricular de *TR* en la mielopoyesis.

5. *TR* regula la expresión de los genes *gcsf* y *mcsf*. Por tanto, la deficiencia de *TR* resulta en la reducción de los niveles de *gcsf* y *mcsf*, alterando el balance *spi1*/*gata1a* en las células sanguíneas y afectando la mielopoyesis. Sin embargo, ni la aparición de las células madre hematopoyéticas ni la eritropoyesis están afectadas por la ausencia de *TR*.